Soliton dynamics and symmetry in CP(^2) Sigma Models

Bull, D.R.

Soliton Dynamics and Symmetry in CP^2 Sigma Models

by

D.R.Bull

A thesis presented for the degree of Doctor of Philosophy at the University of Durham

Department of Mathematical Sciences
University of Durham
Durham DH1 3LE
England

March 1995

Dedicated to the memory of Alison and Tony

Abstract

Soliton Dynamics and Symmetry in CP^2 Sigma Models
by
D.R.Bull

The primary purpose of the work undertaken in this thesis is to investigate soliton scattering in the non linear CP^2 sigma model. This has two spatial and one temporal dimension. The vector fields used to represent the model have three components and hence there exists a global $SU(3)$ symmetry.

The effects of adding an Hopflike term to the basic lagrangian is considered. A review of the model is given in chapter I. The second chapter discusses Noether's theorem which states that each symmetry of the lagrangian has associated with it a conserved charge.

In the third chapter, the eight charges relating to the internal symmetry are calculated. Explanations are provided for the results calculated during the numerical simulations. The results for the CP^1 model are also discussed.

In the fourth chapter, these charges are used to predict the qualitative behaviour of the solitons. It will provide an explanation for the effect of the coefficient of the hopflike term on the scattering. The single soliton ansatz is also investigated.

In the penultimate chapter, an alternative approach is used. This involves looking for the closest static approximation to the evolved solution. It is able to predict the trajectory for pure CP^2 and some confirmation is provided for the ansatz used in the full lagrangian.

The last chapter summarises the results. It also provides some suggestions for further work.

Preface

This thesis is based on work produced whilst at the Department of Mathematical Sciences in the University of Durham between October 1994 and November 1995 under the supervision of Dr. W.J.Zakrzewski. This material has not been submitted previously for any degree, either in this or any other university.

Except for where an explicit reference is given, chapters II ,III, IV and V are claimed to be the original work of the author. The copyright of this thesis remains with the author. No quotation from it should be published without his prior written consent and information obtained from it should be acknowledged fully.

I would like to thank my family and especially my parents for their support during my education. I would also like to mention my appreciation for my friends for helping me to keep my sanity. In particular Ghadeer Abu Leil Cooper, Rasa Greimiene, Nadia Kalogridou, Rachel-Louise Koktava, Richard Costambeys, Richard Hall, Uli Harder, Alex Iskandar, Nick Myers, Michael Young and especially Caroline Brown.

I would also like to thank Wojtek Zakrzewski for his support during my studies. I also acknowledge EPSRC (formally SERC) for their financial support.

Contents

List of Figures

I

Introduction

Nature, and Nature's laws lay hid at night,
God said: let Newton be! And all was light. [1]

It did not last! The Devil shouting ho!
Let Einstein be and restored the status quo. [2]

[1] Alexander Pope, epitaph for Sir Isaac Newton
[2] Sir John Collings

I.i Physical Motivation

The Greek philosopher Democritus postulated around 400 BC, that all matter was constructed from minute, indivisible particles [26]. However, at that time the more widely accepted view was that proposed by Aristotle. He believed that all matter was continuous in structure. This hypothesis dominated until the birth of modern scientific research in the seventeenth and eighteenth centuries. Then the proposed building blocks of matter were given the name atoms, derived from the Greek for indivisible: atomos.

John Dalton is regarded as being the father of modern atomic theory. In 1808 he proposed that all matter was composed of such atoms; that all the atoms of a particular element were identical and that the atoms of different elements differ in mass and other well defined properties. When two or more elements combine, their atoms joined to form molecules. Throughout the nineteenth century experimental results confirmed this theory.

In the 1890s, J.J.Thomson first verified the hypothesis that the atom had an internal structure by confirming the existence of electrons within the atom. This was followed by the discovery of the proton within the hydrogen atom by Rutherford in the 1920s. The existence of a neutron was shown by Chadwick in the 1930s. Thus by the early part of this century, it became clear that atoms were not the fundamental unit of matter. Instead, they are constructed from various combinations of protons, neutrons and electrons.

Protons and neutrons are members of the class of particles known as hadrons (from the Greek word adros, meaning strong). All half integer

spin hadrons are called baryons whilst integral spin hadrons, such as the pion, are called mesons.

After the second world war, high energy accelerators became available and this led to a plethora of new particles being discovered. Hence, a method of classification was urgently required. The quark model was proposed as a means of explaining the internal structure of sub-atomic particles and hence the means by which to classify them [10].

Experimental evidence from deep inelastic scattering in the 1960s indicated that the proton was constructed from smaller components, which Feynman named partons. In an experiment analogous to Rutherford's, it was shown that the charged partons have point-like interactions. It is now believed that quarks are equivalent to these pointlike partons.

Before continuing, a mathematical tool which has proved extremely useful in high energy physics shall be introduced. It is possible to define physical dynamical systems in terms of the difference between the kinetic and potential energy, the Lagrangian. From this can be obtained the equations of motion and other useful information (for an example of this process, see the last two sections of this chapter).

Classical solutions of the Lagrangian fall into four categories [20]:

1. constant solutions (time and space independent);
2. static solutions (time independent but space dependent);
3. time and space dependent solutions
4. instantons (these arise from an analytical continuation of time to an imaginary variable).

However, classical theory is unable to explain physics at microscopic levels. Even quantum mechanics [25] breaks down at high energies. To explain the experimental results, quantum field theories were developed (see [26] for an historical perspective or [34] for an introduction to current methods).

In the quark model [14], it is proposed that baryons are constructed from three quarks whilst mesons are constructed from quark antiquark pairs. They are influenced by the strong force which is short ranged and attractive.

As far as the charged weak interaction is concerned, it is believed that quarks belong to three families, each of which contain a pair of quarks (for example, up and down). These quarks are bound into the hadrons by gluons, the carriers of the strong force.

Quantum Chromodynamics [29] is a model proposed to explain this phenomenon. The quarks are assigned a colour, of which there could be N variations. Experimental evidence suggests that the number of colours in QCD is three.

The quarks cannot exist on their own, but only within the colour neutral hadrons. This is described physically as confinement, which is believed to be a non-perturbative effect.

In QCD, the strong force is described by a $SU(3)$ Yang Mills gauge theory [3]. It is mediated by gluons which carry colour and anti colour. There are thus six colour changing, and two colour non-changing gluons.

The cross section associated with any particular scattering process is complicated. The establishment of asymptotic freedom [8] was an important landmark in the development of QCD. It allowed perturbative techniques to be used to study high energy deep inelastic scatter-

ing (see, for example, [19] and [23]). This provided the experimental verification.

The simplest approach to studying a gauge theory is to use an expansion where each term is given by the sum of all the Feynman diagrams for a particular order of the gauge coupling constant. This method has been helpful in the calculation of high energy processes such as the aforementioned deep inelastic scattering. However, for strong interactions involving hadrons in the infrared limit, the expansion parameter becomes large and an alternative approach is therefore needed.

To understand the alternative method proposed by 't Hooft [17], it is necessary to consider the quantal significance of the solutions of the Lagrangian. For constant solutions it is well known. They are first approximations to the vacuum expectation value of the quantum field.

Frequently they signal the presence of spontaneous symmetry breakdown, for example the Goldstone phenomena. This is the appearance of a massless scalar whenever a continuous symmetry of a physical system is not apparant in the ground state.

The existence of static solutions leads to a new form of state: the soliton. Note that, despite arising from a field theory, they behave like particles. Their energy density is strongly localised, total energy is finite and they are stable.

An important property of most physical field equations is that they are Lorentz invariant. Therefore once a solution $\phi(x)$ has been found, there also exists the boosted solutions $\phi((x-vt)/\sqrt{1-v^2})$. They are able to move within the space.

Most research into time dependent solutions, has been concerned with multisoliton scattering. This has been done by studying the time dependence of field configurations which, for large separations, describe isolated solitons.

It can be shown that some of the quantum properties of these new states (such as the field form factors and soliton mass) are proportional to inverse powers of the coupling constants. This implies that these features are nonperturbative in their nature as they cannot be found in ordinary perturbation theory.

The $1/N$ expansion procedure was proposed as an alternative method by 't Hooft [17] for Quantum Mechanics and Quantum Field Theories [41]. For Yang Mills field theories it involves expanding around the reciprocal of the dimension of the symmetry group $SU(N)$. In QCD this will involve powers of one third. Despite this not being particularly small, the expansion does provide useful results.

The calculations are performed in Euclidean space. This can be considered as an analytic continuation of Minkowski space by using a Wick rotation: $t \rightarrow it$ [3]. This is not a trivial process and before it can be used its validity must be tested.

Of particular interest are the localised finite action solutions of the classical Euclidean field equations. These correspond to the fourth category of classical solutions listed above, the "instantons" (they were given this name by 't Hooft). The requirement of finiteness of energy for solitons is replaced by the requirement of finiteness of the Euclidean action for instantons. The Euclidean action has the same structure as the energy of a static field configuration in one higher spatial dimension.

The vacuum of a Yang Mills theory such as QCD is no longer unique [33]: it degenerates into infinite number of homotopically distinct classes. The true ground should be expressed as

$$|\text{vac}>_\theta = \sum_{-\infty}^{\infty} e^{in\theta}|\text{vac}>_n, \qquad \text{(I.i.1)}$$

where the integer n labels the different homotopy classes. It can be shown this will allow the possibility of tunnelling between two such vacua in Minkowski space.

This scenario in Quantum Theory is called the θ-vacua. One of its most important effects is to lead to the violation of time reversal invariance. However the calculations involving this case are complicated for QCD.

Therefore toy models were sought. The purpose is to be able to study the effects of extended structures within a simpler model. They allow some calculations to be performed analytically, which can only be approximations to the physical theory.

A popular class of such models is known, for historical reasons, as σ-models. In 1960, Gell-Mann and Levy [11] proposed a theory for pion interaction which involved a sigma particle. Physical predictions using this model were eclipsed by the advent of QCD, but in recent years it has proved useful, as a toy model, in the study of non perturbative effects.

These models have four properties in common with the gauge theory in $3+1$ dimensions [40]:

1. They exhibit two dimensional conformal invariance.
2. They are asymptotically free.
3. They possess nontrivial solutions of their equations of motion.
4. They have a parameter expansion which is analogous to the $\frac{1}{N}$ expansion in QCD.

Mathematically they can be described as a field theory defined on a space with Riemannian metric whose nonlinearity arises from the curvature of the target manifold [37].

The above provides the historical reasons for studying sigma models. More recently they have been used in models describing superconductivity and the quantum Hall effect. As an example of harmonic maps, they are also studied in their own right by differential geometers [31].

In 1+1 dimensions, the existence of solitons is associated with the integrability of the model. However, it is not clear whether integrability is a necessary condition or whether other models exist, especially in higher dimensions, with structures which behave like solitons.

In particle theory, the most interesting models are Lorentz invariant. However, in 2+1 dimensions these all appear to be nonintegrable and hence numerical simulations of time evolutions must be used.

Some of these models can be regarded as being "almost integrable" [42]. They have extended structures which resemble solitons in the sense that their scattering is quasi-elastic with little radiation.

Of particular interest to the present work are Grassmanian models in 2+1 dimensions, whose target manifold is represented by the coset space

$$U(N)/(U(M)\times U(N-M)). \tag{I.i.2}$$

There $U(M)$ denotes the group of $M\times M$ unitary matrices. In particular when $M=1$ the CP^{N-1} sigma models are obtained.

To ensure that the total energy is finite, the fields must have the same limit

$$\phi(\mathbf{x}) \to \phi_0 \tag{I.i.3}$$

as $|\mathbf{x}| \to \infty$. This has the effect of compactifying the physical space to a sphere.

The aim of this thesis is to follow on from the work of Piette et al [31]. It is concerned with the scattering of solitons in the modified CP^2 sigma model. In pure CP^2 a head on collision results in scattering at 90 degrees.

However, if a Hopf-like term is added to the basic Lagrangian, the results are more interesting. The solitons now scatter at a non orthogonal angle, the value of which is related to the coefficient associated with the Hopf-like term.

For CP^2 the additional term is no longer a topological term as it cannot be expressed as a total divergence but, for brevity, it will still be referred to as a Hopf term. It will contribute to the classical equations of motion, in contradistinction to CP^1.

The conformal invariance of the models ensures that the extended structures can take any size. Hence during scattering they can change size. Their precise behaviour depends on the details of the interaction. In effect, each soliton is perturbed by the others.

Even a single soliton is unstable to small perturbations. This can result from external factors or from the numerical procedure. The rate of change can be modified by spinning the solitons used in the initial conditions.

The solitons can be stabilised by the addition of a scale defined over the whole space. For example, by adding a potential and Skyrme like term [22]. It was shown that, when separated, the solitons return to their canonical sizes determined by the parameters of the model.

The existence of the $SU(3)$ symmetry in the model leads to eight conserved charges by Noether's theorem. These charges are calculated during numerical simulations of the scattering.

This thesis will consider the effect the additional Hopf-like term has on the classical motion of solitons in CP^2. This will need to be fully understood before the quantised system can be investigated rigorously.

The rest of this chapter will discuss some mathematical methods required for this project. It will then discuss the derivation of the Lagrangian being considered. Chapter II will consider some of the consequences of Noether's theorem.

In the following chapter, the conserved charges associated with the $SU(3)$ symmetry of CP^2 will be derived and compared with the numerical results obtained from the simulations. The fourth chapter will use these charges to investigate the trajectory of the solitons during scattering.

The fifth chapter will describe an alternative method. This will attempt to find the closest static approximation to the predicted solutions during the evolution. Finally the results will be concluded.

The simulations were programmed in FORTRAN 77 [28] and run on various Sun workstations within the Department and Computing Centre at Durham. The graphs were produced by MATLAB [24] and the typesetting performed by LaTeX [21] .

To end this section a few words will be given on the notation used. Superscripts will be used to distinguish between pure CP^2 (0) and the contribution from the Hopf-like term (H). The specific charge under consideration will be labelled by an arabic numeral subscript.

Subscripts shall also be used to indicate differentiation. Roman indices shall specify the spatial dimensions, x_1 and x_2, while Greek indices will cover all dimensions including time, x_0.

The standard shorthand for derivatives will be use in this work

$$\partial_\mu = \frac{\partial}{\partial x_\mu}. \tag{I.i.4}$$

So, for example, ∂_0 will represent the differential operator with respect to time.

I.ii Homotopy Theory

For a good review of homotopy theory, with particular attention paid to its applications in Theoretical Physics, see [12]. Some of the more relevant points for the current work will be summarised here.

Two functions are said to be homotopic if it is possible to continuously deform one into the other. To define this more rigorously, consider two functions $f(x)$ and $g(x)$ where x represents spacetime. They are said to be homotopic if there exists a map $H(x,t)$ which is continuous over the range $0 \leq t \leq 1$ such that

$$\begin{aligned} H(x,0) &= f(x) \\ \text{and} \qquad H(x,1) &= g(x) \end{aligned} \tag{I.ii.1}$$

Thus it is possible to regard classical time evolution as a homotopy between the initial and final state field configurations.

Topological spaces can be partitioned into homotopy classes, $[f]$, inside which all functions are equivalent under the above relationship. A group structure can be formulated using the following operation:

$$[f+g] = [f] + [g] \tag{I.ii.2}$$

Of particular importance to the present work is the group $\pi_n(\mathcal{M})$ which represents all functions of the form:

$$S^n \rightarrow \mathcal{M} \tag{I.ii.3}$$

where S^n is the n dimensional sphere and $\mathcal{M}$ represents the target manifold. For CP^1, this will be isomorphic to the sphere. Note also that the special case $\pi_1(\mathcal{M})$ is known as the fundamental group [2].

An important result follows if the target manifold has the structure of a coset space. Assume that there is a continuous group of symmetries G which acts transitively on the manifold, $\mathcal{M}$. Hence, there will exist a transformation $g \in G$ which will relate any two points, y_1 and y_2, belonging to $\mathcal{M}$, $y_1 = g(y_0)$.

When two elements, g_1 and g_2 for example , of the group give the same point on the manifold, it implies that

$$g_2^{-1} g_1(y_0) = y_0. \tag{I.ii.4}$$

Hence $g_2^{-1} g_1$ is the little group H of y_0: the subgroup of G which leaves the point y_0 unchanged. The little group of G is formally defined by

$$H = \{h \in G | h(p_0) = p_0\} \tag{I.ii.5}$$

The left coset of G with respect to H is the set of elements gh where h varies over H whilst g is kept fixed. It is denoted by

$$gH = \{gh | h \in H\} \tag{I.ii.6}$$

and there is a similar definition for the right coset.

Two group elements acting on a point y_0 will give the same point in the manifold if and only if they belong to the same left coset of G with respect to H. This implies that G may be partitioned into disjoint cosets such that each element of G belongs to one and only one left coset of G with respect to H.

In fact, any point of the manifold can be obtained by the action of a member of some coset gH on y_0. Hence $\mathcal{M}$ can be identified with the space of left cosets G/H

$$\mathcal{M} \simeq G/H = \{gH | g \in G\}. \tag{I.ii.7}$$

This is not, in general, a group. However when H is a normal subgroup (for which the left and right cosets are identical), then a group structure will exist.

When the target manifold is a coset space, the following two useful results can be proved. Provided G is connected ($\pi_0(G) = 0$) and simply connected ($\pi_1(G) = 0$, this requirement is simply that all closed paths in the group can be shrunk to a point), then

$$\begin{aligned} \pi_2(G/H) &= \pi_1(H) \\ \pi_1(G/H) &= \pi_0(H) \end{aligned} \tag{I.ii.8}$$

To have stable topological structures for a d-dimensional system with trivial boundary conditions, it is necessary for $\pi_d(\mathcal{M})$ to be non trivial [12]. In other words, it must have more than one element.

If the group is isomorphic to the integers, Z then it is possible for all homotopy classes to be parametised by an unique number (and conversely all integers have a class associated with it). This number will be topologically invariant.

The Hopf invariant is associated with the group $\pi_{2n-1}(S^n)$ (see [16] or [18]). For this report, the most important case is when n is two for which $\pi_3(S^2)$ is isomorphic to the group of integers.

I.iii CP^n Sigma Models

The basic CP^n model is given by the Lagrangian density

$$L_0 = (D^\mu \mathbf{z})^\dagger D_\mu \mathbf{z} \tag{I.iii.1}$$

where $\mathbf{z}$ is a n+1 dimensional vector field subject to the orthogonality constraint $\mathbf{z}^\dagger \mathbf{z} = 1$ (see [30] and [36]). The covariant derivative is defined to be:

$$D_\mu \psi = \partial_\mu \psi - (\mathbf{z}^\dagger \partial_\mu \mathbf{z})\psi \tag{I.iii.2}$$

for any ψ.

The complex projective space CP^n can be represented by the coset space $SU(n+1)/(SU(n)\mathrm{x}U(1))$. The physical space is two dimensional and the effect of the constraint is to compactify R^2 to the two sphere. Therefore the Lagrangian for static fields can be represented by the map

$$S^2 \rightarrow CP^n \simeq SU(n+1)/(SU(n)\mathrm{x}U(1)). \tag{I.iii.3}$$

To test this for topologically stable structures it is necessary to consider $\pi_2(CP^n)$ which is isomorphic to $\pi_1(SU(n)\mathrm{x}U(1))$ (see previous section). It can be shown (see for example [2]) that the fundamental group of the product space of two path connected Hausdorf spaces [1] is given by

$$\pi_1(X\mathrm{x}Y) = \pi_1(X)\,\mathrm{x}\,\pi_1(Y) \tag{I.iii.4}$$

with the free product being used on the right hand side.

[1] *Hausdorf Space*: A topological space in which every pair of distinct points have a pair of disjoint open neighbourhoods

Therefore as $SU(n)$ has a trivial fundamental group, it follows that

$$\pi_1(CP^n) \simeq \pi_1(U(1)) = Z, \tag{I.iii.5}$$

where Z represents the group of integers. The last result can also be found in Armstrong's book [2]. Hence there exists stable, non-trivial topological structures in the model under consideration.

Before continuing, it will prove useful to consider the specific form of $\mathbf{z}$. The orthogonality condition can be used to simplify the calculations by introducing the new field $\mathbf{f}$, defined by

$$\mathbf{z} = \frac{\mathbf{f}}{|\mathbf{f}|} \tag{I.iii.6}$$

The $U(1)$ invariance of the Lagrangian can then be used to ensure that one of the components of $\mathbf{f}$ is real, or indeed unity. Hence the following ansatz will be used

$$\mathbf{z} = \frac{1}{|\mathbf{f}|}\begin{pmatrix} 1 \\ f_1 \\ \vdots \\ f_n \end{pmatrix} \tag{I.iii.7}$$

Another useful consequence of the constraint is that for any constant matrix M,

$$\mathbf{z}^\dagger M \partial_\alpha \mathbf{z} - \partial_\alpha \mathbf{z}^\dagger M \mathbf{z} = \frac{\mathbf{f}^\dagger M \partial_\alpha \mathbf{f} - \partial_\alpha \mathbf{f}^\dagger M \mathbf{f}}{|\mathbf{f}|^2} \tag{I.iii.8}$$

To proceed it is necessary to consider the topological charge which is defined to be [33]

$$Q^{TOP} = \frac{-i}{2\pi}\int d^2x \, \left(\partial_1 \mathbf{z}^\dagger \partial_2 \mathbf{z} - \partial_2 \mathbf{z}^\dagger \partial_1 \mathbf{z}\right). \tag{I.iii.9}$$

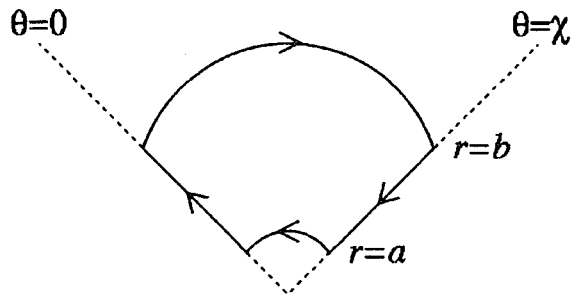

Figure I.1: Polar segment in two space

This can be written as a contour integral by the use of Stoke's theorem (see, for example, [4]). The calculations will be simplified if polar coordinates are used and hence the topological charge should be written in the form

$$Q^{TOP} = \frac{-i}{2\pi} \oint \mathbf{z}^\dagger \frac{\partial \mathbf{z}}{\partial \theta} d\theta + \mathbf{z}^\dagger \frac{\partial \mathbf{z}}{\partial r} dr. \qquad \text{(I.iii.10)}$$

Consider integrating the general function $I = \oint f d\theta + g dr$ over the segment in polar coordinates shown in figure I.1. The integral will be given by

$$\begin{aligned} I = &\int_0^\chi d\theta f(r,\theta)|_{r=b} \quad + \quad \int_b^a dr g(r,\theta)|_{\theta=\chi} \\ &+ \int_\chi^0 d\theta f(r,\theta)|_{r=a} \quad + \quad \int_a^b dr g(r,\theta)|_{\theta=0}. \end{aligned} \qquad \text{(I.iii.11)}$$

The limits $a \to 0$, $b \to \infty$ and $\chi \to 2\pi$ should to be taken to cover all two space.

Consider the radial integral which can be written as

$$I_{\text{radial}} = \int_a^b dr \Big\{ g(r,\theta)|_{\theta=\chi} - g(r,\theta)|_{\theta=0} \Big\}. \qquad \text{(I.iii.12)}$$

Therefore, when the function $g(r,\theta)$ is periodic over $[0, 2\pi]$, which is true for the topological charge and most other calculations considered

in this project, this contribution will trivially tend to zero when the limits are taken. Therefore

$$Q^{TOP} = \frac{-i}{2\pi}\left\{\lim_{b\to\infty}\int_0^{2\pi}\mathbf{z}^\dagger\frac{\partial\mathbf{z}}{\partial\theta}d\theta\Big|_{r=b} - \int_0^{2\pi}\mathbf{z}^\dagger\frac{\partial\mathbf{z}}{\partial\theta}d\theta\Big|_{r=0}\right\}. \qquad \text{(I.iii.13)}$$

It was shown earlier, that the integrand terms can be rearranged into the form

$$\mathbf{z}^\dagger \frac{\partial \mathbf{z}}{\partial \theta} = \frac{(\mathbf{f}^\dagger \partial_\theta \mathbf{f} - \partial_\theta \mathbf{f}^\dagger \mathbf{f})}{|\mathbf{f}|^2}. \tag{I.iii.14}$$

Now consider the following ansatz for $\mathbf{f}$,

$$\mathbf{f} = \begin{pmatrix} 1 \\ \lambda r^n e^{in\theta} \\ \mu r e^{i\theta} \\ \vdots \end{pmatrix} + \text{lower order terms in } r, \tag{I.iii.15}$$

where the second component can be assumed to be of the highest order in r without loss of generality.

For large r, both the numerator and denominator will be of order $2n$ and hence the whole expression will be of order one. When r is zero, the denominator will be unity and hence the integrand will not diverge. However, the numerator will vanish because the derivative operator will ensure that all terms involve a positive power of r.

Hence, when this form is used, the topological charge becomes

$$\begin{aligned} Q^{\text{TOP}} &= \frac{-i}{2\pi} \int_0^{2\pi} in d\theta \\ &= n. \end{aligned} \tag{I.iii.16}$$

Therefore the ansatz given by I.iii.15 will describe the n soliton sector of phase space.

It was mentioned in the introduction, that only static solutions can be found analytically. To obtain a time dependent solution, the parameters associated with equation I.iii.15 can be made time dependent. This is not the general solution, it simply represents giving a static solution a boost.

I.iv Hopf Term

This dissertation is concerned with the effect of adding the following term to the pure CP^2 Lagrangian:

$$\mathcal{L}_H = K\epsilon^{\mu\nu\alpha}\left\{(D_\mu \mathbf{z})^\dagger D_\nu \mathbf{z}\right\}\mathbf{z}^\dagger\partial_\alpha \mathbf{z} \qquad \text{(I.iv.1)}$$

It is the only additional term which has no more than three derivative terms that does not break the global symmetries of the Lagrangian [31].

On its own, this would be an arbitrary way of enhancing the target manifold of the Lagrangian. However, a more rigorous justification for this term can be given for the simpler CP^1 model (see, for example, [42]).

Consider a time evolution over the period $[0, T]$. If the final field configuration is identical to the initial field configuration, then the time orbit can be treated as if it were periodic. The physical space can therefore be represented by $S^2 \mathrm{x} S^1$ which is *locally* isomorphic to S^3.

The action can thus be viewed as a map of the form

$$S^3 \rightarrow CP^1 \simeq S^2 \qquad \text{(I.iv.2)}$$

which can be described by the homotopy group $\pi_3(S^2)$. As discussed earlier, this is isomorphic to the group of integers. Hence the map is infinitely connected and will allow fractional statistics ([9] and [39]).

To see this, take a single soliton and rotate it through 2π during this period. Feynman postulated that this would correspond to the wave-function acquiring a factor of e^{iS}, where S is the action corresponding to the adiabatic rotation [38]. The angular momentum is then defined by

$$e^{iS} = e^{i2\pi J}. \qquad \text{(I.iv.3)}$$

For pure CP^2, the action is quadratic in time. It is a standard result from dynamics that an object moving at constant angular velocity around a circle has velocity inversely proportional to its period (see, for example, [13]). Therefore, S^0 will be of order $\frac{1}{T}$, where T is the end time point. Now consider taking the limit $T \to \infty$. It can be clearly seen that S^0 will go to zero and hence pure CP^1 has zero angular momentum [35].

Wilczek and Zee [38] showed that it was possible to add a topological term to CP^1 which satisfied the mathematical criteria of a Hopf invariant. It is locally a total derivative and as such does not affect the classical equations of motion. However, it does affect the quantum system describing the "spin" of the extended structures.

They constructed the topological current

$$j^\mu = \frac{1}{2\pi}\epsilon^{\mu\nu\lambda}(D^\nu \mathbf{z})^\dagger D_\lambda \mathbf{z} \qquad \text{(I.iv.4)}$$

which is clearly conserved. Hence it can be expressed as the curl of the gauge field,

$$A_\mu = \mathbf{z}^\dagger \partial_\mu \mathbf{z} \qquad \text{(I.iv.5)}$$

and taking $KA_\mu j^\mu$ in the Lagrangian density results in the form given by equation I.iv.1. This term is linear in time and hence can be expected to give a nontrivial contribution to the angular momentum.

The Hopf term can be shown to be analogous to the Chern Simons term in gauge theory and the θ-vacua in QCD [9]. To see the relationship with the former result, define the tensor

$$F^{\nu\mu} = \partial_\nu A_\mu. \qquad \text{(I.iv.6)}$$

If a current is defined in terms of this by,

$$j^{\mu} = \frac{1}{2}\epsilon^{\mu\nu\lambda}F_{\nu\lambda}, \tag{I.iv.7}$$

it can be shown to be equivalent to the earlier definition as

$$\begin{aligned} j_{\mu} &= \frac{1}{2}\epsilon^{\mu\nu\lambda}\partial_{\nu}A_{\lambda} \\ &= \frac{1}{2}\epsilon^{\mu\nu\lambda}\partial_{\nu}\mathbf{z}^{\dagger}\partial_{\lambda}\mathbf{z} \\ &= \frac{i}{2}\epsilon^{\mu\nu\lambda}(D^{\nu}\mathbf{z})^{\dagger}D_{\lambda}\mathbf{z} \text{ plus symmetric terms.} \end{aligned} \tag{I.iv.8}$$

For a single soliton, spatial rotation is isomorphic to isospin rotation. It can thus be shown that the soliton will have angular momentum $\kappa/2\pi$, where $\kappa = 2\pi K$. To see this, it is simpler to use the equivalent $O(3)$ sigma model, which is related to CP^1 by

$$\phi_i = \mathbf{z}^{\dagger}\sigma^i\mathbf{z} \tag{I.iv.9}$$

where σ^i are the usual Pauli matrices [25].

The following argument is taken from the canonical quantisation procedure given in [5]. They defined the gauge potential associated with the conserved current j_{μ} by

$$j_{\mu} = \epsilon_{\mu\nu\lambda}\partial^{\nu}A^{\lambda}. \tag{I.iv.10}$$

When the model is canonically quantised using the radiation gauge, $\partial_i A_i = 0$, it can be shown to be given by

$$A_i(x) = \epsilon_{ik}\ \partial_k \int d^2x' D(x-x')j_0(x') \tag{I.iv.11}$$

$D(x-x')$ is the Green's function which is defined by

$$\nabla^2 D(x) = -\delta(x). \tag{I.iv.12}$$

The canonical momentum conjugate is found by using

$$\pi^a(x) = \frac{\delta \mathcal{L}}{\delta(\partial_0 \phi^a(x))}. \tag{I.iv.13}$$

From this can be derived the Dirac brackets required for quantisation. For further details of this, the interested reader is referred to Bowick's paper.

The standard definition of angular momentum in d spatial dimensions is given by [34]

$$J = \epsilon_{ij} \int d^d\, x x^i\, T^{0j}. \tag{I.iv.14}$$

$T^{\mu\nu}$ is the stress energy tensor.

However this definition, when applied to a two dimensional system, leads to an ambiguity because the generators will be scalar [5]. Hence they will not satisfy any nontrivial lie algebra and the angular momentum will be arbitrary up to a constant.

This ambiguity can be resolved by including the temporal dimension in the algebra. The full symmetry in Minkowski space will be $SO(2,1)$ and this can be used to define angular momentum as the commutator of the Lorentz boost generators

$$J = \frac{1}{2} i \epsilon_{ij} [J^{0i}, J^{0j}] \tag{I.iv.15}$$

It is thus possible to define the following two Poincare generators

$$\begin{aligned} P_\mu &\equiv \int d^2x T^{0\mu}, \\ J^{\mu\nu} &\equiv \int d^2x \left(x^\mu T^{0\nu} - x^\nu T^{0\mu} \right) \end{aligned} \tag{I.iv.16}$$

which satisfy the Poincare algebra

$$\begin{aligned} [P^\mu, P^\nu] &= 0, \\ i[P^\mu, J^{\nu\lambda}] &= g^{\mu\lambda}P^\nu - g^{\mu\nu}P^\lambda, \\ i[J^{\mu\nu}, J^{\kappa\lambda}] &= g^{\nu\lambda}J^{\mu\kappa} - g^{\mu\lambda}J^{\nu\kappa} + g^{\mu\kappa}J^{\nu\lambda} - g^{\nu\kappa}J^{\mu\lambda}. \end{aligned} \quad \text{(I.iv.17)}$$

In Bowick's paper, it was shown that this satisfies the relevant covariance criterion.

From the last condition of I.iv.17, it can be seen that

$$\begin{aligned} \frac{1}{2}\epsilon_{ij}[j^{0i}, j^{0j}] &= \frac{1}{2}\epsilon_{ij}j^{ij} \\ &= \epsilon_{ij}\int d^2x x^i T^{0j}. \end{aligned} \quad \text{(I.iv.18)}$$

Hence this more rigorous definition still satisfies the earlier, naive ansatz given for the angular momentum.

Up until equation I.iv.15, the calculation holds for the general Lagrangian. However, introducing the stress energy tensor ties the calculation to a specific model. For example, for CP^1, it will be given by

$$T_{\mu\nu} = (D_\nu \mathbf{z})^\dagger D_\mu \mathbf{z} - (D_\mu \mathbf{z})^\dagger D_\nu \mathbf{z} - \mathcal{L}\delta_{\mu\nu}. \quad \text{(I.iv.19)}$$

Using the above algebra it is possible to show that the angular momentum can written in the following form

$$\begin{aligned} J &= \int d^2x \epsilon^{ij} x_i \pi^a(x) \partial_j \phi^a(x) \\ &- \frac{\kappa}{2\pi}\int d^2x\ \epsilon_{ij}\epsilon_{kl}\epsilon^{abc}\ x_i A_k(x)\phi^b(x)\ \partial_l^c\phi(x)\partial_j\phi^a(x) \end{aligned} \quad \text{(I.iv.20)}$$

where π^a is the momentum conjugate to ϕ as defined in I.iv.13.

The first term is the standard orbital angular momentum. The second term can be rewritten as

$$J_2 = -2\kappa \int d^2x \epsilon_{ij}\epsilon_{kl}\epsilon_{lj} x_i A_k(x) j^0(x) \quad \text{(I.iv.21)}$$

by using the identity

$$\epsilon_{\mu\nu\lambda} j^{\mu} \phi^{a} = \frac{1}{4\pi} \epsilon^{abc} \partial_{\nu} \phi^{b} \partial_{\lambda} \phi^{c}. \qquad \text{(I.iv.22)}$$

Substituting for the gauge potential by using equation I.iv.11, a few lines of calculation will show that

$$\begin{aligned} J_2 &= \frac{\kappa}{\pi} \int d^2x d^2x' \frac{x(x-x')}{|x-x'|^2} j^0(x') j^0(x) \\ &= \frac{\kappa}{\pi} \int d^2x d^2x' \left\{ 1 + \frac{x'(x-x')}{|x-x'|^2} \right\} j^0(x') j^0(x) \\ &= \frac{\kappa}{2\pi} Q^2 \end{aligned} \qquad \text{(I.iv.23)}$$

where Q is the topological charge, defined in this interpretation by

$$Q = \int d^2x j_0(x). \qquad \text{(I.iv.24)}$$

This is equivalent to the earlier definition given by I.iii.9.

Therefore it has been established that the Hopf term is responsible for the fractional spin. It cannot be removed by a redefinition of the generators as J is fixed as the commutator of lorentz boosts.

By considering soliton and antisoliton pairs, it is possible to show that the Hopf invariant corresponds to the topological linking number (this next section follows the calculation of [38]). This can be shown heuristically by considering the maps $S^3 \rightarrow S^2$. The reverse image of a point in S^2 can be thought of as a curve in R^3 with infinity identified as a single point through stereo projection.

Consider two special cases of ϕ for a single soliton. $\phi = (0,0,1)$ corresponds to the great circle $|z_1| = 1, z_2 = 0$ and (0,0,-1) to interchanging the components of **z**. Express the components of the fields in

the form

$$(z_1, z_2) = (\cos\psi, \sin\psi\cos\theta, \sin\psi\sin\theta\cos\phi, \sin\psi\sin\theta\sin\phi) \quad \text{(I.iv.25)}$$

and stereographically project to $r(\psi)(\cos\theta, \sin\theta\cos\psi, \sin\theta\sin\psi)$ in R^3. The function r ranges monotonically from infinity to zero as ψ varies from zero to π. It can then be clearly seen that the two curves will link only once for one soliton.

Exotic statistics can be explored by considering soliton antisoliton pairs. To be able to use the above results, it is necessary for them to be created from a vacuum and for the evolution to result in their ultimate destruction. Consider one such pair and rotate them through 2π (if they were not rotated, the map would be homotopically trivial). This will correspond to an Hopf invariant of one. Hence the trajectories will link only once.

Now consider two such pairs and during the evolution exchange the two solitons. This will also have an Hopf invariant of one which can be seen by plotting the trajectories of each soliton and antisoliton. This is easier than calculating the Hopf invariant directly. Thus the Skyrmions obey exotic statistics which interpolate continuously between Bose and Fermi statistics.

Before leaving this section, it is worth emphasizing why the above calculation does not hold in CP^2. The Hopf like term makes a contribution like a stress force to this model and is no longer purely topological. An alternative way of looking at it is to regard stress as being a Hopf like term.

This thesis is concerned with the effect of this additional term on the classical scattering of solitons in the higher dimensional system. This is done through an analysis of the conserved charges associated with the symmetries of the Lagrangian. The next chapter will consider Noether's theorem.

I.v Equations of motion

To finish this chapter, the equations of motion will be calculated for the sigma model under consideration. The coefficient associated with the Hopf term ensures that it is possible to consider the contribution from $\mathcal{L}^0$ and $\mathcal{L}^H$ separately.

Recall that the Lagrangian for pure CP^n, with the addition of the associated Lagrange multiplier for the constraint, is

$$\mathcal{L}^0 = (D_\mu \mathbf{z})^\dagger D_\mu \mathbf{z} + \lambda(\mathbf{z}^\dagger \mathbf{z} - 1). \tag{I.v.1}$$

It can be shown that

$$\frac{\partial \mathcal{L}^0}{\partial(\partial_\rho z_e^\dagger)} = D_\rho z^e \tag{I.v.2}$$

and

$$\frac{\partial \mathcal{L}^0}{\partial(z_e^\dagger)} = \mathbf{z}^\dagger \partial_\rho \mathbf{z} D_\rho z^e, \tag{I.v.3}$$

from which it follows that the equations of motion for pure CP^n is

$$D^\rho D_\rho \mathbf{z} - \lambda \mathbf{z} = 0 \tag{I.v.4}$$

and its complex conjugate.

Now consider the contribution from the Hopf term,

$$\mathcal{L}^H = K\epsilon^{\mu\nu\alpha}\left\{(D_\mu \mathbf{z})^\dagger D_\nu \mathbf{z}\right\} \mathbf{z}^\dagger \partial_\alpha \mathbf{z}, \tag{I.v.5}$$

for which

$$\frac{\partial \mathcal{L}^H}{\partial(\partial_\rho z_e^\dagger)} = K\epsilon^{\rho\nu\alpha} D_\nu z_e \mathbf{z}^\dagger \partial_\alpha \mathbf{z} \tag{I.v.6}$$

and

$$\frac{\partial \mathcal{L}^H}{\partial(z_e^\dagger)} = K\epsilon^{\rho\nu\alpha} \partial_\nu z_e \left\{(D_\rho \mathbf{z})^\dagger D_\alpha \mathbf{z}\right\}. \tag{I.v.7}$$

Therefore equation I.v.5 will contribute

$$2K\epsilon^{\rho\nu\alpha}D_\alpha \mathbf{z}\{(D_\rho \mathbf{z})^\dagger D_\nu \mathbf{z}\} \qquad \text{(I.v.8)}$$

to the Euler Lagrange equations. Note that this will not contribute for CP^1. However for higher dimensional models, such as CP^2, it will play an important role.

It now remains to calculate the Lagrange multiplier, λ. This is found by taking the scalar product of equation I.v.4 (after inserting the additional term given above) with z_e and using the constraint, $\mathbf{z}^\dagger\mathbf{z} = 1$. Hence the full equations of motion are given by

$$(1 - \mathbf{z}\mathbf{z}^\dagger)D^\mu D_\mu \mathbf{z} - 2K\epsilon^{\rho\nu\alpha}D_\alpha \mathbf{z}\{(D_\rho \mathbf{z})^\dagger D_\nu \mathbf{z}\} = 0 \qquad \text{(I.v.9)}$$

and its complex conjugate.

II

Conserved Charges

If it looks like a duck, walks like a duck and quacks like a duck, then it probably is a duck. [1]

[1] Senator Bob Dole

II.i Noether's theorem

According to Noether's theorem, all symmetries of the Lagrangian have associated with them a conserved charge [34]. To see this consider the general form of the Lagrangian for a constrained dynamical system,

$$\begin{aligned}\mathcal{L} &= \mathcal{L}(\phi_r, \partial_\mu \phi_r, \lambda_i) \\ &= \mathcal{L}'(\phi_r, \partial_\mu \phi_r) + \lambda_i f_i(\phi_r, \partial_\mu \phi_r)\end{aligned}$$

where for the model under consideration ϕ_r will be $\mathbf{z}$ or its complex conjugate. The functions f_i represent the constraints on the system and λ_i their associated Lagrange multipliers. For CP^n it will be a function of ϕ_r only.

Now add an infinitesimal variation to ϕ_r,

$$\phi_r \rightarrow \phi_r + \delta\phi_r \tag{II.i.1}$$

and the corresponding variation in $\mathcal{L}$ can be shown to be

$$\delta\mathcal{L} = \left(\frac{\partial\mathcal{L}}{\partial\phi_r} - \partial_\mu\left(\frac{\partial\mathcal{L}}{\partial(\partial_\mu\phi_r)}\right)\right)\delta\phi_r + \partial_\mu\left(\frac{\partial\mathcal{L}}{\partial(\partial_\mu\phi_r)}\delta\phi_r\right) + \frac{\partial\mathcal{L}}{\partial\lambda_i}\delta\lambda_i. \tag{II.i.2}$$

The first term is simply the field equations. The constraint in CP^n is unaffected by an $SU(n+1)$ rotation. Therefore the third term will not contribute and hence can be ignored.

If the Lagrangian is invariant under the variation in ϕ_r, then the second term must be zero, and so

$$j_\mu = \text{constant}\left(\frac{\partial\mathcal{L}}{\partial(\partial_\mu\phi_r)}\delta\phi_r\right) \tag{II.i.3}$$

is conserved. The constraints will only contribute to this when they are dependent on the derivatives, which is not the case for the current model.

The constant obviously has no effect on the conservation of the charge and thus can be dropped. Rearranging $\partial_\mu j^\mu$ as

$$\partial_0 j^0 = -\partial_i j^i \tag{II.i.4}$$

and integrating will lead to the conserved charge being defined as

$$Q = \int d^2x \; j_0, \tag{II.i.5}$$

provided j^1 and j^2 vanish on the boundary.

For a complex scalar field with a gauge invariant constraint, the charge density is

$$j_\mu \propto \frac{\partial \mathcal{L}}{\partial(\partial_\mu \mathbf{z})}\delta\mathbf{z} + \delta\mathbf{z}^\dagger \frac{\partial \mathcal{L}}{\partial(\partial_\mu \mathbf{z}^\dagger)} \tag{II.i.6}$$

As mentioned earlier, the constraint $|\mathbf{z}|^2 = 1$ will not contribute to this.

The purpose of this work is to shed some light on the meaning of the Hopf term. It makes no contribution to the energy momentum tensor [31]. Also each term of the contribution to the Euler-Lagrange equations is dependent on time derivatives. Therefore, it will not contribute to these equations when the fields are static and, although this may seem a trivial result, it will prove useful later.

The results of Piette et al [31] suggest that the term can be thought of as an "internal magnetic" field. They also used it to test the validity of the collective coordinate approximation.

In the above derivation the field equations were assumed to be true. There are other more rigorous proofs (see, for example, [19], [23] or [34]), but none as succinct as the above. However it is interesting to note that the equations of motions themselves can be shown to be a consequence of Noether's theorem.

They are obtained by assuming the Lagrangian is invariant under a total variation in the field as before. However an additional constraint is placed by assuming that the variations are restricted to those which vanish on the boundary. For a physical system, this must leave $\mathcal{L}$ unchanged.

The total derivative terms will then be trivially zero and the only term which is left will lead to the Euler-Lagrange Equations. Note, though, that these equations involve terms of the form $\partial\mathcal{L}/\partial\phi_r$ and hence the constraint will affect the result in CP^n.

II.ii Preliminary Calculations

All the calculations to be considered in this thesis have the same form for the denominator when expressed in terms of renormalised fields. Although this is not conserved it will prove useful to consider this term in detail first. The following calculations shall be restricted to CP^2, from which the results for CP^1 can easily be deduced.

It is now necessary to consider the representation used to describe the solitons. Recall from the previous chapter, that the $U(1)$ invariance in the Lagrangian could be used to set the first component of the field $\mathbf{z}$ to unity. Therefore, the term to be considered is of the form

$$d = 1 + |W|^2 + |W^1|^2 \tag{II.ii.1}$$

raised to some power. In most calculations it will be squared.

Using the notation introduced in the previous chapter, the standard ansatz for the complex fields used in the present work is given by

$$\mathbf{f} = \begin{pmatrix} 1 \\ W \\ W^1 \end{pmatrix}, \tag{II.ii.2}$$

where

$$W = \eta \frac{\Pi_{i=1}^{k}(x_+ - a_i)}{\Pi_{j=1}^{l}(x_+ - a_j)}, \tag{II.ii.3}$$

$$x_+ = x + iy, \tag{II.ii.4}$$

and Π represents the multiplication operator. A similar expression exists for W^1.

Two assumptions have been made. Firstly that $l \leq k$ and secondly that none of the factors cancel. It will correspond to the topological charge being k in units of 2π.

For most simulations it is possible to use a simplification. It can be assumed that the denominator and the coefficient η both tend to infinity, whilst their ratio remains finite. In this scenario, the dependency on x_+ is restricted to the numerator.

An additional approximation which can be used is to assume that the ansatz can be expressed in the form

$$\begin{aligned} W &= \rho(x_+^n - a), \\ W^1 &= \mu(x_+^m - b). \end{aligned} \qquad \text{(II.ii.5)}$$

The powers n and m are positive integers and it can be assumed, without loss of generality, that $n \geq m$.

Two solitons are represented by taking n to be two and m to be one. In this particular case, when b is zero and they are well separated, the position of the solitons is approximately given by $\sqrt{a}$.

It is worth emphasizing that this is only an approximation. When the position is calculated numerically (by looking for the location of the maximum of the energy density), there could be a noticeable difference which will increase as they both approach the origin.

In particular, when the solitons pass through each other, the solitons themselves are not well defined. Hence, during this stage of the evolution the position of the individual lumps can not be determined analytically. The trajectory of each soliton can thus only be given subjectively during the actual scattering process.

When the above ansatz is substituted into the denominator, it becomes

$$|f|^2 = 1 + |\rho|^2(r^{2n} + |a|^2 - r^n\Omega_a) + |\mu|^2(r^{2m} + |b|^2 - r^m\Omega_b), \quad \text{(II.ii.6)}$$

where the Ω functions are defined to be

$$\begin{aligned} \Omega_a &= ae^{-in\theta} + \bar{a}e^{in\theta} \\ \Omega_b &= be^{-im\theta} + \bar{b}e^{im\theta}. \end{aligned} \tag{II.ii.7}$$

This is of order $2n$ for large r. Therefore for most calculations, for which $|\mathrm{f}|^2$ is squared, the denominator will be approximately of order r^{4n}. When the Jacobian for converting the integrals to polar coordinates is taken into account, it can be seen that the integrals will diverge if

$$k \geq 2(2n-1), \tag{II.ii.8}$$

where k is the order of the numerator.

Hence, as non trivial conserved charges will be finite, the range of physically relevant values of n and m can be deduced. There will not be a problem at the origin, because of the existence of the constant term in the denominator. So, for example, for two solitons the order of the numerator must be less than six to obtain a finite result.

To proceed further, it is necessary to consider special cases. Firstly, assume that m and n are equal. In this case, the denominator can be simplified to

$$1 + (|\mu|^2 + |\rho|^2)r^{2n} - (|\mu^2|^2\Omega_b + |\rho|^2\Omega_a)r^n + |\mu|^2|b|^2 + |\rho|^2|a|^2 \tag{II.ii.9}$$

To deduce any useful results, either a and b must be assumed to be equal, or b must be zero. In both cases, the above will reduce to an expression of the form

$$A + Br^m \cos 2m\theta + Cr^{2m}, \tag{II.ii.10}$$

where A, B and C are real constants. This is odd in θ and hence, any term in the numerator which is even, for example $\sin 2m\theta$, will trivially integrate to zero over the whole two space.

Now assume that when $n = 2m$ the following relations hold

$$\begin{aligned} \rho &= \lambda^2 \\ \text{and} \qquad \mu &= \sqrt{2}\lambda. \end{aligned} \tag{II.ii.11}$$

Once again, nothing can be deduced for general a and b. However, if b is taken to be zero, then the denominator becomes

$$(1 + |\lambda|^2 r^n)^2 + |\lambda|^2(|a|^2 - r^n \Omega_a) \tag{II.ii.12}$$

Now consider in detail Ω_a. This can be written in the form

$$\Omega_a = (a + \bar{a}) \cos n\theta - i(a - \bar{a}) \sin n\theta \tag{II.ii.13}$$

Therefore, by defining η implicitly using

$$\begin{aligned} \cos\eta &= a + \bar{a} \\ \text{and} \qquad \sin\eta &= i(a - \bar{a}), \end{aligned} \tag{II.ii.14}$$

the omega function reduces to

$$\Omega_a = \cos(n\theta + \eta). \tag{II.ii.15}$$

This, in turn, leads to the obvious change in variables of

$$\begin{aligned} \phi &= \theta - \frac{\eta}{n} \\ \text{and} \qquad s &= |\lambda|^2 r^n. \end{aligned} \tag{II.ii.16}$$

The denominator will now take the form

$$(1 + s)^2 + |\lambda|^2 |a|^2 - s \cos n\theta \tag{II.ii.17}$$

Any term in the numerator which is even in ϕ will trivially integrate to zero. For example, it can be shown that

$$e^{in\theta} \sim 2a \cos n\phi \qquad \text{(II.ii.18)}$$

under integration, where ϕ is as defined in equation II.ii.16.

Before leaving this section, consider the two soliton static model when the lumps are situated at the origin. For general ρ and μ, they will form a ring like structure, as shown in figure II.1.

However, when the two coefficients are expressed in terms of the complex parameter λ defined by equation II.ii.11, then the ansatz corresponds to the two solitons having a single peak at the origin, as in figure II.2.

Also, the parameter λ can initially be taken to be real without loss of generality and this is the ansatz used for the initial conditions in the numerical approximations. It should be noted though, that this coefficient can not be assumed to remain real throughout the predicted evolution.

For most simulations b is initially taken to be zero. Time evolution is simulated by the use of a Galilean boost,

$$a(t) = a(0)(1 - vt)^2 \qquad \text{(II.ii.19)}$$

where v is defined to be the velocity of the solitons. The most general scenario would be to assume that ρ, μ and b are also time dependent.

II.ii. Preliminary Calculations

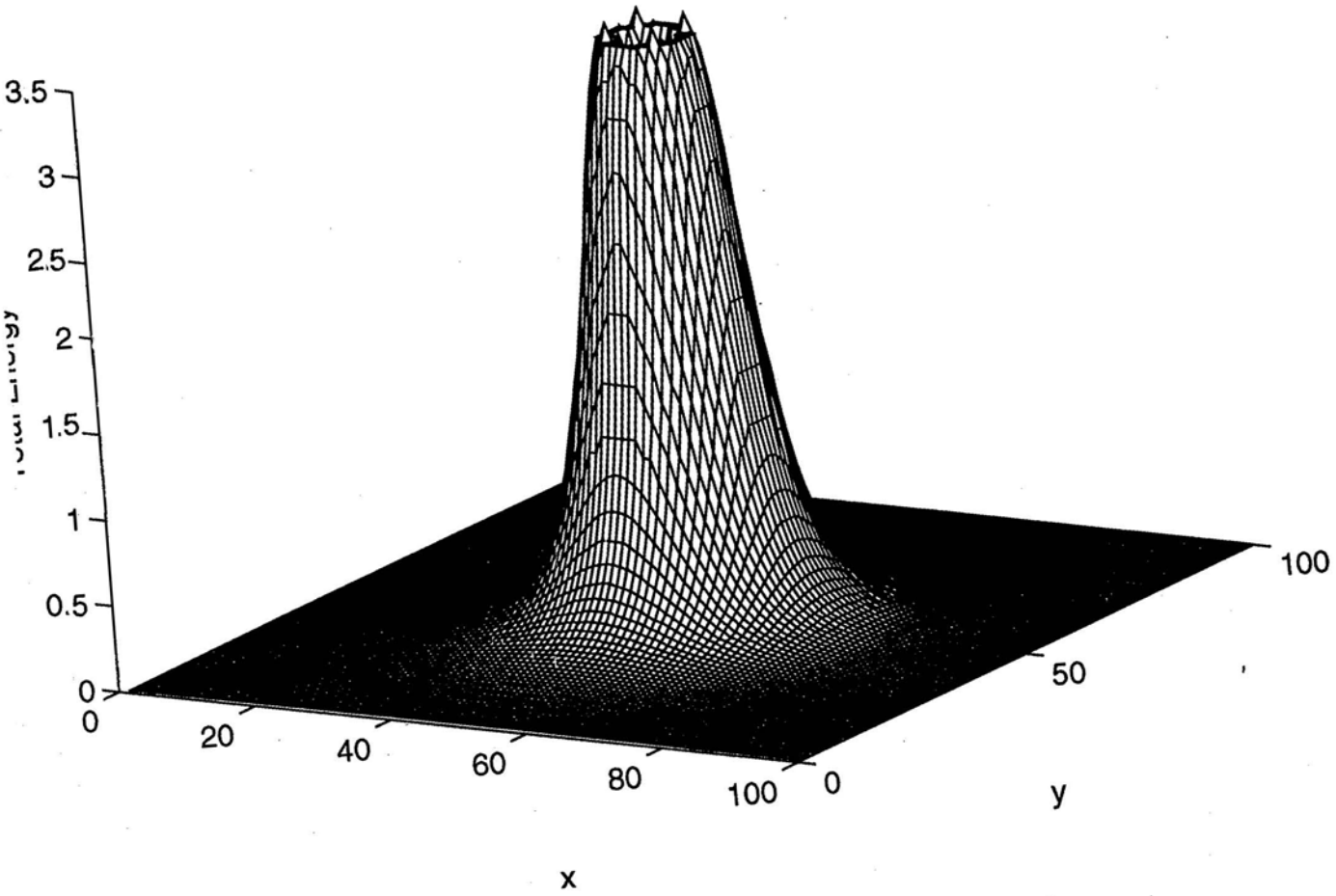

Figure II.1: Two solitons at the origin with general ρ and μ.

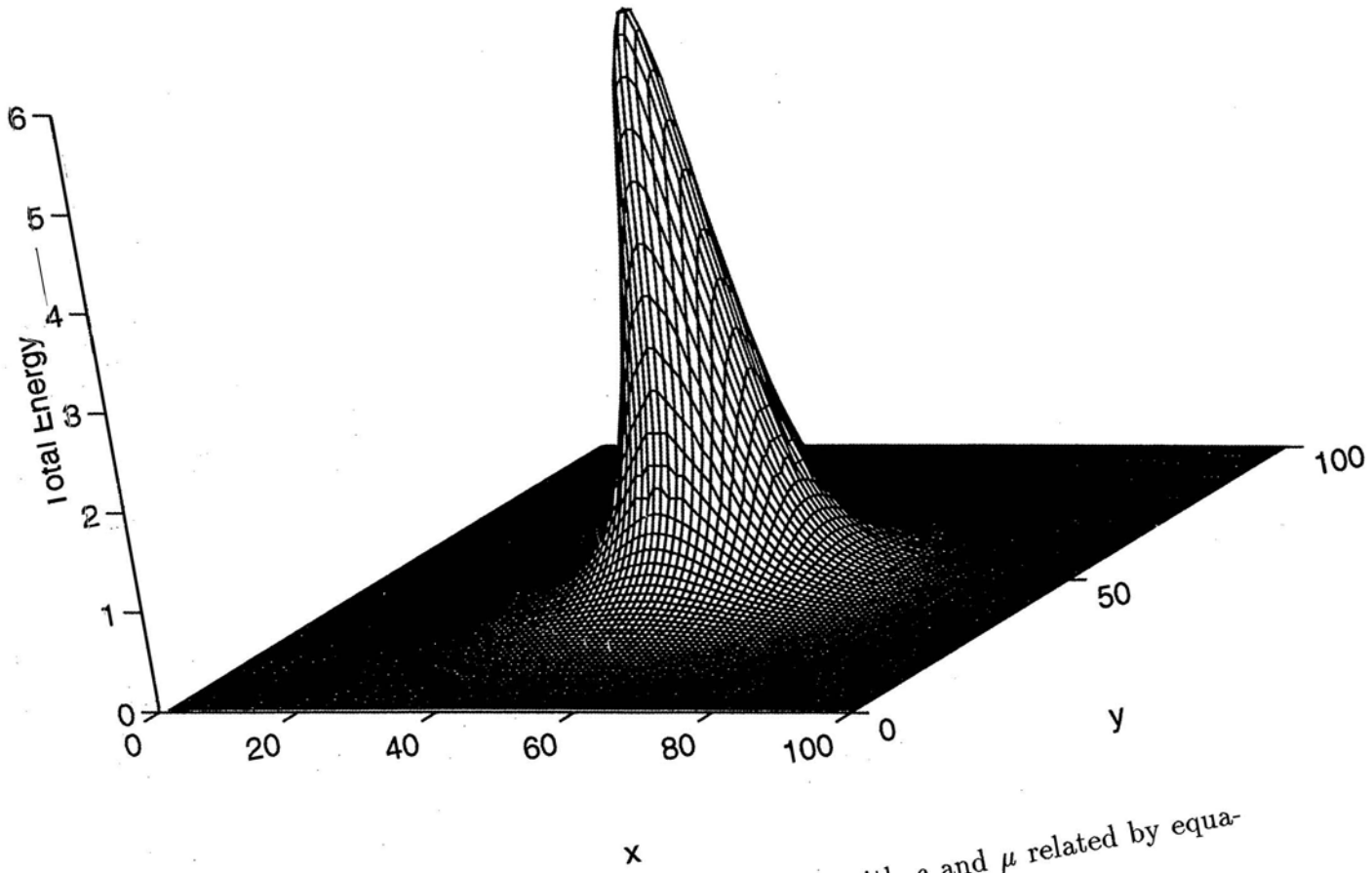

Figure II.2: Two solitons at the origin with ρ and μ related by equation II.ii.11

It is of interest to know, how valid an approximation the boost given by equation II.ii.19 is. In the remainder of this chapter and the next, the charge densities of interest will be calculated for the general case. The expressions will then be given for the programme ansatz. These results will be used in chapter IV to predict the behaviour of the solitons during scattering.

II.iii Energy Momentum Tensor

An important consequence of Noether's theorem is the conservation of the energy momentum tensor and, in particular, the Hamiltonian [34]. Assume invariance under translations and after a few lines of calculation the standard result is obtained

$$T^{\mu}_{\nu} = \frac{\delta \mathcal{L}}{\delta(\partial_{\mu}\mathbf{z})}\partial_{\nu}\mathbf{z} + \partial_{\nu}\mathbf{z}^{\dagger}\frac{\delta \mathcal{L}}{\delta(\partial_{\mu}\mathbf{z}^{\dagger})} - \mathcal{L}\delta^{\mu}_{\nu} \qquad \text{(II.iii.1)}$$

For CP^n, it takes the form:

$$T^{\mu}_{\nu} = (D_{\nu}\mathbf{z})^{\dagger}D^{\mu}\mathbf{z} + (D^{\mu}\mathbf{z})^{\dagger}D_{\nu}\mathbf{z} - \mathcal{L}\delta^{\mu}_{\nu} \qquad \text{(II.iii.2)}$$

and, as discussed in [31], this tensor will receive no contribution from the Hopf term. The energy density, or hamiltonian, is given by T_{00}, and is a conserved charge density. With a Minkowski metric, it is simply:

$$H = (D_0\mathbf{z})^{\dagger}D_0\mathbf{z} + (D_i\mathbf{z})^{\dagger}D_i\mathbf{z}. \qquad \text{(II.iii.3)}$$

Expressed in terms of the analytic functions W and W^1, the hamiltonian becomes

$$H = \frac{1}{|\mathbf{f}|^4}\left\{\overline{W}_{\mu}W_{\mu} + \overline{W}^1_{\mu}W^1_{\mu} + (W^1W_{\mu} - WW^1_{\mu})(\overline{W^1}\overline{W}_{\mu} - \overline{W}\overline{W}^1_{\mu})\right\} \qquad \text{(II.iii.4)}$$

The kinetic energy is given by setting $\mu = 0$ and the potential energy by summing the contributions from when μ equals 1 and μ equals 2.

II.iii.a Kinetic Energy

Substituting for components of the field reduces the numerator of the kinetic energy density to:

$$
\begin{aligned}
T_{\text{num}} &= |\rho_0|^2(r^{2n} + |a|^2 - r^n\Omega_a) + |\rho|^2\ |a_0|^2 \\
&\qquad - \rho a_0\left[\bar{\rho_0}(r^n e^{-in\theta} - \bar{a})\right] - \bar{\rho}\bar{a}_0\left[\rho_0(r^n e^{in\theta} - a)\right] \\
&+ |\mu_0|^2(r^{2m} + |b|^2 - r^m\Omega_b) + |\mu|^2\ |b_0|^2 \\
&\qquad - \mu b_0\left[\bar{\mu_0}(r^m e^{-im\theta} - \bar{b})\right] - \bar{\mu}\bar{b_0}\left[\mu_0(r^m e^{im\theta} - b)\right] \\
&+ |\mu\rho_0 - \mu_0\rho|^2 \Big\{r^{2(m+n)} + r^{2n}|b|^2 + r^{2m}|a|^2 + |ab|^2 \\
&\qquad\qquad + ab\left[r^{m+n}e^{-i(m+n)\theta} - r^n\bar{b}e^{-in\theta} - r^m\bar{a}e^{-im\theta}\right] \\
&\qquad\qquad + \bar{a}\bar{b}\left[r^{m+n}e^{i(m+n)\theta} - r^n be^{in\theta} - r^m ae^{im\theta}\right] \\
&\qquad\qquad - r^{m+2n}\Omega_a - r^{2m+n}\Omega_b - r^{n+m}\Omega_{ab})\Big\} \\
&+ |\mu\rho|^2\Big\{|a_0|^2(r^{2m} + |b|^2 - r^m\Omega_b) - |b_0|^2(r^{2n} + |a|^2 - r^n\Omega_a) \\
&\qquad - \bar{a}_0 b_0\left[r^{n+m}e^{-i(m-n)\theta} + a\bar{b} - r^m ae^{-im\theta} - r^n\bar{b}e^{in\theta}\right] \\
&\qquad - a_0\bar{b}_0\left[r^{n+m}e^{i(m-n)\theta} + \bar{a}b - r^m\bar{a}e^{im\theta} - r^n be^{-in\theta}\right]\Big\} \\
&- \Big\{\left(|\mu|^2\bar{\rho}\rho_t - |\rho|^2\bar{\mu}\mu_t\right)\Big[\bar{a}_t\Big(r^{n+2m}e^{in\theta} + r^m e^{-im\theta}ab - ar^{2m} \\
&\qquad\qquad - br^{n+m}e^{i(n-m)\theta} - \bar{b}r^{n+m}e^{i(n+m)\theta} + a|b|^2 \\
&\qquad\qquad - a\bar{b}r^m e^{im\theta} - |b^2|^2 r^n e^{in\theta}\Big) \\
&\qquad\qquad \bar{b}_t\Big(r^{m+2n}e^{im\theta} + r^n e^{-in\theta}ba - br^{2n} \\
&\qquad\qquad - ar^{m+n}e^{i(m-n)\theta} - \bar{a}r^{m+n}e^{i(m+n)\theta} + b|a|^2 \\
&\qquad\qquad - b\bar{a}r^n e^{in\theta} - |a^2|^2 r^m e^{im\theta}\Big)\Big] \\
&\qquad + \text{complex conjugate}\Big\}
\end{aligned}
\tag{II.iii.5}
$$

where the additional Ω function is defined to be

$$\Omega_{ab} = a\bar{b}e^{i(m-n)\theta} + \bar{a}be^{i(m-n)\theta} \qquad \text{(II.iii.6)}$$

It is known that the total energy is conserved and will not diverge. For large values of r the numerator is clearly of order $2(n+m)$. Therefore by using the test given in equation II.ii.8 it is clear that T will only be finite when $n-m \geq 1$. This does not place much constraint because of the assumption that m is not larger than n, but it does imply that the ansatz used within the programme will lead to a divergence.

However, it can be clearly seen that, except for the special case when m and n are equal to one, the divergent terms arise from the time dependency of μ and ρ. If these are taken to be constant, then the kinetic energy will be finite for all n as it reduces to:

$$\begin{aligned} T_{\text{num}} = \frac{1}{|f|^4}\Big\{ & |\mu\rho|^2\Big[|a_t|^2(r^{2m}+|b|^2-r^m\Omega_b)+|b_t|^2(r^{2n}+|a|^2-r^n\Omega_a) \\ & -a_t\bar{b}_t(r^{n+m}e^{i(m-n)\theta}-r^nbe^{-in\theta}-r^m\bar{a}e^{im\theta}+\bar{a}b) \\ & -\bar{a}_tb_t(r^{n+m}e^{-im-n\theta}-r^n\bar{b}e^{in\theta}-r^mae^{-im\theta}+a\bar{b})\Big] \\ & +|\rho|^2|a_t|^2+|\mu|^2|b_t|^2\Big\} \end{aligned} \qquad \text{(II.iii.7)}$$

The order of the numerator is now $2n$ and hence if ρ and μ are constant throughout the evolution, then the kinetic energy will be finite for all $n > 1$, for any value of m.

It would thus appear to be reasonable to take λ to be initially constant in equation II.ii.11 when considering scattering. For completeness, the kinetic energy will be given below for this ansatz

$$T_{\text{num}} = \frac{|\lambda|^4}{|f|^4}|a_t|^2(1+2|\lambda|^2r^2) \qquad \text{(II.iii.8)}$$

When m and n are both one, then there exists other infinite terms in the expression which are proportional to the derivative of the parameter a. Therefore, for the kinetic energy to be finite it is necessary for these divergences to cancel. Hence for this single soliton ansatz, it is necessary for the parameters ρ and μ to remain time dependent.

II.iii.b Potential Energy

The numerator for the potential energy density is given by:

$$\begin{aligned} V_{\text{num}}=2\Big\{ & |\rho|^2 n^2 r^{2(n-1)} + m^2|\mu|^2 r^{2(m-1)} \\ + \quad & |\rho\mu|^2 \Big[n^2 r^{2(n-1)}(r^{2m} + |b|^2 - r^m \Omega_b) \\ & + m^2 r^{2(m-1)}(r^{2n} + |a|^2 - r^n \Omega_a) \\ & - nm r^{n+m-2}(2r^{n+m} + \Omega_{ab} - r^m \Omega_a - r^n \Omega_b)\Big]\Big\} \end{aligned} \tag{II.iii.9}$$

and the denominator is the same as for the kinetic energy. The order of V is $2(m+n-1)$ and thus is clearly finite for all n greater than one.

For completeness, this will also be given in terms of the simpler ansatz with b equal to zero

$$V = \frac{4|\lambda|^2}{|f|^4}\left((1+|\lambda|^2 r^2)^2 + |\lambda|^4|a|^2 + |\lambda|^2 r^2 \Omega_a\right) \tag{II.iii.10}$$

When m and n are equal both to one, it can be shown that the divergences cancel if ρ is also equal to μ. The numerator simplifies to

$$V = 2|\lambda|^2(2 + |\lambda|^2|a|^2), \tag{II.iii.11}$$

which is clearly finite.

II.iii.c Angular Momentum

The angular momentum will now be considered. It was mentioned in the previous chapter that the angular momentum is not well defined in two dimensions. Therefore as before, the standard definition for three dimensions will be utilised by using the time dimension as a means to overcome the ambiguity.

The following derivation was taken from [34]. The action for a physical system must be invariant under spatial rotations. If the Lagrangian is defined to be a function of $\phi(x_i)$, then this corresponds to the variations

$$\begin{aligned} \delta x^i &= \epsilon^{ij} x^j \\ \text{and} \qquad \delta\phi &= 0. \end{aligned} \tag{II.iii.12}$$

Furthermore, as the rotation group is a subgroup of the Lorentz group [5], this can be generalised by replacing the roman indices with greek indices.

For a symmetric hamiltonian, this will lead to the definition of the angular momentum used in the model under consideration.

$$M = \int d^2x \, \left(T^{0i} x^j - T^{0j} x^i \right) \tag{II.iii.13}$$

and after a few lines of calculations it can be shown that for the current model this will give the following expression for the integrand of M

$$\begin{aligned} M &= \frac{1}{|\mathbf{f}|^2} \left(\partial_\theta \mathbf{f}^\dagger \partial_t \mathbf{f} + \partial_t \mathbf{f}^\dagger \partial_\theta \mathbf{f} \right) \\ &- \frac{1}{|\mathbf{f}|^4} \left(\partial_t \mathbf{f}^\dagger \mathbf{f} \; \mathbf{f}^\dagger \partial_\theta \mathbf{f} + \partial_\theta \mathbf{f}^\dagger \mathbf{f} \; \mathbf{f}^\dagger \partial_t \mathbf{f} \right). \end{aligned} \tag{II.iii.14}$$

When expressed in terms of the components of $\mathbf{f}$, it simplifies to:

$$\begin{aligned} M &= \frac{1}{|\mathbf{f}|^4}\Big\{W_\theta \overline{W}^1_t \overline{W} W^1 + W^1_t \overline{W}_\theta \overline{W}^1 W \\ &\quad + W^1_\theta \overline{W}_t \overline{W}^1 W + W_t \overline{W^1}_\theta \overline{W} W^1 \\ &\quad - (1+|W^1|^2)(\overline{W}_t W_\theta + \overline{W}_\theta W_t) \\ &\quad - (1+|W|^2)(\overline{W^1}_t W^1_\theta + \overline{W}^1_\theta W^1_t)\Big\}. \end{aligned} \qquad \text{(II.iii.15)}$$

Substituting for W and W^1 results in the angular momentum being expressed as

$$M = \frac{2i\mathrm{Im}(A)}{|\mathbf{f}|^4} \qquad \text{(II.iii.16)}$$

where

$$\begin{aligned} A &= \mu\bar{\mu}_0\Big\{n|\rho|^2 r^n\Big[r^{n+2m} - r^{n+m}\Omega_b - r^n \bar{a} e^{in\theta} + r^n|b|^2 \\ &\qquad + r^m(\bar{a}b e^{-i(m-n)\theta} + \bar{a}\bar{b}e^{i(m+n)\theta}) - \bar{a}|b|^2 e^{in\theta}\Big] \\ &\qquad + [1+|\rho|^2(r^{2n}+|a|^2 - r^n\Omega_a)][mr^{2m} + r^m \bar{b} e^{im\theta}]\Big\} \\ &+ \rho\bar{\rho}_0\Big\{m|\mu^2|r^m\Big[r^{2n+m} - r^{n+m}\Omega_a - r^m \bar{b} e^{im\theta} + r^m|a|^2 \\ &\qquad + r^n(a\bar{b}e^{i(m-n)\theta} + \bar{a}\bar{b}e^{i(n+m)\theta}) - \bar{b}|a|^2 e^{im\theta}\Big] \\ &\qquad + [1+|\mu|^2(r^{2m}+|b|^2 - r^m\Omega_b)][nr^{2n} + r^n \bar{a} e^{in\theta}]\Big\} \\ &+ a_0\Big\{m|\mu|^2|\rho|^2\Big[r^{n+2m}e^{-in\theta} + \bar{a}br^m e^{-im\theta} - r^{2m}\bar{a} - r^{n+m}be^{-i(n+m)\theta}\Big] \\ &\qquad - [1+|\mu|^2(r^{2m}+|b|^2 - r^m\Omega_b)]|\rho|^2 nr^n e^{-in\theta}\Big\} \\ &+ b_0\Big\{n|\mu|^2|\rho|^2\Big[r^{2n+m}e^{-im\theta} + a\bar{b}r^n e^{-in\theta} - r^{2n}\bar{b} - r^{n+m}ae^{-i(n+m)\theta}\Big] \\ &\qquad - [1+|\rho|^2(r^{2n}+|a|^2 - r^n\Omega_a)]|\mu|^2 mr^m e^{-im\theta}\Big\} \end{aligned} \qquad \text{(II.iii.17)}$$

The order of this is the same as for the kinetic energy numerator, $2(m+n)$, and hence it will diverge for the same range of values. How-

ever, once again the problem is circumvented if ρ and μ are assumed to be constant.

In this case, the order is $m-2n$ and hence the angular momentum will now be finite for n greater than one, if m is zero or one. The expression will reduce to

$$\begin{aligned} A &= a_0\Big\{m|\mu|^2|\rho|^2\Big[r^{n+2m}e^{-in\theta}+\bar{a}br^m e^{-im\theta}-r^{2m}\bar{a}-r^{n+m}be^{-i(n+m)\theta}\Big] \\ &\qquad -[1+|\mu|^2(r^{2m}+|b|^2-r^m\Omega_b)]|\rho|^2 nr^n e^{-in\theta}\Big\} \\ &+ b_0\Big\{n|\mu|^2|\rho|^2\Big[r^{2n+m}e^{-im\theta}+a\bar{b}r^n e^{-in\theta}-r^{2n}\bar{b}-r^{n+m}ae^{-i(n+m)\theta}\Big] \\ &\qquad -[1+|\rho|^2(r^{2n}+|a|^2-r^n\Omega_a)]|\mu|^2 mr^m e^{-im\theta}\Big\} \qquad \text{(II.iii.18)} \end{aligned}$$

The simplified expression for the ansatz used in the simulations is given below

$$\begin{aligned} M &= \frac{i}{|\mathbf{f}|^4}2a_0\Big\{|\lambda|^6\Big[r^4e^{-i2\theta}-r^2\bar{a}\Big]-2\Big[1+2|\lambda|^2r^2\Big]|\lambda|^4r^2e^{-i2\theta} \\ &\qquad -\text{complex conjugate}\Big\}. \qquad \text{(II.iii.19)} \end{aligned}$$

Expressed in terms of the new variables this becomes

$$M=\frac{i}{|\mathbf{f}|^4}|\lambda|^2\Big\{a_0\bar{a}\Big[s^2e^{-i2\phi}-s|\lambda|^2\Big]-2[1+2s]se^{-i2\phi}-\text{c.c.}\Big\} \qquad \text{(II.iii.20)}$$

Now consider the case when m and n are both unity. There will be divergent terms arising from the coefficients of a_0 as well as from ρ_0 and μ_0. Therefore the angular momentum can only be finite when both a and the coefficients of x_+ are time dependent. This confirms the earlier conclusion deduced from the calculation of the kinetic energy.

II.iv Summary

After a brief review of Noether's theorem, it was shown that it was reasonable to use the following simplified ansatz for the field components,

$$\begin{aligned} W &= \rho(x_+^n - a), \\ W^1 &= \mu(x_+^m - b) \end{aligned}$$

This thesis is primarily concerned with scattering and hence for most of the work m is taken to be one whilst n is assumed to be 2. The coefficients ρ and μ are chosen so as to ensure that when the two solitons are both located at the origin, they will have a single peak when b is zero.

The last section of this chapter considered the energy momentum tensor. It was shown that when n is less than three, then both the kinetic energy and the angular momentum will diverge.

For the two soliton ansatz, this problem is resolved by assuming that ρ and μ are both constant. In this scenario, both these conserved quantities will be finite.

For the single soliton model the converse is true. The quantities can only be finite if all four (three, if b is taken to be zero) complex parameters are time dependent. If ρ and μ are constant, then the resultant charges will be divergent.

III

Charges Arising From The Internal Symmetry

Three's the magic number,
not one nor two but three.
Three's the magic number. [1]

[1] De La Soul

III.i Introduction

In the last chapter it was shown that every symmetry of the Lagrangian has associated with it a conserved charge. The CP^n sigma models under consideration have associated with them a global $SU(n+1)$ symmetry. There will thus be a set of charges corresponding to this internal symmetry.

CP^1 will have three conserved quantities whilst CP^2 shall have eight. They are obtained from the following generators of the complex projective space

$$\begin{aligned} \delta z &= \frac{i\lambda^\gamma}{2}\epsilon_\gamma z \\ \delta z^\dagger &= -z^\dagger\frac{i\lambda^\gamma}{2}\epsilon_\gamma \end{aligned} \qquad \text{(III.i.1)}$$

where ϵ_γ is infinitesimal.

In the simpler CP^1 model, the Pauli matrices give a suitable representation for the gamma matrices. In CP^2 the Gell-Mann-Low matrices will be used,

$$\lambda^1 = \begin{pmatrix} 0 & 1 & 0 \\ 1 & 0 & 0 \\ 0 & 0 & 0 \end{pmatrix} \quad \lambda^2 = \begin{pmatrix} 0 & -i & 0 \\ i & 0 & 0 \\ 0 & 0 & 0 \end{pmatrix}$$

$$\lambda^3 = \begin{pmatrix} 1 & 0 & 0 \\ 0 & -1 & 0 \\ 0 & 0 & 0 \end{pmatrix} \quad \lambda^4 = \begin{pmatrix} 0 & 0 & 1 \\ 0 & 0 & 0 \\ 1 & 0 & 0 \end{pmatrix}$$

$$\lambda^5 = \begin{pmatrix} 0 & 0 & -i \\ 0 & 0 & 0 \\ i & 0 & 0 \end{pmatrix} \quad \lambda^6 = \begin{pmatrix} 0 & 0 & 0 \\ 0 & 0 & 1 \\ 0 & 1 & 0 \end{pmatrix}$$

$$\lambda^7 = \begin{pmatrix} 0 & 0 & 0 \\ 0 & 0 & -i \\ 0 & i & 0 \end{pmatrix} \quad \lambda^8 = \begin{pmatrix} 1 & 0 & 0 \\ 0 & 1 & 0 \\ 0 & 0 & -2 \end{pmatrix} \qquad \text{(III.i.2)}$$

where λ^8 has an additional normalisation factor $1/\sqrt{3}$. However, because the charges are only defined up to an overall arbitrary constant, normalisations factors such as these, and the halves given in equation III.i.1, can be ignored.

By using equation I.v.2, it can be shown that for general λ^γ, the charge density can be split into the following two components

$$\begin{aligned} j_0^0 &= i\left(\partial_0 \mathbf{z}^\dagger \lambda^\gamma \mathbf{z} - \mathbf{z}^\dagger \lambda^\gamma \partial_0 \mathbf{z} + 2(\mathbf{z}^\dagger \partial_0 \mathbf{z}) \mathbf{z}^\dagger \lambda^\gamma \mathbf{z}\right) \\ j_0^H &= iK\epsilon^{\nu\alpha}\left(\partial_\nu \mathbf{z}^\dagger \partial_\alpha \mathbf{z}\ \mathbf{z}^\dagger \lambda^\gamma \mathbf{z} - \mathbf{z}^\dagger \partial_\alpha \mathbf{z}\ \partial_\nu (\mathbf{z}^\dagger \lambda^\gamma \mathbf{z})\right) \end{aligned} \quad \text{(III.i.3)}$$

Six of the charges can be regarded as being pairs. They are $[Q_1, Q_2]$, $[Q_4, Q_5]$ and $[Q_6, Q_7]$. This can be deduced from the form of the Gell-Mann-Low matrices given on the previous page. Each element of a pair will correspond to the real and imaginary components of a covering function.

Furthermore, the first pair is related to the second by interchanging W and W^1 in the expressions. Hence the second pair can be deduced from Q_1. These links reduce the amount of calculations which need to be performed to four.

It can be shown explicitly that the sum of j^0 and j^H will be conserved on integration. Consider first taking the time derivative of the contribution from the pure CP^2 Lagrangian

$$\partial_0 j_0^0 = i\left[\partial_0^2 \mathbf{z}^\dagger \lambda^\gamma \mathbf{z} - \mathbf{z}^\dagger \lambda^\gamma \partial_0^2 \mathbf{z} + 2\left\{\partial_0(\mathbf{z}^\dagger \partial_0 \mathbf{z}) \mathbf{z}^\dagger \lambda^\gamma \mathbf{z} + (\mathbf{z}^\dagger \partial_0 \mathbf{z}) \partial_0 (\mathbf{z}^\dagger \lambda^\gamma \mathbf{z})\right\}\right] \quad \text{(III.i.4)}$$

Now substitute for the second derivative using the equation of motion. The Lagrange multiplier will not be explicitly given, as it will make the calculation easier to read. Once the Euler-Lagrange equation

has been rearranged into the form

$$\begin{aligned}\partial_0^2\mathbf{z} &= \lambda\mathbf{z} + \partial_0(\mathbf{z}^\dagger\partial_0\mathbf{z}) + 2(\mathbf{z}^\dagger\partial_0\mathbf{z})\partial_0\mathbf{z} - (\mathbf{z}^\dagger\partial_0\mathbf{z})(\mathbf{z}^\dagger\partial_0\mathbf{z})\mathbf{z} \\ &+ D_i D^i\mathbf{z} \\ &+ 2Ki\epsilon^{\mu\nu\alpha}\left\{(D_\mu\mathbf{z})^\dagger D_\nu\mathbf{z}\right\}(D_\rho\mathbf{z})^\dagger, \qquad \text{(III.i.5)}\end{aligned}$$

the substitution becomes clear.

After a few lines of calculation, it is possible to show that the terms on the first line of the right hand side of the above equation will cancel the other terms in equation III.i.4. It thus only remains to consider the effect of the other two contributions.

The second term in equation III.i.5 can be expressed in terms of a total divergence. It can be shown that this will vanish due to the action being finite. Therefore, it has been confirmed that the charges will converge for pure CP^2.

Now consider the effect of switching on the Hopf term, which corresponds to the third term given above. This can be shown to reduce to

$$-\partial_0 j_0^H + \text{surface integral terms.} \qquad \text{(III.i.6)}$$

For the ansatz under consideration, the surface integral can easily be shown to vanish.

Therefore, on integration of these charge densities, it becomes clear that

$$\partial_0 Q^0 = -\partial_0 Q^H. \qquad \text{(III.i.7)}$$

In other words, the total charge will be conserved, but there is no reason to believe that Q^0 and Q^H will be individually conserved.

III.ii Numerical Predictions

III.ii.a CP^1

The simpler CP^1 model will be considered first. There will only be three conserved charges. However, the simulations for this model were run using the CP^2 simulation codes, with W^1 being identically zero. Hence eight quantities were calculated.

Now consider the contribution to the first three charges from the pure CP^1 part of the Lagrangian. The first two, as predicted in the previous section, behaved like the real and imaginary component of a covering function.

In particular, when a was real, Q_1 was finite whilst Q_2 was zero. This can be seen in figure III.1. It was confirmed numerically that they were approximately proportional to the real and imaginary component of the velocity respectively.

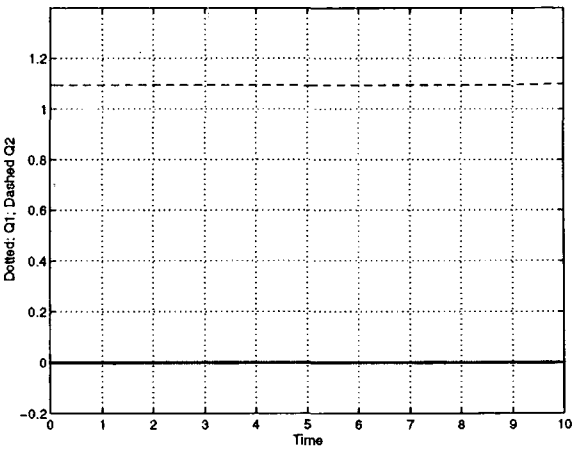

Figure III.1: Q_1 and Q_2 for CP^1 when $Q^{TOP} = 2$

The third charge was also numerically shown to be zero. All the terms in the remaining five charges involved the third component of the CP^2 field and hence need not be considered for this reduced phase space.

As mentioned in the introduction to this chapter, the Hopf term will be a total divergence in this scenario and hence will not contribute to the classical equations of motion. It was therefore expected that the charge density coming from the Hopf term would have no meaning and hence unlikely to be conserved. However, it was found that for two of the charges, the contributions from the Hopf term were conserved, see figure III.2.

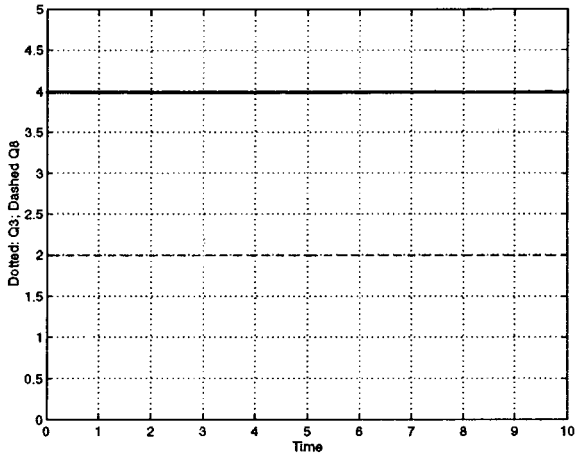

Figure III.2: Q_3^H and Q_8^H for CP^1 when $Q^{TOP} = 2$

It was also noticed that the ratio of these two unexpected conserved charges was integral. As the Hopf term should not introduce any new conserved quantities into the model, these charges had to be proportional to an existing charge. The most likely candidate for this rôle would be the topological charge.

III.ii.b CP^2

Several numerical simulations were performed for various values of the input parameters, from which the following table was compiled.

Charge	CP^2	CP^2+ Hopf term
Q_1	$\propto Im$(velocity)	indirectly $\propto$ velocity
Q_2	$\propto Re$(velocity)	indirectly $\propto$ velocity
Q_3	zero	$\propto$ topological charge
Q_4		zero
Q_5		zero
Q_6		zero
Q_7		zero
Q_8	zero	$\propto$ topological charge

List of SU(3) Hopf Charges

The nontrivial charges for a typical value of K are shown in figures III.3 and III.4. The initial velocity for this evolution was low, $v = 0.1$ and the grid size was set to be ± 12 in both spatial coordinates.

To show the effect of the velocity on the first two charges, they are plotted in figure III.5 for a higher velocity, $v = 0.5$. All other parameters are set to be the same so as to emphasise the dependency on this initial boost.

Finally, for completeness, the sole non trivial charges for pure CP^2 when the initial velocity is real (in this case $v = 0.2$) is shown in figure III.6. This was calculated from a smaller grid (± 8 in each direction).

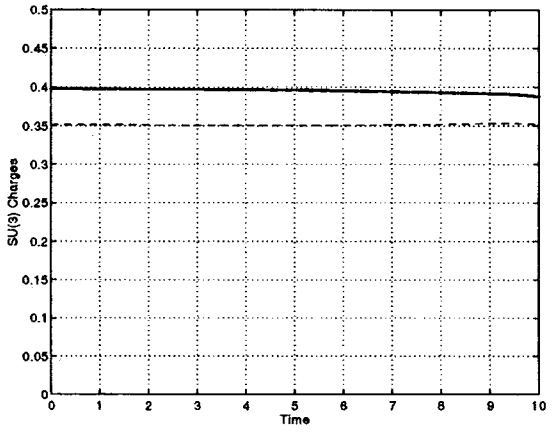

Figure III.3: Q_1 (solid) and Q_2 (dashed) for CP^2 when $K = 1$ with a low initial velocity

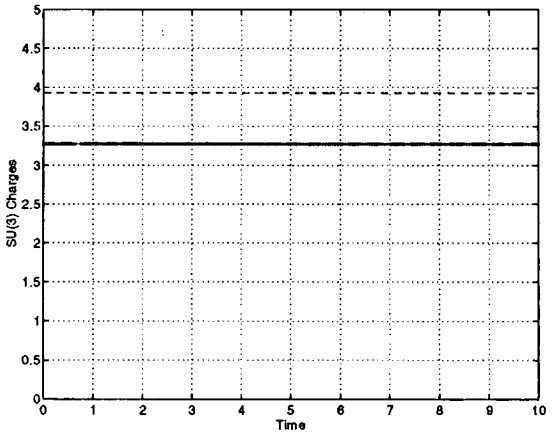

Figure III.4: Q_3 (solid) and Q_8 (dashed) for CP^2 when $K = 1$ with a low initial velocity

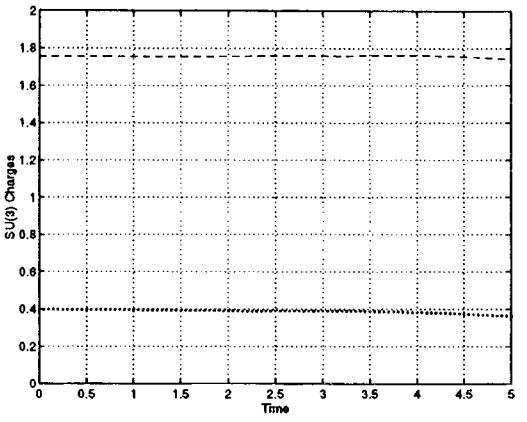

Figure III.5: Q_1 (solid) and Q_2 (dashed) for CP^2 when $K = 1$ with an high initial velocity

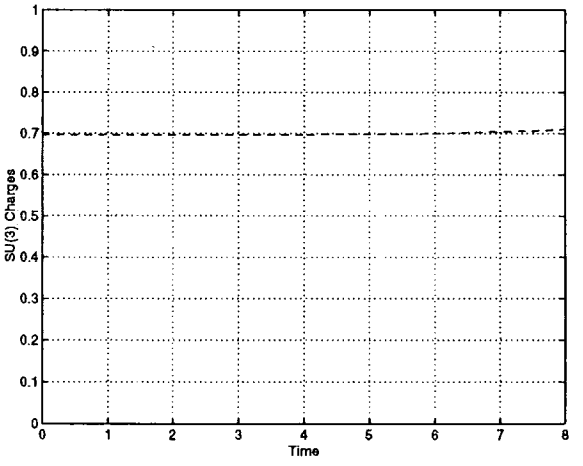

Figure III.6: Q_2 for pure CP^2 when the initial velocity is real

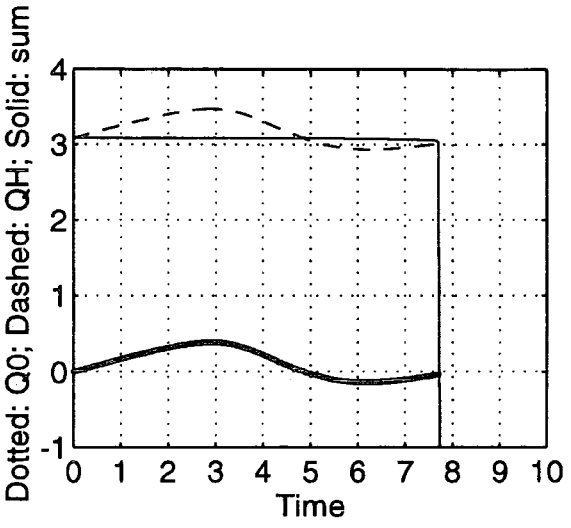

Figure III.7: Component of Q_3 during scattering for two solitons with $K = 1$

When the Hopf term was added, Q_1 and Q_2 have a small additional contribution which is independent of the velocity. It was also confirmed that Q^0 and Q^H are not conserved separately unless $K = 0$ (see, for example, figure III.7: larger grid, $v = 0.2$). These results can be confirmed analytically for two static solitons placed at the origin.

Hence, to summarise. The internal symmetry gives rise to four nontrivial charges. Of these, Q_1 and Q_2 are also nontrivial for pure CP^2 (with the proviso that Q_2 is zero when the initial velocity is real). The remaining two, Q_3 and Q_8, are of the most interest. This pair only arise when the additional term is switched on in the full model. They are independent of the initial velocity which would suggest the possibility of a link with the topological charge.

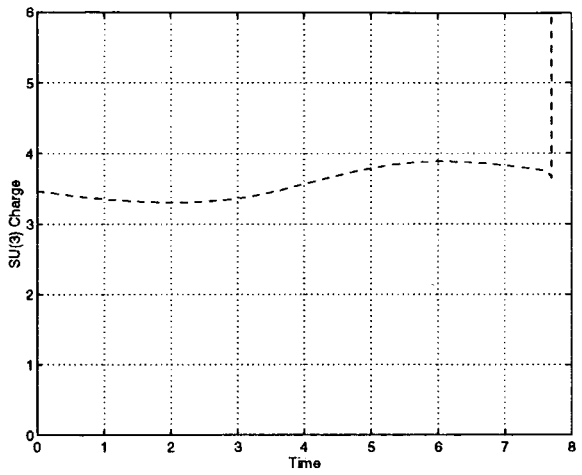

Figure III.8: Q_8 charge when boundary is at ± 8

It was noticeable that Q_8 was much more sensitive to the boundary conditions. If the boundary was cut off too close to the solitons, the charge conservation was noticeably affected (see figure III.8. In figure III.3 the boundary was at $r = 12$). This is probably due to it being a more complicated expression. Q_1 and Q_2 are also affected by the boundary, but they are still approximately conserved for such an abrupt cut-off.

The boundary should obviously be at infinity, but this causes computational problems and hence an approximation of some form must be used. For most purposes, it is sufficient to approximate the plane with a finite grid because of the nature of the field distribution. It was believed that the errors this brought in would be insignificant.

To test this hypothesis, that the errors produced by a finite boundary are minimal, some calculations were performed on a pseudo infinite grid. This was created by using the map

$$m = \frac{Sx}{1 + S|x|} \tag{III.ii.1}$$

with a similar map for y. It maps zero to zero and infinity to one. The coefficient S is simply a scale factor.

Although there still had to be a cutoff (as there would be problems with the upper boundary value, $m = 1$) it enabled a much larger grid in real space to be used without introducing excessive computational time. The results from these simulations confirmed the validity of the cruder approximation. Hence the simpler method was used as it was able to run significantly faster.

III.iii Explicit Calculations of Charges

III.iii.a Q_1 and Q_2

Consider Q_1 for pure CP^2. The charge density will be:

$$\begin{aligned} j_1^0 &= \frac{1}{|\mathbf{f}|^2}(\overline{W}_0 - W_0) \\ &+ \frac{1}{|\mathbf{f}|^4}(\mathbf{f}^\dagger\partial_0\mathbf{f} - \partial_0\mathbf{f}^\dagger\mathbf{f})(W + \bar{W}) \end{aligned} \tag{III.iii.1}$$

After a few lines of calculations to combine the two terms, the numerator of the charge density can be shown to be

$$\begin{aligned} i\Big\{&\overline{W}_0(1 - WW + |W^1|^2) - W_0(1 - \overline{WW} + |W^1|^2) \\ &-(W + \overline{W})(\overline{W}^1 W_0^1 - \overline{W}_0^1 W^1)\Big\} \end{aligned} \tag{III.iii.2}$$

Substituting the general anatz for the fields and combining the terms, the numerator becomes the real component of the following

$$\begin{aligned} 2i\Big\{&\Big[\bar{\rho}_0(r^n e^{-in\theta} - \bar{a}) - \bar{\rho}\bar{a}_t)\Big]\Big[1 - \rho^2(r^{2n}e^{i2n\theta} - 2are^{in\theta} + a^2) \\ &+|\mu|^2(r^{2m} + |b|^2 - r^m\Omega_b)\Big] \\ &-\Big[(\bar{\mu}\mu_0 - \bar{\mu}_0\mu)(r^{2m} + |b|^2 - r^m\Omega_b) \\ &-(b_0 e^{-im\theta} - \bar{b}_0 e^{im\theta})r^m|\mu|^2 - (b_0\bar{b} - \bar{t}_0 b)\Big] \\ &\Big[r^n(\bar{\rho}e^{-in\theta} + \rho e^{in\theta}) - \bar{\rho}\bar{a} + \rho a\Big]\Big\} \end{aligned} \tag{III.iii.3}$$

The order of this expression is $3n$ and therefore, by using the formula deduced in the last chapter it can be seen that this will diverge for n less than or equal to two.

Consider the two cases separately, and initially take n to be two. From this it follows that m must be one or two, as it has been assumed that the order of W^1 is less than or equal to the order of W.

Once again, it is necessary to assume that ρ and μ are constant to ensure the numerator of the charge density is finite. When m is one, it will reduce to the real component of

$$2i\Big\{\bar{\rho}\bar{a}_0\Big[1-\rho^2(r^4e^{i4\theta}-2ar^2e^{i2\theta}+a^2)-|\mu|^2(r^2+|b|^2-r\Omega_b)\Big] +\Big[(b_0e^{-i\theta}-\bar{b}_0e^{i\theta}r)|\mu|^2r+(b_0\bar{b}-\bar{b}_0b)\Big] \Big[r^2(\bar{\rho}e^{-2\theta}+\rho e^{-2\theta})-(\bar{\rho}\bar{a}+\rho a)\Big]\Big\} \quad \text{(III.iii.4)}$$

This will be of order 4 and hence the charge Q_1^0 will be finite in this scenario. It can similarly be shown, that the equivalent expression for when m is also equal to two will be finite.

Now consider the ansatz used in the programme. The numerator of the charge density simplifies to be the real part of

$$2\Big\{\bar{\lambda}^2\bar{a}_0[1-\lambda^4(2r^4\cos 4\theta-4ar^2\cos 2\theta+a^2)-2\lambda r^2]\Big\} \quad \text{(III.iii.5)}$$

This will be proportional to the time derivative of a, which is usually taken to be the velocity of the solitons.

For small λ, it will be approximately proportional to the imaginary component of the velocity. This can be confirmed analytically when a is zero, as all the terms involving trigonometric functions will trivially vanish on integration in this particular case.

Unfortunately, it is not possible to integrate analytically for non-trivial a. However, this does confirm the numerical results for pure CP^2 as the charge will be independent of the initial value of this parameter.

When m and n are both unity, there will be two divergences in the charge density. One of these is the coefficient of the time derivative of ρ, as above, but the other is multiplied by the a_0. These will have to cancel each other for the charge to be finite. Hence, it confirms the requirement for the coefficients of x_+ in the single soliton ansatz to be time dependent.

Now consider the Hopf contribution to the charge density which will be, in terms of the renormalised fields,

$$j_1^H = K\epsilon^{\mu\nu}\frac{1}{|\mathbf{f}|^4}\Big\{(W+\overline{W})\partial_\mu(\mathbf{f}^\dagger\partial_\nu\mathbf{f}) \\ -\tfrac{1}{2}\partial_\nu(W+\overline{W})(\mathbf{f}^\dagger\partial_\mu\mathbf{f}-\partial_\mu\mathbf{f}^\dagger\mathbf{f})\Big\}. \qquad \text{(III.iii.6)}$$

It is now simply a matter of substituting for the components of $\mathbf{f}$ using the standard ansatz. After some elementary algebra, this will result in

$$\begin{aligned} j_1^H &= -\frac{K}{|\mathbf{f}|^4}\Big\{\left[n^2|\rho|^2r^{2(n-1)}+2m^2|\mu|^2r^{2(m-1)}\right] \\ &\qquad \left[r^n(\rho e^{in\theta}+\bar{\rho}e^{-in\theta})-(\rho a+\bar{\rho}\bar{a})\right] \\ &\quad -nmr^{n+m-2}|\mu|^2\left[\rho e^{im\theta}+\bar{\rho}e^{-im\theta}-\rho b e^{i(n-m)\theta}\right. \\ &\qquad \left.-\bar{\rho}\bar{b}e^{-i(n-m)\theta}\right]\Big\} \qquad \text{(III.iii.7)} \end{aligned}$$

This will be of order $3n-2$. Therefore, it has been shown to be finite for all n.

With the ansatz used in the programme, this will simplify to

$$\begin{aligned} j_1^H &= -\frac{4\lambda^4K}{|\mathbf{f}|^4}\Big\{(1+\lambda^2r^2)\left[r^2(e^{i2\theta}+e^{-i2\theta})-(a+\bar{a})\right] \\ &\qquad -(1+\lambda^2r^2)\left[r^2(e^{i2\theta}+e^{-i2\theta})\right]\Big\} \qquad \text{(III.iii.8)} \end{aligned}$$

Hence there will be a nonzero contribution to Q_1 from the Hopf term which is independent of the velocity.

The Q_2 charge is obtained from Q_1 and hence does not need to be discussed in detail. However, it does provide an useful check on the calculations. It also confirms that for small λ, Q_2^0 is approximately proportional to the real component of the velocity. For pure CP^2, and always when located at the origin, the proportionality is direct. Q_2^H also introduces a component which is independent of the velocity.

III.iii.b Q_3

Q_3^0 will now be considered. Expressed in terms of the normalised fields it becomes:

$$Q_3^0 = i\int\int d^2x \frac{1}{|\mathbf{f}|^2}(\partial_0\mathbf{f}^\dagger\lambda^3\mathbf{f} - \mathbf{f}^\dagger\lambda^3\partial_0\mathbf{f}) + \frac{(1-|W|^2)}{|\mathbf{f}|^4}(\mathbf{f}^\dagger\partial_0\mathbf{f} - \partial_0\mathbf{f}^\dagger\mathbf{f}) \tag{III.iii.9}$$

After some simple algebra, this can be expressed in the simpler form

$$\begin{aligned} j_3^0 \;&= \frac{i}{|\mathbf{f}|^4}\Big\{(2+|W^1|^2)(W_0\overline{W} - W\overline{W}_0) \\ &\qquad (1-|W|^2)(W_0^1\overline{W}^1 - W^1\overline{W}_0^1)\Big\} \end{aligned} \tag{III.iii.10}$$

Substituting for W and W^1, this expands out to

$$\begin{aligned} j_3^0 \;=\; &\frac{i}{|\mathbf{f}|^4}\Big\{\Big[2+|\mu|^2(r^{2m}+|b|^2-r^m\Omega_b)\Big] \\ &\qquad \Big[(r^{2n}+|a|^2-r^n\Omega_a)(\bar\rho\rho_0 - \bar\rho_0\rho) \\ &\qquad\quad -|\rho|^2\Big(r^n(a_0e^{-in\theta} - \bar a_0 e^{in\theta}) - (\bar a a_0 - \bar a_0 a)\Big)\Big] \\ &+\Big[1-|\rho|^2(r^{2n}+|a|^2-r^n\Omega_a)\Big] \\ &\qquad \Big[(r^{2m}+|b|^2-r^m\Omega_a)(\bar\mu\mu_0 - \bar\mu_0\mu) \\ &\qquad\quad -|\mu|^2\Big((b_0e^{-im\theta} - \bar b_0 e^{im\theta})r^m - (\bar b b_0 - \bar b_0 b)\Big)\Big]\Big\} \end{aligned} \tag{III.iii.11}$$

The order of this expression for large r is $2(m-n)$, although if μ and ρ are identical the divergences will cancel. This means that j_3^0 will diverge on integration if $n - m \leq 1$.

However, once again, when n is two the problem is removed if ρ and μ are assumed to be constant. In this scenario, the divergence will only arise if $2n \leq m+2$ and the density simplifies to

$$\begin{aligned} j_3^0 &= \frac{-i}{|\mathbf{f}|^4}\Big\{\Big[2+|\mu|^2(r^{2m}+|b|^2-r^m\Omega_b)\Big] \\ &\qquad |\rho|^2\Big[(a_0e^{-in\theta}-\bar{a}_0e^{in\theta})r^n-(\bar{a}a_0-\bar{a}_0a)\Big] \\ &\quad +\Big[1-|\rho|^2(r^{2n}+|a|^2-r^n\Omega_a)\Big] \\ &\qquad |\mu|^2\Big[(b_0e^{-im\theta}-\bar{b}_0e^{im\theta})r^m-(\bar{b}b_0-\bar{b}_0b)\Big]\Big\} \end{aligned} \tag{III.iii.12}$$

For the ansatz used in the programme, this becomes

$$\begin{aligned} j_3^0 &= i\frac{2|\lambda|^4}{|\mathbf{f}|^4}\Big\{(1+|\lambda|^2r^2)\Big[(\bar{a}a_0-\bar{a}_0a) \\ &\qquad -r^2(a_0e^{-in\theta}-a_0e^{in\theta})\Big]\Big\} \end{aligned} \tag{III.iii.13}$$

At the origin this will trivially integrate to zero. There will not be any contribution from the time derivative of a. Hence for pure CP^2, this charge will be trivially zero, thus explaining the numerical results.

When n and m are both unity, then there will be divergent factors associated with the time derivative of a. Once again, the charge can only be finite if the divergent term associated with the time derivatives of ρ and μ cancels with the other infinite quantity. Thereby confirming the need for more than one parameter to vary with time for a single soliton.

Now consider the Hopf contribution to Q_3.

$$Q_3^H = iK \iint d^2x \epsilon^{\mu\nu} \partial_\mu (\mathbf{z}^\dagger \partial_\nu \mathbf{z}) \mathbf{z}^\dagger \lambda^3 \mathbf{z} - \mathbf{z}^\dagger \partial_\nu \mathbf{z} \partial_\mu (\mathbf{z}^\dagger \lambda^3 \mathbf{z}) \qquad \text{(III.iii.14)}$$

Substituting for $\mathbf{z}^\dagger \lambda^3 \mathbf{z}$ and rearranging, it can be shown that:

$$Q_3^H = (2\pi K Q^{TOP} - I_3), \qquad \text{(III.iii.15)}$$

where

$$\begin{aligned} I_3 \;=\; i \iint d^2x \frac{\epsilon^{\mu\nu}}{|\mathbf{f}|^2} \Big\{ & \partial_\mu (\mathbf{z}^\dagger \partial_\nu \mathbf{z}) (2|W|^2 + |W^1|^2) \\ & + \big(\mathbf{f}^\dagger \partial_\mu \mathbf{f} - \partial_\mu \mathbf{f}^\dagger \mathbf{f}\big) \partial_\nu (\mathbf{z}^\dagger \lambda^3 \mathbf{z}) \Big\} \end{aligned} \qquad \text{(III.iii.16)}$$

and Q^{TOP} is the topological charge, as defined in equation I.iii.9.

Hence, because Q^{TOP} is by definition conserved, it follows that $Q_3^0 - KI_3$ must also be conserved. It is this expression which will be considered in detail. As discussed on page 54, there is no evidence to suggest that for general K either term would be separately conserved. Note that I_3 does not involve time derivatives and hence will not vanish for static fields.

Expressed in terms of the components of the normalised field, this expression simplifies to

$$\begin{aligned} I_3 \;=\; & \frac{i}{|f|} \Big\{ |W^1|^2 (\overline{W}_x W_y - \overline{W}_y W_x) + 2|W|^2 (\overline{W}^1_x W^1_y - \overline{W}^1_y W^1_x) \\ & - \frac{1}{2} [\overline{W W^1} (W_x W^1_y - W_y W^1_x) + W W^1 (\overline{W}_x \overline{W}^1_y - \overline{W}_y \overline{W}^1_x)] \\ & + \frac{3}{2} [\overline{W} W^1 (W_x \overline{W}^1_y - W_y \overline{W}^1_x) - W \overline{W^1} (\overline{W}_x W^1_y - \overline{W}_y W^1_x)] \Big\} \end{aligned} \qquad \text{(III.iii.17)}$$

Now consider the special case for CP^1, where either W or W^1 is zero. It is obvious that in this case, the above will trivially vanish. For

this model, Q_3^H is an integral multiple of the topological charge, thus explaining the numerical results illustrated by figure III.2.

Returning to CP^2 and substituting for the components, the contribution from the Hopf term becomes

$$\begin{aligned} I_3 \;=\; \frac{-1}{|f|^4}\Big\{ & 2|\mu|^2|\rho|^2\Big[n^2r^{2(n-1)}(r^{2m}+|b|^2-r^m\Omega_b) \\ & +2m^2r^{2(m-1)}(r^{2n}+|a|^2-r^n\Omega_a)\Big] \\ & -3nmr^{n+m-2}\Big[2r^{n+m}\Omega_{ab}-r^n\Omega_b-r^m\Omega_a\Big]\Big\} \end{aligned} \tag{III.iii.18}$$

where the Ω functions are as defined previously in equation II.ii.7. When n is greater than m, this will clearly be finite.

However, it appears to be divergent when n equals m. However, a few lines of calculations will show that in this scenario, the divergences will cancel. Therefore this integral will be finite for all values of n and m.

When the ansatz used in the programme is considered, it reduces to

$$I_3 = -4\frac{|\lambda|^6}{|f|^4}\big(2|a|^2+r^2\Omega_a\big) \tag{III.iii.19}$$

This will be zero at the origin, but is nontrivial away from there.

III.iii.c Q_4 and Q_5

The pair $[Q_4, Q_5]$ does not need to be considered in detail as they can be deduced from Q_1. It is just necessary to interchange W and W^1. This corresponds to interchanging n, a and ρ with m, b and μ respectively, in the above equations.

However, in the analysis it was assumed that n would never be smaller than m. Therefore the order of the full equation for Q_4^0, assuming time dependency of the coefficients of x_+, will be $2m + n$. Hence it will diverge for $2n \leq 2 + m$. It is thus necessary to discuss the cases for which n is either one or two.

The solution is the same as for Q_1^0. If the parameters ρ and μ are taken to be constant, then the divergences will not contribute. In this scenario, when n is two, the charge density reduces to

$$\begin{aligned} 2\Big\{ & \bar{\mu}\bar{b}_0\Big[1 + \mu^2(r^2e^{i2\theta} - 2bre^{i\theta} + b^2) + |\rho|^2(r^4 - r^2\Omega_a + |a|^2)\Big] \\ & -\mu b_0\Big[1 + \bar{\mu}^2(r^2e^{i2\theta} - 2\bar{b}re^{i\theta} + \bar{b}^2) + |\rho|^2(r^4 - r^2\Omega_a + |a|^2)\Big] \\ & +\Big[(a_0e^{-i2\theta} - \bar{a}_0e^{i2\theta})r^2|\rho|^2 + (a_0\bar{a} - \bar{a}_0a)\Big] \\ & \Big[r(\bar{\mu}e^{\theta} + \mu e^{-\theta}) - (\bar{\mu}\bar{b} + \mu b)\Big]\Big\} \end{aligned} \qquad \text{(III.iii.20)}$$

With the particular ansatz used in the simulation, b is taken to be zero. Therefore the expression will become

$$2\Big\{\Big[(a_0e^{-i2\theta} - \bar{a}_0e^{i2\theta})r^2|\rho|^2 + (a_0\bar{a} - \bar{a}_0a)\Big]\Big[r(\bar{\mu}e^{\theta} + \mu e^{-\theta})\Big]\Big\}. \qquad \text{(III.iii.21)}$$

To analyse this, it is necessary to expand the exponential terms. Those terms involving $\sin k\theta$, for any integer k will trivially integrate to zero. It thus becomes the imaginary component of of

$$2a_0r\Big[(\bar{\mu}\cos\theta + \mu\cos(3\theta))|\rho|^2r^2 + \bar{a}\Re(\mu)\cos\theta\Big] \qquad \text{(III.iii.22)}$$

When a is zero, this will vanish trivially on integration. Therefore as it is conserved, Q_4^0 will be zero for pure CP^2. A similar argument will show that Q_5^0 will also be zero.

Now consider the Hopf contribution. This will be of order $2n+m-2$ and hence will always be finite. When b is zero, the numerator will take the form

$$Kr\Re(\mu)|\mu|^2 r^2 \cos\theta \qquad \text{(III.iii.23)}$$

This is trivially zero at the origin but it is not obvious what happens away from the origin. However, because the total charge is trivially zero at the origin, it must be zero everywhere. Hence this confirms the numerical results.

When m and n are both equal to one, then the charges will have two divergent terms. Therefore it confirms the requirement that for this ansatz, the coefficients of x_+ must also depend on time.

III.iii.d Q_6 and Q_7

The contribution from the CP^2 Lagrangian to the charge density can be shown to be:

$$\begin{aligned} j_6^0 &= \frac{i}{|f|^4}\Big\{(1+|W^1|^2)(\bar{W}_0 W^1 - W_0\bar{W}^1) \\ &\quad +(1+|W|^2)(\bar{W}_0^1 W - W_0^1\bar{W}) \\ &\quad -WW\overline{W}^1\overline{W}_0 + \overline{W}\overline{W}W^1W_0 \\ &\quad -W^1W^1\overline{W}\overline{W}_0^1 + \overline{W}^1\overline{W}^1WW_0^1\Big\} \end{aligned} \tag{III.iii.24}$$

When the components are substituted for, the charge can be expressed as

$$Q_6 = 2i\iint r dr d\theta \frac{\mathrm{Im A}}{|f|^4} \tag{III.iii.25}$$

where the integrand function is defined to be:

$$\begin{aligned} A &= [1+|\mu|^2(r^{2m}+|b|^2 - r^m\Omega_b)] \\ &\quad [\bar{\rho}_t\mu(r^{n+m}e^{i(m-n)\theta} + \bar{a}b - (\bar{a}r^m e^{im\theta} + br^n e^{-in\theta})) \\ &\quad -\bar{\rho}\mu\bar{a}_0(r^m e^{im\theta} - b)] \\ &+ [1+|\rho|^2(r^{2n}+|a|^2 - r^n\Omega_a)] \\ &\quad [\bar{\mu}_0\rho(r^{n+m}e^{-i(m-n)\theta} + a\bar{b} - (ar^m e^{-im\theta} + \bar{b}r^n e^{in\theta})) \\ &\quad -\rho\bar{\mu}\bar{b}_0(r^n e^{in\theta} - a)] \\ &- [\rho^2(r^{2n}e^{i2\theta} + a^2 - 2ar^n e^{in\theta}] \\ &\quad [\bar{\mu}\bar{\rho}_0(r^{m+n}e^{-i(n+m)\theta} + \bar{a}\bar{b} - \bar{a}r^m e^{-im\theta} - \bar{b}r^n e^{-in\theta}) \\ &\quad -\bar{\mu}\bar{\rho}\bar{a}_0(r^m e^{-im\theta} - \bar{b})] \\ &- [\mu^2(r^{2m}e^{i2\theta} + b^2 - 2br^n e^{in\theta})] \\ &\quad [\bar{\mu}_0\bar{\rho}(r^{m+n}e^{-i(m+n)\theta} + \bar{a}\bar{b} - \bar{a}r^m e^{-im\theta} - \bar{b}r^n e^{-in\theta}) \\ &\quad -\bar{\mu}\bar{\rho}\bar{b}_0(r^n e^{-in\theta} - \bar{a})] \end{aligned} \tag{III.iii.26}$$

This will lead to a divergent integral when $n - m \leq 2$.

However, even when ρ and μ are taken to be constant, the charge will still be infinite for $n \leq 2$ as the integrand becomes proportional to the imaginary component of

$$\begin{aligned} A &= [1 + |\mu|^2(r^{2m} + |b|^2 - r^m\Omega_b) + |\rho|^2(r^{2n}e^{-i2\theta} + \bar{a}^2 - 2\bar{a}r^n e^{-in\theta})] \\ &\qquad [\bar{\mu}\rho a_0(r^m e^{-im\theta} - \bar{b})] \\ &+ [1 + |\rho|^2(r^{2n} + |a|^2 - r^n\Omega_a) + |\mu|^2(r^{2m}e^{i2\theta} + \bar{b}^2 - 2\bar{b}r^n e^{-in\theta})] \\ &\qquad [\mu\bar{\rho}b_0(r^n e^{in\theta} - \bar{a})]. \end{aligned} \tag{III.iii.27}$$

This would appear to contradict the numerical results which predicted Q_6 to be zero. However, it can be seen that the divergent term is dependent on b. If this parameter is set to zero (as it is in the numerical simulations), then the charge density will be finite when n is two.

When ansatz II.ii.11 is used, the charge density function becomes

$$A = \sqrt{2}\lambda^2\Big\{1 + 2\lambda^2 r^2 + \lambda^4(r^4 e^{-i2\theta} + \bar{a}^2 - 2\bar{a}r^2 e^{-i2\theta})\lambda a_0 r^m e^{-i\theta}\Big\}. \tag{III.iii.28}$$

which is clearly finite. It can be seem that when a is also zero, then all terms are proportional to a trigonometric function. Therefore for pure CP^2 this charge will be trivial, confirming the numerical results.

When n is unity, then there will be a divergent term associated with a_0. Once again, this is confirmation that in the single soliton ansatz, the coefficients of x_+ must be time dependent.

Now consider the contribution from the Hopf term. The charge density can be shown to be:

$$\begin{aligned} j_6^H &= \frac{iK}{2|f|^4}\{(\overline{W}W^1+\overline{W}^1W)(\overline{W}_xW_y-\overline{W}_yW_x+\overline{W}^1_xW^1_y-\overline{W}^1_yW^1_x) \\ &+ (|W|^2+|W^1|^2)(\overline{W}_xW^1_y-\overline{W}_yW^1_x+\overline{W}^1_xW_y-\overline{W}^1_yW_x) \\ &+ (W^1W^1-WW)\overline{W}_x\overline{W}^1_y+(\overline{WW}-\overline{W^1W^1})W_xW^1_y\}. \end{aligned} \tag{III.iii.29}$$

Expressing this as a function of the imaginary component of a variable A, in an analogous way to the above, and substituting for the components W and W^1, results in the integrand being a function of

$$\begin{aligned} A &= 2\left[n^2|\rho|^2r^{2(n-1)}+m^2|\mu|^2r^{2(m-1)}\right] \\ &\qquad \left[r^{n+m}\rho\bar{\mu}e^{i(m-n)\theta}-r^n\bar{\rho}\mu be^{-in\theta}-r^m\bar{\mu}\rho ae^{-im\theta}+\bar{\rho}\mu\bar{a}b\right] \\ &+ 2nm\left[|\rho|^2(r^{2n}+|a|^2-r^n\Omega_a)\right. \\ &\qquad \left.+|\mu|^2(r^{2m}+|b|^2-r^m\Omega_b)\right]\rho\bar{\mu}r^{m+n-2}e^{-(m-n)\theta} \\ &- nm\left[\mu^2(r^{2m}e^{i2m\theta}+b^2+2be^{im\theta})+\rho^2(r^{2n}e^{i2n\theta}+a^2+2ae^{in\theta})\right] \\ &\qquad \rho\bar{\mu}r^{n+m-2}e^{-i(m-n)\theta} \end{aligned} \tag{III.iii.30}$$

This will only lead to a divergent integral only when m equals n.

For completeness, it will be given for the ansatz used in the programme

$$\begin{aligned} A &= 4\sqrt{2}\lambda^2\bar{\lambda}e^{-i\theta}\Big\{r^3(1+2|\lambda|^2r^2)+r\left[|\lambda|^2(r^4+|a|^2-r^2\Omega_a)+2r^2\right] \\ &\qquad -2\lambda^2r^2e^{i2\theta}+\lambda^4(r^4e^{i4\theta}+a^2+2ae^{i2\theta})\Big\} \end{aligned} \tag{III.iii.31}$$

By using a similar argument to before, It is possible to see that this will also vanish on integration. Thus, for the ansatz used in the simulations, Q_6 will always be trivial.

For a single soliton, $m = n = 1$, then the same argument as used for Q_1 can be followed. This will confirm the need for all three parameters to be time dependent for this charge to be finite.

The value of charge Q_7 can be obtained from Q_6 by taking the real component of the two functions defined above as A, thus confirming the numerical prediction that this should also be zero.

III.iii.e Q_8

The contribution from pure CP^2 to the charge density for Q_8 can easily be shown to be

$$j_8^0 = \frac{3i}{|f|^4}\Big\{|W^1|^2(\overline{W}_0 W - \overline{W}W_0) + (1+|W|^2)(\overline{W^1}_0 W^1 - \overline{W^1}W_0^1)\Big\} \tag{III.iii.32}$$

and substituting for W and W^1 gives the expression:

$$\begin{aligned} j_8^0 \;=\; & \frac{3i}{|f|^4}\Big\{|\mu|^2(r^{2m}+|b|^2-r^m\Omega_b) \\ & [\rho\bar{\rho}_0(r^{2n}+|a|^2-r^n\Omega_a) - |\rho|^2(r^n e^{in\theta}-a)\bar{a}_0 \\ & -(\bar{\rho}\rho_0(r^{2n}+|a|^2-r^n\Omega_a) - |\rho|^2(r^n e^{-in\theta}-\bar{a})a_0)] \\ & +[1+|\rho|^2(r^{2n}+|a|^2-r^n\Omega_a)] \\ & [\mu\bar{\mu}_0(r^{2m}+|b|^2-r^m\Omega_b) - |\mu|^2(r^m e^{im\theta}-b)\bar{b}_0 \\ & -(\bar{\mu}\mu_0(r^{2m}+|b|^2-r^m\Omega_b) - |\mu|^2(r^m e^{-im\theta}-\bar{b})b_0)]\Big\} \end{aligned} \tag{III.iii.33}$$

This will give a divergent charge if $n-m \leq 1$, in particular if n is two and n is one. The assumption that ρ and μ are constant will once again surmount this problem for all cases except m and n being equal to one.

This simplification is given below.

$$\begin{aligned} j_8^0 \;=\; & \frac{3i}{|f|^4}\Big\{|\mu|^2(r^{2m}+|b|^2-r^m\Omega_b) \\ & |\rho|^2[(r^n e^{-in\theta}-\bar{a})a_0 - (r^n e^{in\theta}-a)\bar{a}_0] \\ & +[1+|\rho|^2(r^{2n}+|a|^2-r^n\Omega_a)] \\ & |\mu|^2[(r^m e^{-im\theta}-\bar{b})b_0 - (r^m e^{im\theta}-b)\bar{b}_0]\Big\} \end{aligned} \tag{III.iii.34}$$

This will give a divergent answer when $2n - m \leq 1$. For the ansatz used in the numerical work, the charge density reduces to

$$j_8^0 = \frac{3i}{|f|^4}\{2\lambda^6 r^2[(r^2 e^{-i2\theta} - \bar{a})a_0 - (r^2 e^{i2\theta} - a)\bar{a}_0]\} \qquad \text{(III.iii.35)}$$

As with j_3^0, this involves terms involving just the temporal derivative of a. Therefore, it may be finite even at the origin. Hence it doesn't contradict the numerical results.

Also like the third charge, when m and n are both equal to one, there will be two divergences. Hence Q_8^0 can only be finite if ρ and μ are also time dependent.

Now consider the Hopf contribution. This takes the form

$$\begin{aligned} Q_8^H &= iK \int\int d^2x \epsilon^{\mu\nu} \Big\{ \partial_\mu(\mathbf{z}^\dagger \partial_\nu \mathbf{z})(1 + |W|^2 - 2|W^1|^2)\frac{1}{|\mathbf{f}|^2} \\ &\qquad -\mathbf{z}^\dagger \partial_\mu \mathbf{z} \partial_\mu(\mathbf{z}^\dagger \lambda^8 \mathbf{z}) \Big\} \qquad \text{(III.iii.36)} \end{aligned}$$

and hence in an analogous argument to that for Q_3, it can be shown that $Q_8^0 - KI_8$ must be conserved, where

$$I_8 = i \int\int d^2x \epsilon^{\mu\nu} \left\{ \frac{|W^1|^2}{|\mathbf{f}|^2} \partial_\mu(\mathbf{z}^\dagger \partial_\nu \mathbf{z}) + \mathbf{z}^\dagger \partial_\nu \mathbf{z} \partial_\mu \left(\frac{|W^1|^2}{|\mathbf{f}|^2} \right) \right\}. \qquad \text{(III.iii.37)}$$

This is clearly zero for CP^1. Hence Q_8^H has also been shown to be an integral multiple of the topological charge for this model, agreeing with the numerical results shown in figure III.2.

For CP^2 the integrand simplifies to

$$\begin{aligned} I_8 &= \frac{3}{2}\frac{i}{|f|^4}\{[2|W^1|^2(\overline{W}_x W_y - \overline{W}_y W_x) \\ &- \overline{W}^1 \overline{W}(W_x^1 W_y - W_y^1 W_x) + W^1 W(\overline{W}_x^1 \overline{W}_y - \overline{W}_y^1 \overline{W}_x) \\ &+ W^1 \overline{W}(\overline{W}_x^1 W_y - \overline{W}_y^1 W_x) - \overline{W}^1 W(W_x^1 \overline{W}_y - W_y^1 \overline{W}_x)]\}. \end{aligned} \qquad \text{(III.iii.38)}$$

Substituting for the components gives the following expression.

$$\begin{aligned} I_8 \;=\; & -3\frac{1}{|f|^4}|\mu|^2|\rho|^2\Big\{2n^2r^{2(n-1)}(r^{2m}+|b|^2-r^m\Omega_b) \\ & -nmr^{n+m-2}\Big[2r^{n+m}+\overline{a}be^{-i(m-n)\theta}+a\overline{b}e^{i(m-n)\theta} \\ & -r^m\Omega_a-r^n\Omega b\Big]\Big\} \end{aligned} \tag{III.iii.39}$$

and this will obviously be a finite quantity if $m \neq n$.

When n is two and the programme ansatz is used, this becomes

$$I_8 = -6\frac{|\lambda|^6}{|f|^4}\Big[4r^4-r^2\Omega_a\Big] \tag{III.iii.40}$$

Note that this will definitely be nonzero at the origin.

When m and n are equal , a similar calculation to that for Q^3 will show that the divergent terms will cancel. Thus this term will be finite for all values of n and m.

III.iv Summary of Results

In the general ansatz for CP^2, the components of the vector fields are taken to be 1, W and W^1. It is assumed that W is of order n and W^1 of order m where $n \geq m$. There are problems with divergences arising from all eight charges for $n \leq 2$.

When n is equal to two, then taking the coefficients of x_+ (μ and ρ) to be constant solves most of the problems. Q_6 and Q_7 will still be divergent unless b, the term in W^1 independent of the spatial coordinates, is assumed to be constantly zero. The other six charges charges, however, will be finite for all values of b.

When the particular ansatz used in the programme is taken, then in pure CP^2 two of the charges (Q_1 and Q_2) are dependent on the velocity of the solitons. The remaining six charges are trivially zero. When the Hopflike term is added, these two charges have an additional contribution which is independent of the velocity.

In addition, the two charges Q_3 and Q_8 are no longer trivial in the enhanced model. They are now related to the topological charge. In the simpler CP^1 model, the relationship can be shown to be an equivalence.

However, there is also an additional contribution which is separately conserved. Hence, these two charges are of the most interest to the current project.

When m and n are both equal to one, then it is necessary for the coefficients of x_+ in W and W^1 to be dependent on time. Otherwise most of the charges will diverge. This confirms the result from earlier work. However for two or more solitons, it is possible for these parameters to be conserved.

IV

Trajectory of Solitons

Well Toto, I guess we ain't in Kansas anymore. [1]

[1] Dorothy in Wizard of Oz

IV.i Introduction

In the preceding chapter, the charges arising from the internal symmetry of sigma models were discussed. The numerical results from simulations were explained by explicit calculations of the charges. This section will primarily be concerned with two solitons in the CP^2 model using the ansatz defined by equation II.ii.11.

It was mentioned in the introduction, that the equations of motion cannot be solved explicitly for time dependent solitons. Instead, static solutions are given a Galilean boost in the programme to emulate evolution.

The predicted scattering of two solitons has been documented in [31]. For pure CP^2, the impact results in orthogonal scattering, as shown in figure IV.1.

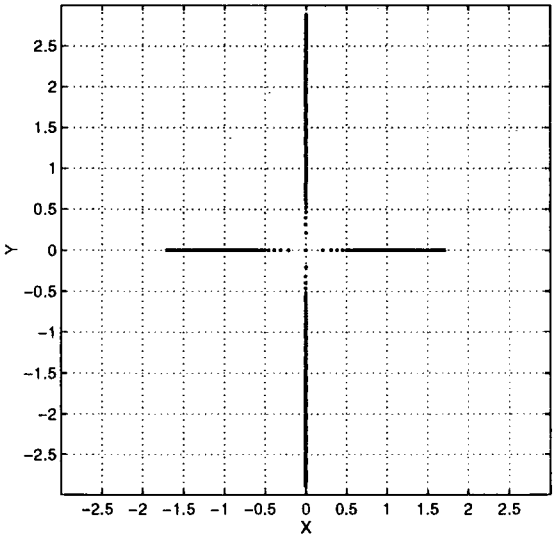

Figure IV.1: Soliton trajectory for pure CP^2

However, when the Hopf term is added to the Lagrangian, the scattering angle becomes acute. The results for a typical value of this parameter is shown below. The reason for this was suggested to be that the Hopf term represented an internal rotation of the soliton.

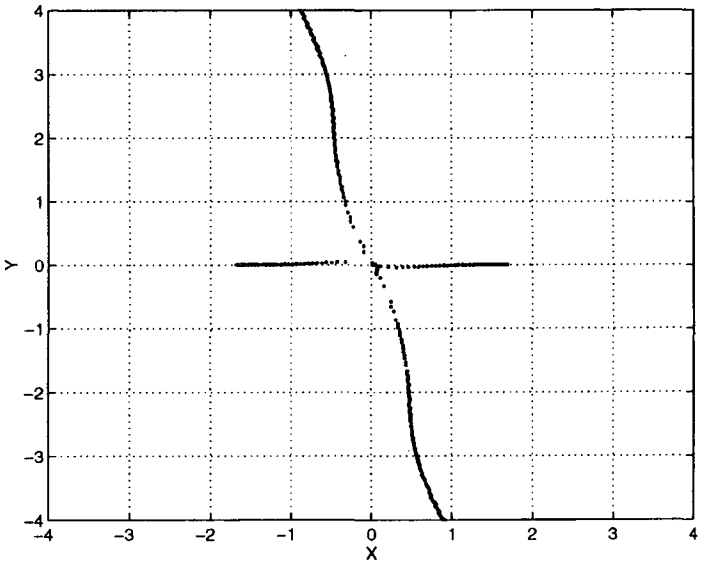

Figure IV.2: Soliton trajectory for CP^2 with $K = 1$

In reference [30], the solitons were given a phase angle so that they rotated away from the real axis. This enabled a non zero impact parameter to be considered. The results predicted scattering at an obtuse angle.

The purpose of this chapter is to try and understand these results. This will be done by considering the charges arising from the internal symmetry, in particular Q_3 and Q_8. The energy density will also be used. It was also hoped that the results would be able to predict the trajectory of the solitons.

The chapter will end with a brief discussion of the single soliton phase space. It was hoped that this would confirm and, possibly even add to, the interpretation of the Hopf term given in earlier work.

IV.ii Two Solitons

IV.ii.a Simplified ansatz

In this section, it shall be assumed that the initial ansatz used in the programme will remain valid throughout the simulation. Therefore, b in equation II.ii.5 will be constantly zero and the two coefficients ρ and μ will be given by the functions in equation II.ii.11. Furthermore, as the parameter λ can be taken to be real without loss of generality, only two equations will be needed to solve for all the variables in the ansatz.

Now consider the equations arising from the two $SU(3)$ charges Q_3 and Q_8. Expressed in terms of the variables ϕ and s, they are

$$\begin{aligned} Q_3^0 - KI_3 &= (a^\dagger a_t - a_t a^\dagger)\left[|\lambda|^2(\alpha+\beta) - 2(\delta+\epsilon)\right] \\ &\quad -2K|\lambda|^2\left[2|\lambda|^2|a|^2\alpha + \delta\right] \\ Q_8^0 - KI_8 &= 3\left\{(a^\dagger a_t - a_t a^\dagger)\left[2\epsilon - \beta|\lambda|^2\right] - K(2\gamma - |\lambda|^2\delta)\right\} \end{aligned} \tag{IV.ii.1}$$

where the results from equation II.ii.18 have been used to combine the terms in the contributions from pure CP^2.

The five standard integrals are given by

$$\begin{aligned} \alpha &= \iint ds d\phi \frac{1}{|\mathbf{f}|^4} \\ \beta &= \iint ds d\phi \frac{s}{|\mathbf{f}|^4} \\ \gamma &= \iint ds d\phi \frac{s^2}{|\mathbf{f}|^4} \\ \delta &= \iint ds d\phi \frac{s\cos 2\phi}{|\mathbf{f}|^4} \end{aligned}$$

and

$$\epsilon = \iint ds d\phi \frac{s^2 \cos 2\phi}{|\mathbf{f}|^4} \qquad \text{(IV.ii.2)}$$

with the denominator being

$$|\mathbf{f}|^2 = (1+s)^2 + |a|^2 - s\cos 2\phi. \qquad \text{(IV.ii.3)}$$

The initial behaviour of pure CP^2 can be seen at this stage when the solitons are initially placed on the real axis. As a is real, the right hand sides of the first two equations are zero. Thus the two solitons will move along the real axis until they collide. However, it is not clear from this first impression what will happen when a is zero or imaginary.

This deduction is confirmed by the numerical results obtained from this and earlier work (see, for example, figure IV.1). The coefficients of x_+^2 and x_+ were chosen so as to ensure that two solitons will form a peaked topological structure if they are both placed at the origin.

To proceed, it proves convenient to express the parameter a in terms of complex polar coordinates,

$$a(t) = p(t)e^{i\psi(t)}. \qquad \text{(IV.ii.4)}$$

Hence

$$a\bar{a}_t - \bar{a}a_t = -2ip^2\frac{\partial\psi}{\partial t}. \qquad \text{(IV.ii.5)}$$

Therefore the two equations reduce to

$$\begin{aligned} Q_3^{\text{NUM}} - 4\pi &= 2p^2\frac{\partial\psi}{\partial t}\left[|\lambda|^2(\alpha+\beta) - 2(\delta+\epsilon)\right] + 2K|\lambda|^2\left[2|\lambda|^2p^2\alpha + \delta\right] \\ Q_8^{\text{NUM}} - 4\pi &= 3\left\{p^2\frac{\partial\psi}{\partial t}\left[2\epsilon - \beta|\lambda|^2\right] - 2K\left[2\gamma - |\lambda|^2\delta\right]\right\} \end{aligned} \qquad \text{(IV.ii.6)}$$

where the left hand sides have been expressed in terms of the numerical prediction of the charges from the programme. Both of these equations are of the form

$$p^2 \frac{d\psi}{dt} F(p) = K\,(G(p) - 4\pi) + Q^{\mathrm{NUM}} \qquad \text{(IV.ii.7)}$$

Consider first pure CP^2. The function $G(p)$ does not contribute because both Q_3^0 and Q_8^0 have be shown to be zero. This can be seen from the numerical results or, alternatively, it can be calculated when the solitons are at the origin.

It therefore confirms that for pure CP^2 the phase will remain constant for all p except when $p = 0$. At this value, which corresponds to the two solitons being located at the origin, the derivative is undefined.

Therefore the two solitons will move in a straight line both before and after the impact. Hence it provides an explanation for the numerical results.

Unfortunately, the actual scattering angle cannot be deduced analytically from this. But the empirical evidence gives an orthogonal scattering angle.

Now consider the full model. It is clear from this equation that the velocity of the soliton picks up an imaginary component which rotates the solitons away from the real axis. Thus there is no longer a head on collision between them. The two solitons no longer go through the origin, they only skirt around it before scattering.

However, it should be remembered that p is a parameter which only approximates the position when the two solitons are far apart. Therefore the possibility that p becomes zero needs to be considered. When this happens, the rate of change in the phase is undefined.

The numerical values were found to be close to 4π and hence $G(p)$ will be small. Hence the rate of change of the phase is approximately directly proportional to K before the impact. This thus predicts differing angles of scattering for various values of this parameter.

This agrees qualitatively with the numerical result. After the lorentz boost has been applied, the soliton position does start to pick up a small complex component. However it is so small that it is easy to miss on the usual position plots (see figure IV.3 for the effect of K on the trajectory).

Soliton scattering with a non zero impact parameter was considered for pure CP^2 in [42] and shown to result in non orthogonal scattering. However the scattering angle obtained was obtuse and not acute. It should be recalled, however, that when the solitons are close together, their positions are not well defined. Hence the trajectory through the origin is a subjective path. The difference between an obtuse and an acute scattering angle is simply a matter of interpretation.

The fact that the rate of change of the phase angle is small suggests an acute angle, but it is no more than a suggestion. It is not possible to calculate what happens when the parameter p is zero and, because it is simply a parameter, it is not possible to assume it doesn't become zero during the impact.

Even if p doesn't become zero, as may be expected in the naive interpretation, then the positions of the solitons during the scattering are not well defined. Hence it is not possible to give a definite relationship between the solitons going into the scattering and those coming out.

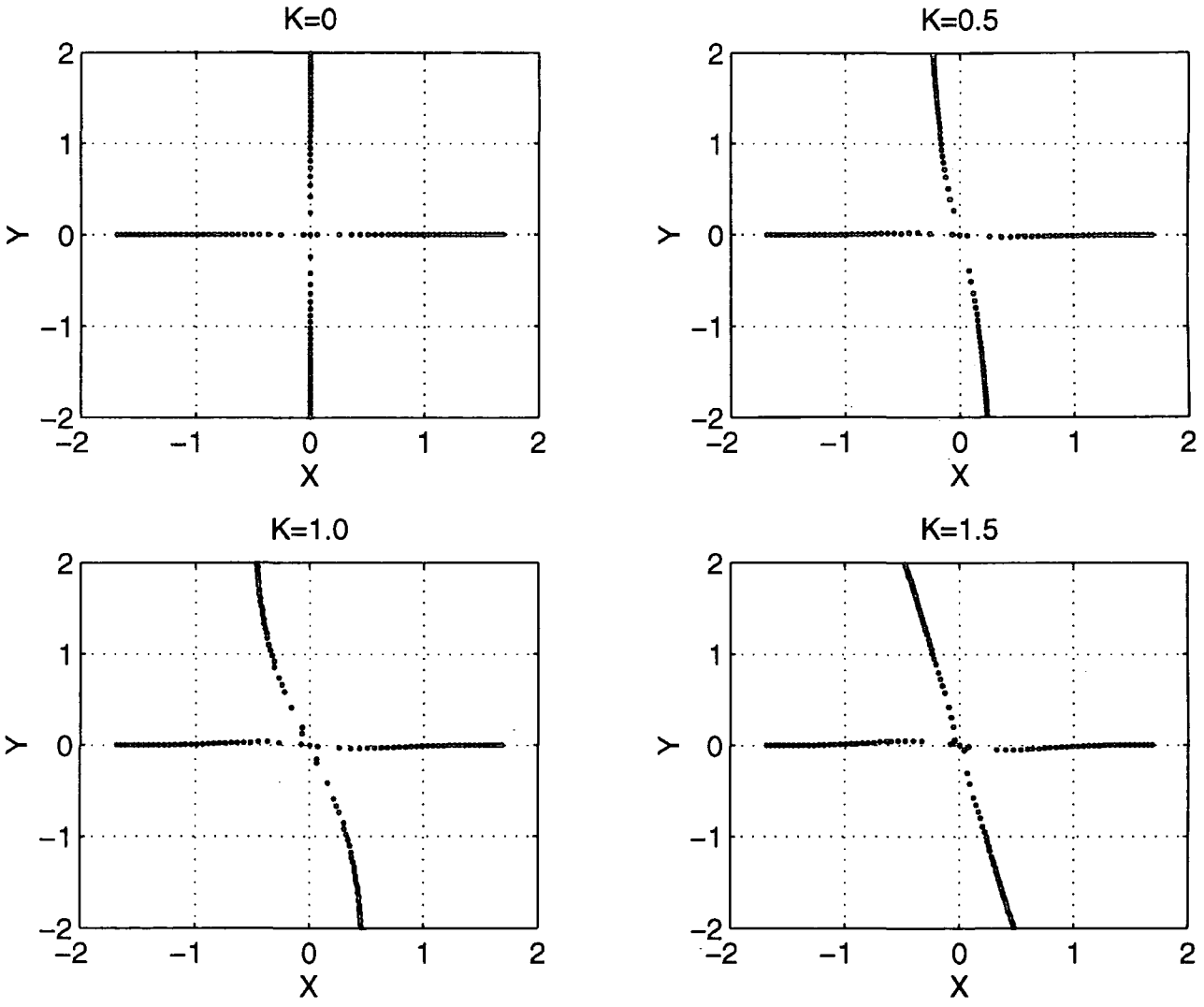

Figure IV.3: Distance trajectory predicted by programme for various values of K

Notice that the two Hopf charges being considered give the same information. This can be used to provide a test for the validity of the simple ansatz under consideration, in particular the assumption that only one parameter is time dependent.

To see the rate of change in the distance from the origin, it is necessary to consider a third equation. The simplest candidate is the total energy which, in terms of the new variables and standard integrals, becomes

$$T + V = \frac{1}{2}|a_t|^2(\alpha + 2\beta) + 2\Big((1 + |\lambda|^4|a|^2)\alpha + 2\beta + 2|\lambda|^2\delta\Big) \quad \text{(IV.ii.8)}$$

When expressed in terms of p and ψ the right hand side reduces to

$$\frac{1}{2}\left[\left(\frac{dp}{dt}\right)^2 + p^2\left(\frac{d\psi}{dt}\right)^2\right]p^2(\alpha + 2\beta) + 2\left((1 + |\lambda|^4p^2)\alpha + 2\beta + 2|\lambda|^2\delta\right) \quad \text{(IV.ii.9)}$$

It is expected that $\frac{d\psi}{dt}$ will be small relative to $\frac{dp}{dt}$. Therefore, the above equation is approximately of the form

$$\frac{dp}{dt} = H(p). \quad \text{(IV.ii.10)}$$

Note, though, that this will *not* hold during scattering. It thus predicts that before scattering, the distance from the origin will be independent of the Hopf coefficient K. This is also in agreement with the numerical results, see figure IV.4.

The difference after scattering will be partly because there will be a large phase change during the scattering. Even for pure CP^2 it will change by $\frac{\pi}{2}$ during this process.

Also other parameters, including the velocity, will be affected by the Hopf term. Therefore the energy and hence the rate of change of p after scattering, will be indirectly dependent on the value of K.

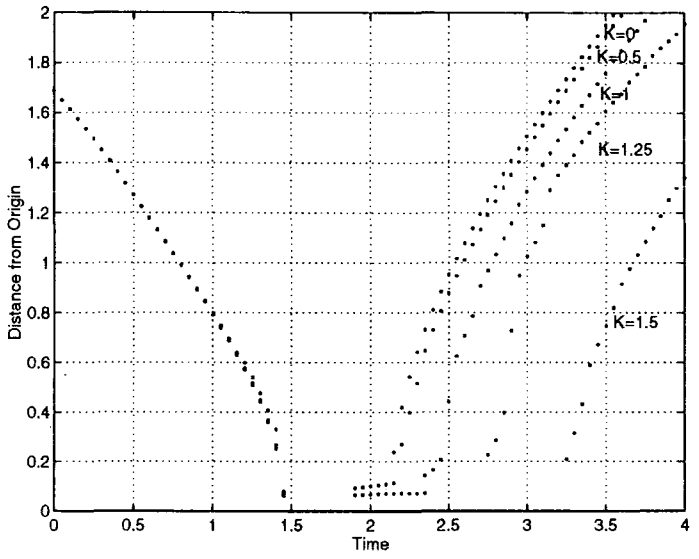

Figure IV.4: Effect of K on distance trajectories

So far, the arguments given have all been subjective. It is now necessary to consider qualitative values if any more information is to be obtained.

It has not been possible to integrate directly the integrals in IV.ii.2, even for this simple case. They can only be expressed in terms of elliptic integrals. Therefore, a mixed analytical and numerical scheme was required.

The angular integration region was performed analytically using tables (see for example [6]). Only three results were needed,

$$\int_0^{\frac{\pi}{2}} d\phi \frac{d\phi}{(B + C\cos a\phi)^2} = -\frac{B}{C^2 - B^2} \int_0^{\frac{\pi}{2}} d\phi \frac{d\phi}{(B + C\cos a\phi)}$$

$$\int_0^{\frac{\pi}{2}} d\phi \frac{d\phi \cos a\phi}{(B + C\cos a\phi)^2} = -\frac{C}{B^2 - C^2} \int_0^{\frac{\pi}{2}} d\phi \frac{d\phi}{(B + C\cos a\phi)}$$

and

$$\int_0^{\frac{\pi}{2}} d\phi \frac{d\phi}{(B + C\cos a\phi)} = \frac{2}{A\sqrt{(B^2 - C^2)}} \frac{\pi}{2} \qquad \text{(IV.ii.11)}$$

where

$$B = (1+s)^2 + p^2$$

and

$$C = -s. \qquad \text{(IV.ii.12)}$$

The integrals will now be in a suitable form for numerical integration. This was performed using Xmaple [7] and checked by using NAG subroutines [27] to perform the double integration.

As mentioned earlier, equation IV.ii.7 also provided a useful check on the calculations, as the two equations have to be consistent for all p. Therefore these will be considered in detail first. The two equations can be written in the form

$$\begin{aligned} Q_3^0 - KI_3 &= A_3 \frac{d\psi}{dt} + KB_3 \\ Q_8^0 - KI_8 &= A_8 \frac{d\psi}{dt} + KB_8 \end{aligned} \qquad \text{(IV.ii.13)}$$

where the values of the coefficients on the right hand sides can be read off from equation IV.ii.6. The left hand sides should be taken from the numerical predictions.

At $t = 0$, the Hopf charges will corresponds to those for a static solution. Therefore, as $Q_3^0(0)$ and $Q_8^0(0)$ are both zero, the equations will reduce to

$$\begin{aligned} A_3(t)\frac{d\psi}{dt} + KB_3(t) &= -KI_3(0) \\ A_8(t)\frac{d\psi}{dt} + KB_8(t) &= -KI_8(0) \end{aligned} \qquad \text{(IV.ii.14)}$$

For these two equations to be consistent, it is necessary for the two ratios $(I_3 + B_3)|A_3$ and $(I_8 + B_8)|A_8$ to be equal. This is not true in general and therefore a more general ansatz needs to be considered.

A difficulty with this analysis is that any numerical integration procedure will require a value for p. Hence, the differential equations can only be solved for fixed values of the parameters.

Thus it can only reliably predict the situation for the period just after the starting time. The possibility that the inconsistencies are caused by the crudeness of the integration method cannot be ruled out.

IV.ii.b Nonconserved b

The simplified ansatz leads to inconsistent equations for the rate of change in the phase. A more general ansatz thus needs to be used.

Therefore, it was initially assumed that only the phase of b was dependent on time. As it was initially taken to be zero in the simulation, then its absolute value would remain zero during the evolution. Hence it would ensure a compatibility between the two approaches.

The denominator will still be the same as it was in the previous section. Hence, terms which can be expressed in terms of the sine function in the numerator will still trivially integrate to zero. An additional standard integral is needed. This takes the form

$$\zeta = \iint ds\, d\phi\, \frac{\sqrt{s}\cos\phi}{\sqrt{2}|f|^4}. \qquad \text{(IV.ii.15)}$$

Therefore, the two $SU(3)$ charges under consideration will now lead to the following

$$\begin{aligned}
Q_3^0 - KI_3 &= 2\psi_t\Big\{2p^2|\lambda|^2(\alpha+\beta) + 2K(2|\lambda|^2p^2\alpha+\delta) \\
&- \Big[1-(s^2-2|\lambda|^2\delta+|\lambda|^4p^2)\Big] \\
&\quad \Big[(b_t+\bar{b}_t)\sqrt{(2p)}\cos\frac{\psi}{2} \\
&\quad +i\left((b_t-\bar{b}_t)\sqrt{(2p)}\sin\frac{\psi}{2}\right)\Big]\zeta\Big\} \\
Q_8^0 - KI_8 &= 3\psi_t\Big\{p^2(2\epsilon-2\beta|\lambda|^2) + 2K(22\gamma-|\lambda|^2\delta) \\
&- \Big[1+(s^2-2|\lambda|^2\delta+|\lambda|^4p^2)\Big] \\
&\quad \Big[(b_t+\bar{b}_t)\sqrt{(2p)}\cos\frac{\psi}{2} \\
&\quad +i\left((b_t-\bar{b}_t)\sqrt{(2p)}\sin\frac{\psi}{2}\right)\Big]\zeta\Big\} \qquad \text{(IV.ii.16)}
\end{aligned}$$

It is now necessary to consider the phase of b. Assume that it takes the form

$$b = qe^{i\epsilon} \tag{IV.ii.17}$$

Therefore the derivative takes the form

$$b_t = (q_t + iq\epsilon_t)e^{i\epsilon} \tag{IV.ii.18}$$

Hence, if b is zero, the terms involving the derivative of its phase will vanish.

Weakening the constraint, so that q is taken to be sufficiently small as to make q^2 approximately zero, will complicate the issue. This is because the denominator will now have to include the term $r\Omega_b$. All that can be said is that odd terms in the numerator will still vanish on integration.

Therefore, the problem reduces to solving the following two coupled ODEs

$$\begin{aligned}
Q_3^0 - KI_3 &= 2\psi_t\Big\{2p^2|\lambda|^2(\alpha+\beta) + K(2|\lambda|^2p^2\alpha + \delta) \\
&+ \Big[1 - (s^2 - 2|\lambda|^2\delta + |\lambda|^4p^2)\Big] \\
&\quad q\epsilon_t e^{i\epsilon}\sqrt{(2p)}\sin\frac{\psi}{2}\zeta\Big\} \\
Q_8^0 - KI_8 &= 3\psi_t\Big\{p^2(\alpha - 2\alpha\delta) + K(2\delta + \gamma) \\
&+ \Big[1 + (s^2 - 2|\lambda|^2\delta + |\lambda|^4p^2)\Big] \\
&\quad q\epsilon_t e^{i\epsilon}\sqrt{(2p)}\sin\frac{\psi}{2}\zeta\Big]\Big\}
\end{aligned} \tag{IV.ii.19}$$

where the standard integrals have to be modified accordingly. Note that equations IV.ii.2 are no longer valid.

As the integrals can only be solved numerically, values for p and q are required. The initial conditions dictate the value of p and, therefore, it can be taken to be equal to two.

What to take for q presents more of a problem. It should be approximately zero. However, it was necessary to establish whether it could be taken to be zero without affecting the accuracy of the analysis.

Assuming that q was sufficiently small so as to be able to approximate q^2 as zero does not help. There will still be a term in the denominator which depends on the square root of s.

The alternative is to assume that q will remain real, but with a varying magnitude. Again, this will cause problems as the differential equations cannot be solved analytically as it will involve the value of q in the numerator and denominator.

The problem is even worse if b is assumed to vary both its phase and its magnitude. The integrals cannot be solved analytically, and numerical procedures will not be very reliable.

Therefore the regrettable conclusion is that this procedure cannot give quantitative results. It can only give qualitative predictions for the behaviour of the solitons.

IV.iii Single Soliton

This chapter shall conclude with a brief look at the simplest single soliton ansatz. Consider first the denominator which is, in general,

$$(1+(|\mu|^2+|\rho|^2)r^2 - r(|\mu|^2\Omega_b + |\rho|^2\Omega_a) + |\mu|^2|b|^2 + |\rho|^2|a|^2) \quad \text{(IV.iii.1)}$$

To be able to obtain a feel for the results, it is necessary to make some assumptions to simplify the calculations. Firstly assume that b is zero and that μ and ρ are equal. Then, the above will reduce to

$$(1+2|\mu|^2r^2 - r|\rho|^2\Omega_a + |\rho|^2|a|^2) \quad \text{(IV.iii.2)}$$

Now consider the kinetic energy. Under the above assumptions, this will become

$$\begin{aligned} T &= |\rho_t|^2(2r^2+|a|^2-2ar\cos\phi) + |a_t|^2(|\rho|^2+r^2|\rho|^4) \\ &- \bar{\rho}\rho_t\bar{a}_t(2ar\cos\phi - a) - \bar{\rho}_t\rho a_t(2\bar{a}r\cos\phi - \bar{a}) \end{aligned} \quad \text{(IV.iii.3)}$$

For this to be finite, the following relationship must hold

$$|\rho_t|^2 = -\frac{1}{2}|\rho|^4|a_t|^2. \quad \text{(IV.iii.4)}$$

This emphasises the requirement for ρ to be time dependent in this phase space.

Now consider the charge Q_3. The contribution from the pure CP^2 Lagrangian can be shown to be the integral of the following charge density

$$j_3^0 = \left[\bar{\mu}\mu_t - \bar{\mu}_t\mu\right]\left[3r^2|a|^2 - 4r\cos\phi\right] + \left[\bar{a}a_t - \bar{a}_t a\right]\left[|\mu|^2r^2+2\right]\left[1-2r\cos\phi\right]|\mu|^2 \quad \text{(IV.iii.5)}$$

The contribution from the Hopf term is

$$I_3 = -|\mu|^4(4|a|^2 + 2r\cos\phi) \qquad \text{(IV.iii.6)}$$

For the total charge to be finite it is necessary for the coefficient of r^2 to be zero. This provides the constraint

$$3r^2(\bar{\mu}\mu_0 - \bar{\mu}_0\mu) = |\mu|^4 r^2(2r\cos\phi - 1)(\bar{a}a_0 - a\bar{a}_0) \qquad \text{(IV.iii.7)}$$

However, before this can be used to express the derivative of μ in terms of a_0, it must be checked for consistency with the equivalent expression derived from Q_8^0.

The contribution to this from the $\mathcal{L}^0$ is

$$j_8^0 = 3i\Big\{\big[\bar{\mu}\mu_0 - \bar{\mu}_0\mu\big]r^2 + \big[\bar{a}a_0 - \bar{a}_0 a\big]\big[|\mu|^4 r^2(2r\cos\phi - 1)\big]\Big\} \qquad \text{(IV.iii.8)}$$

For completeness, the Hopf contribution is

$$I_8 = -6|\mu|^4 r\cos\phi. \qquad \text{(IV.iii.9)}$$

All terms in the contribution from the pure CP^2 Lagrangian are infinite. The constraint to make this zero is not consistent with the previous constraint for Q_3. Therefore quantitative predictions cannot be made.

If this problem is overlooked, then the finite contribution from $\mathcal{L}^0$ to Q_3 is

$$j_3^0 = -\big[\bar{\mu}\mu_0 - \bar{\mu}_0\mu\big]\big[2p^2 - 2r\cos\phi\big] + 2\big[\bar{a}a_0 - \bar{a}_0 a\big]\big[1 - 2r\cos\phi\big]. \qquad \text{(IV.iii.10)}$$

This does not provide any new qualitative information about the behaviour of a single soliton.

The same conclusions which were drawn for the two soliton case may be applied here. The ansatz being tested is only an approximation to the solution. To proceed further it would be necessary to consider more general cases, with particular regard to which components should be taken to be time dependent.

V

Shadowing of Solitons

Have you ever danced with the Devil in the pale moonlight?
I ask that of all my prey, I just like the sound of it. [1]

[1] The Joker in the film Batman

V.i Introduction

Following on from the work in [32] and the doubts raised by the previous section, it was decided to test whether the solitons do follow the expected homotopy of static solutions using the simplified ansatz described in section IV.i. This was done by stopping the simulation at regular, short time intervals and finding the static approximation which best matched the numerical data.

It was first necessary to consider what was meant by the closest solution. A method was proposed for the O(3) sigma model in [32]. However this only involved comparing one field. Various ways of generalising to two fields were considered. It was initially decided to concentrate on two methods.

The first involved finding the smallest error in $|f|^2$. This had the advantage of testing boths components with one comparison test and that it would never be zero. It was therefore possible to consider both absolute and relative error distributions.

The second test used was to generalise the method used in Piette's paper [32] and consider the sum of the absolute difference in each field:

$$\text{error} = |W_{\text{evolved}} - W_{\text{static}}|^2 + |W^1_{\text{evolved}} - W^1_{\text{static}}|^2 \qquad \text{(V.i.1)}$$

As there remains the possibility that either or both of the fields could be zero, only the absolute error could be used for this test.

It then remained to consider whether the maximum absolute error or the average should be minimised. It was decided to initially use both on the first test and see which performed better.

An alternative but much cruder test is to pick five points from the field distribution for each component. These are then used to match the five complex coefficients given by

$$w(z) = \lambda \frac{(z-a)(z-b)}{(z-c)(z-d)}. \qquad \text{(V.i.2)}$$

Some useful results can be obtained from this.

The scattering behaviour in pure CP^2 is fairly well understood (see for example [42] for a review) and therefore it was an obvious choice to test the various comparison procedures.

When the data in this chapter is compared with earlier work, it should be borne in mind that for the initial results, the velocity used was set low. This meant the scattering period was prolonged and allowed more information to be taken from it.

Also to be remembered is that in all the numerical simulations time is relative as it depends on the algorithm used. It is expressed in terms of seconds for aesthetical reasons alone.

V.ii Pure CP^2

V.ii.a Introduction

The initial results from the comparison procedure over a short time period suggested that b in equation II.ii.5 remains zero throughout the numerical simulation. Therefore, it appeared to be justified to take b to be constant in equations IV.ii.8.

There was though a problem when the solitons passed through the origins. It did not give, as expected, the best static approximation to be two solitons on top of each other at the origin. This meant that it was necessary to investigate whether the test procedure or the initial ansatz was fundamentally flawed.

For this reason, the ansatz for the fields were modified to be

$$\begin{aligned} W &= h(r)x_+^2 \\ \text{and} \qquad W^1 &= g(r)x_+. \end{aligned} \tag{V.ii.1}$$

For a static solution of this form, the Euler Lagrange equations will give the following second order ODEs for h and g

$$\begin{aligned} (1+g^2r^4+h^2r^2)(g_{rr}r+5g_r) &= gr^4(rg_r^2+4gg_r) \\ &+ hr^2(rg_rh_r+hg_r+2gh_r) \\ (1+g^2r^4+h^2r^2)(h_{rr}r+3h_r) &= hr^2(rh_r^2+2hh_r) \\ &+ gr^4(rg_rh_r+hg_r+2gh_r) \end{aligned} \tag{V.ii.2}$$

For equation V.ii.1 to be a valid ansatz, the above equalities must be trivially true.

Assume that a polynomial approximation can be used in the region close to $r = 0$,

$$\begin{aligned} h(r) &= a_0 + a_1 r + a_2 r^2 + \ldots \\ g(r) &= b_0 + b_1 r + b_2 r^2 + \ldots \end{aligned} \qquad \text{(V.ii.3)}$$

It is clear that the constant term trivially satisfies the ODEs.

Substitute the polynomial expansions into the differential equations. There will be a divergent term of order $\frac{1}{r}$ and, as the Euler Lagrange equations must be finite, the coefficient to this must be trivial. Therefore this will imply that a_1 and b_1 must be zero.

However, consistency in the two equations will require a_2 and b_2 (and also, by induction, a_n and b_n, for all n) to be zero. Therefore this analysis simply confirmed that the coefficients g and h must be independent of r in pure CP^2.

Further examination of the data with the comparison procedure, revealed the true nature of the problem. The distance trajectory predicted by the programme appeared to suggest that the solitons were at the origin for a finite length of time (see, for example, figure V.1).

However this is misleading. By looking at the contour plots for CP^2 at a time period taken to be within the scattering process, it becomes clear that the two solitons are not coincident, see figures V.2.

They are overlapping, but the small separation distance between them causes a distortion in the energy distribution which pushes the maximum of the field to be between the two centres of the solitons. The programme uses this maximum to calculate the position of the solitons and hence fails to pick out the true structure.

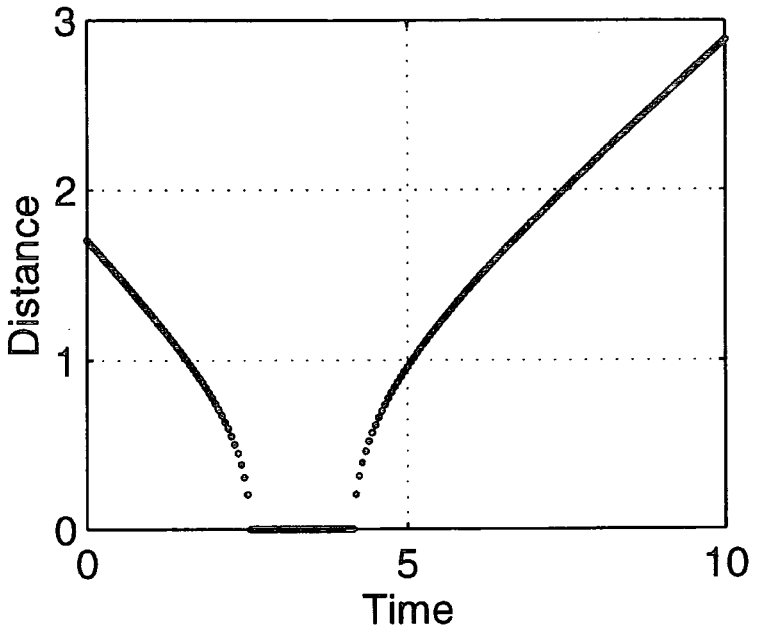

Figure V.1: Distance trajectory predicted by programme for pure CP^2

The real picture is that the solitons pass through the origin but do not remain there for a finite period of time. However this should be qualified: the individual solitons are not well defined when there is so much overlap. Therefore this can only be a subjective description.

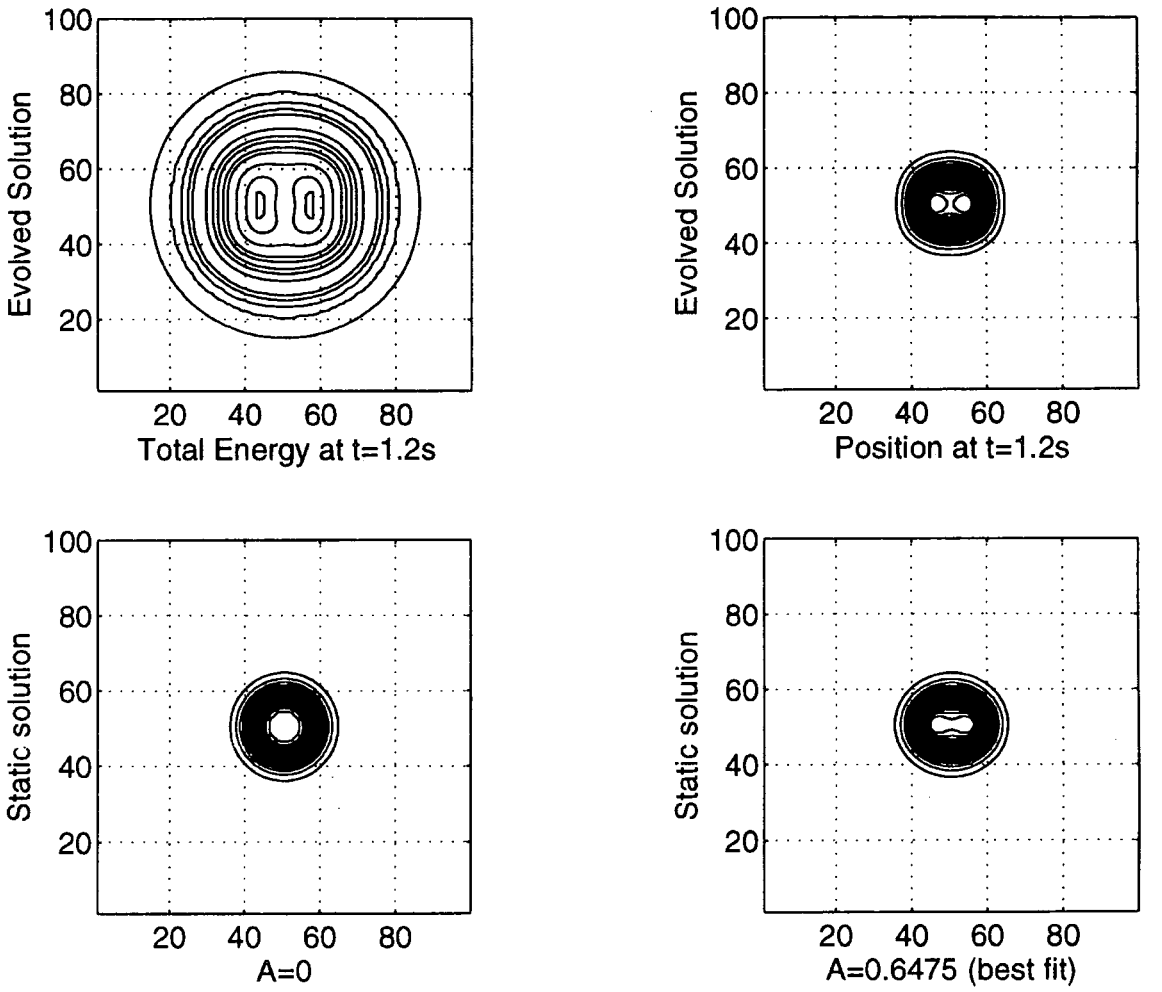

Figure V.2: Comparison of Contour Plots

V.ii.b Minimising the denominator

It now remains to decide which of the minimising procedures to use. In figure V.3 the trajectory for CP^2 is shadowed using the first procedure.

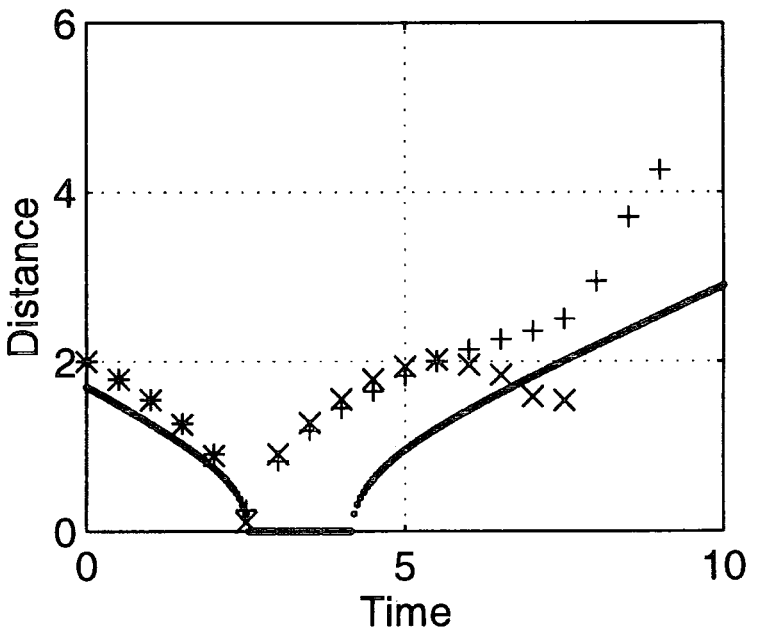

Figure V.3: Numerical prediction compared with predicted static solutions

+++ when average error is minimised
xxx when maximum error is minimised

The two types of error tested agree closely up until scattering. The slight discrepancy between the simulation and the predicted solution is due to the closeness of the two solitons: they are not "well separated".

However they do not predict the same trajectory afterwards and both methods diverge away from the expected result soon after the

scattering. This result, taken at face value, would suggest that the simple ansatz is beginning to break down. It is therefore important to consider whether the procedure being used is valid. It is necessary to look for the main cause of the discrepancy.

The programme uses the energy density to calculate the position. Therefore the maximum total and kinetic energy are plotted in figure V.4. They are well behaved over the time evolution and hence there is no reason to believe that this could be the cause of the problem.

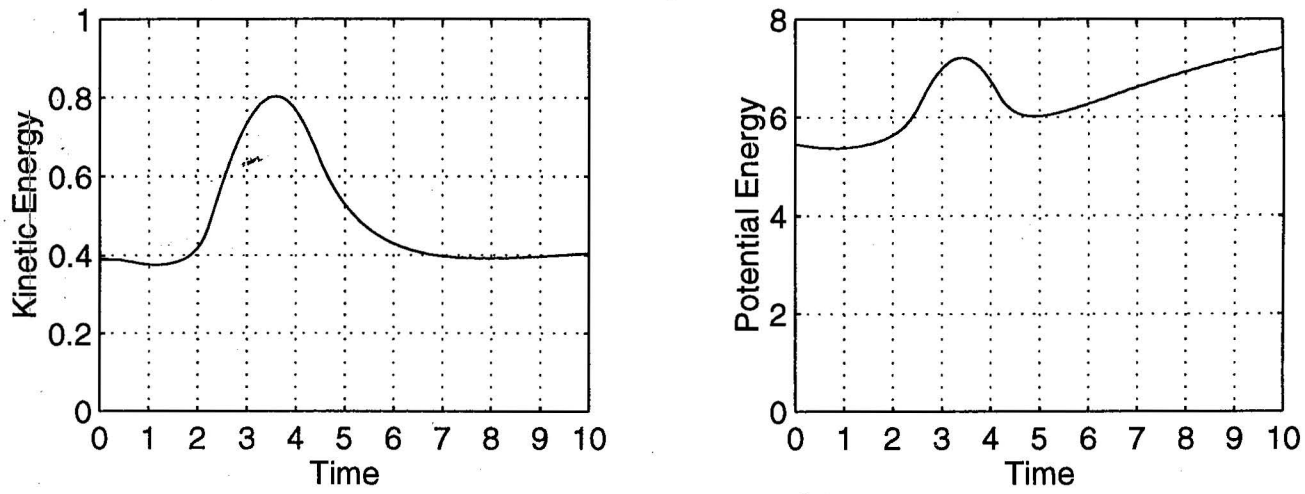

Figure V.4: Kinetic Energy for CP^2

Also the value of $|f|^2$ is always strictly greater than one. Therefore the calculational errors brought into the comparison procedure should be small. The problem appears to be in the test used.

The distribution of errors around the optimal values of the parameters were recorded. There is no clear way to represent graphically the variation in three complex parameters on a single graph. Therefore, a way had to be found for expressing this information in two or three dimensional plots.

As all the evidence indicated that b was constantly zero, the error distribution in this was not calculated. Initially, μ was kept constant and three dimensional graphs were plotted for the variation in a.

Consider the error distribution around optimal parameters for the closest static solution corresponding to t being ten seconds in figure V.3 (the error distributions for positions just after the starting are expected to be insignificant and hence are not of much use). Figure V.5 shows the maximum error distribution, figure V.6 the average error distribution for the absolute error, and the next two graphs give the same distribution for the relative errors.

It can be seen from these results that the distributions are not well defined. Therefore it would appear that the position of the minimum becomes blurred and hence the procedure becomes unreliable.

V.ii. **Pure** CP^2

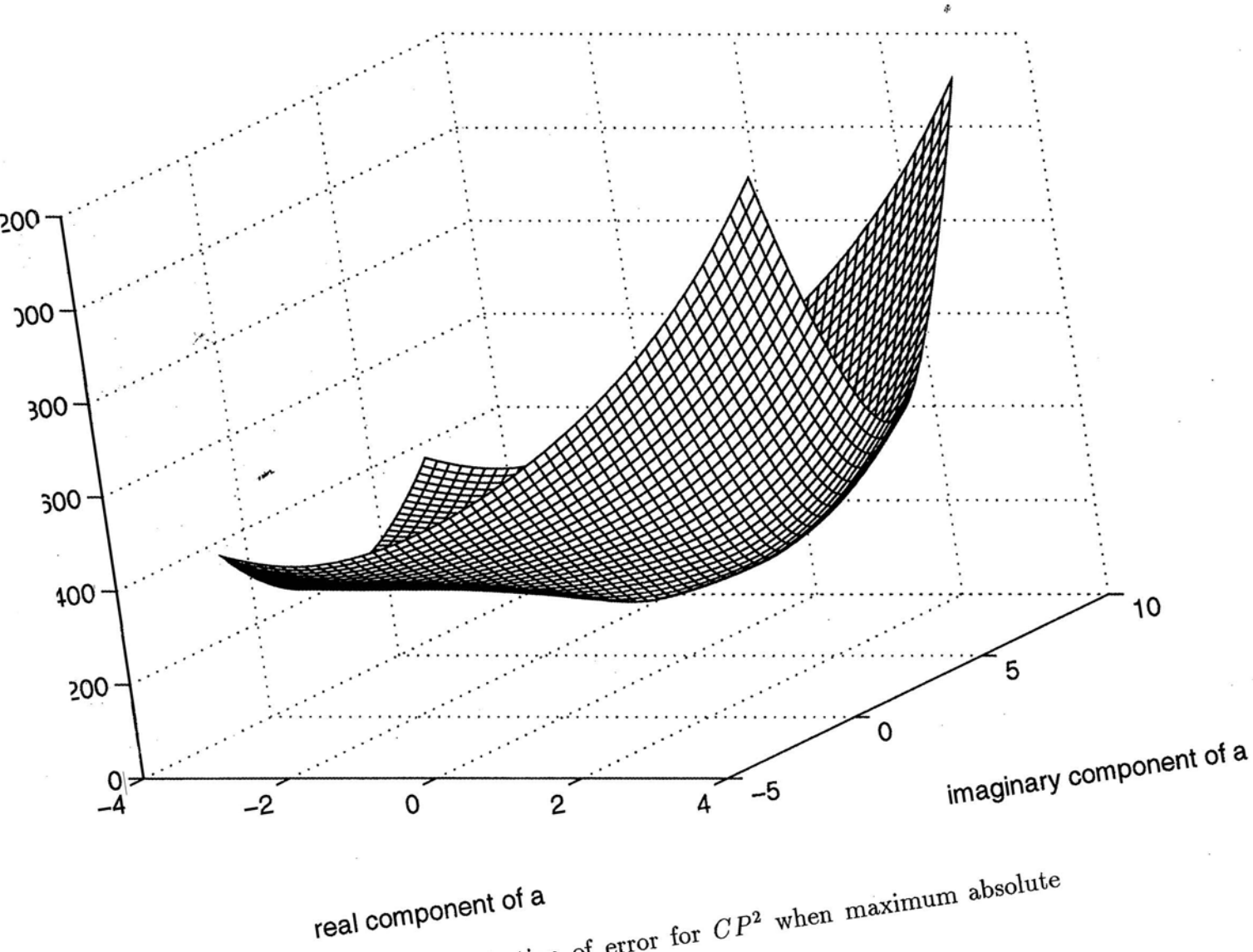

Figure V.5: Distribution of error for CP^2 when maximum absolute error in $|f|^2$ is minimised

V.ii. **Pure** CP^2

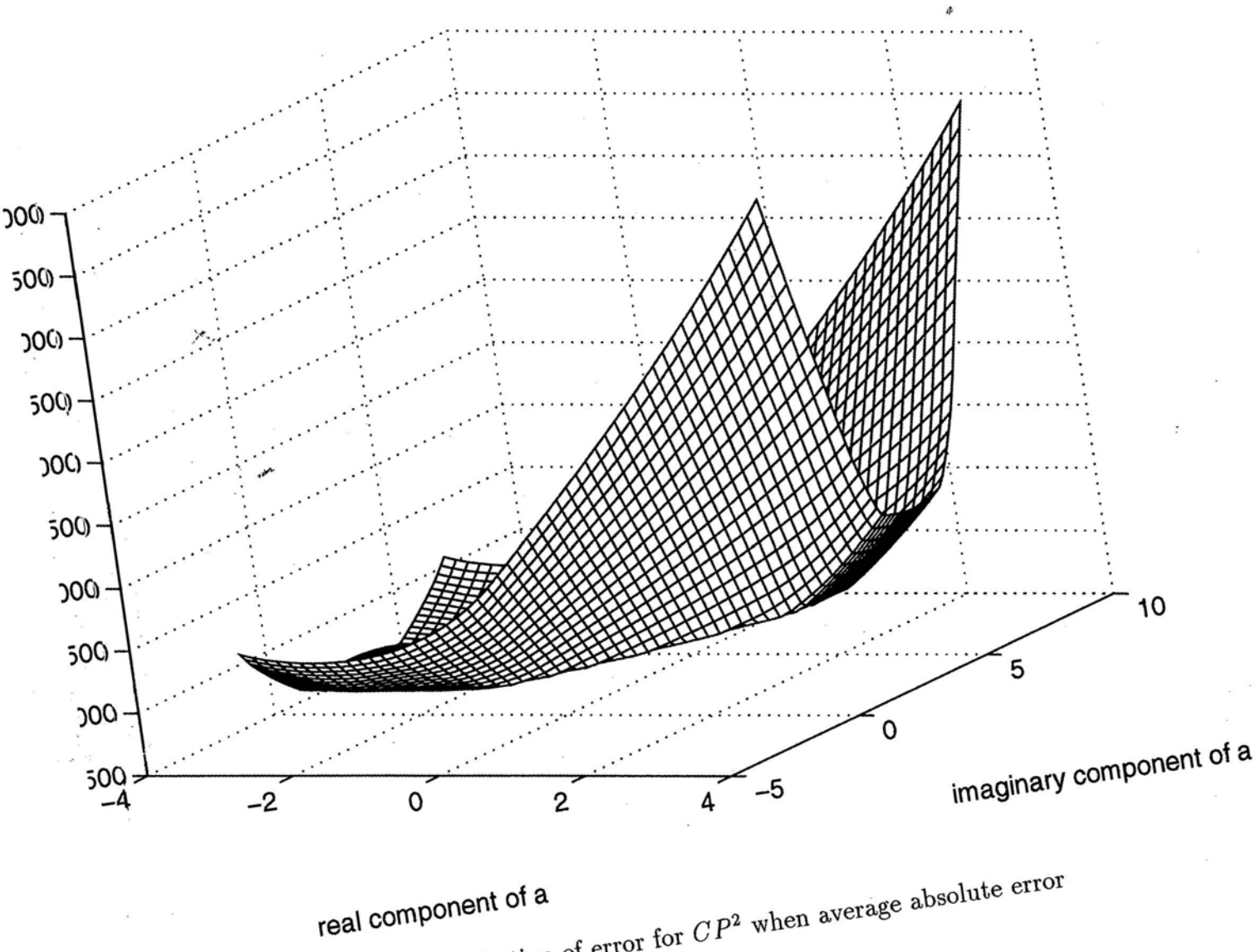

Figure V.6: Distribution of error for CP^2 when average absolute error in $|f|^2$ is minimised

V.ii. **Pure** CP^2

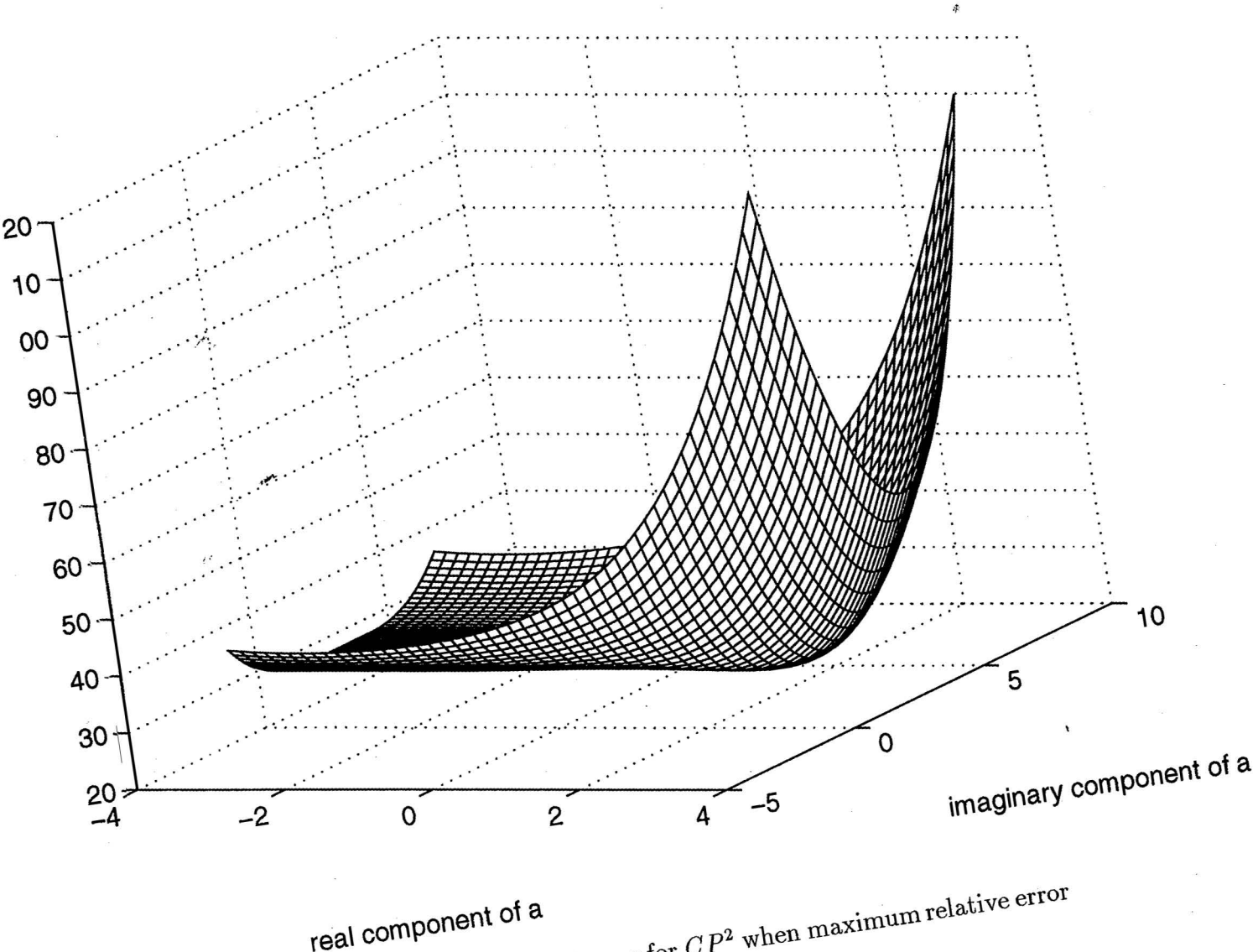

Figure V.7: Distribution of error for CP^2 when maximum relative error in $|f|^2$ is minimised

V.ii. **Pure** CP^2

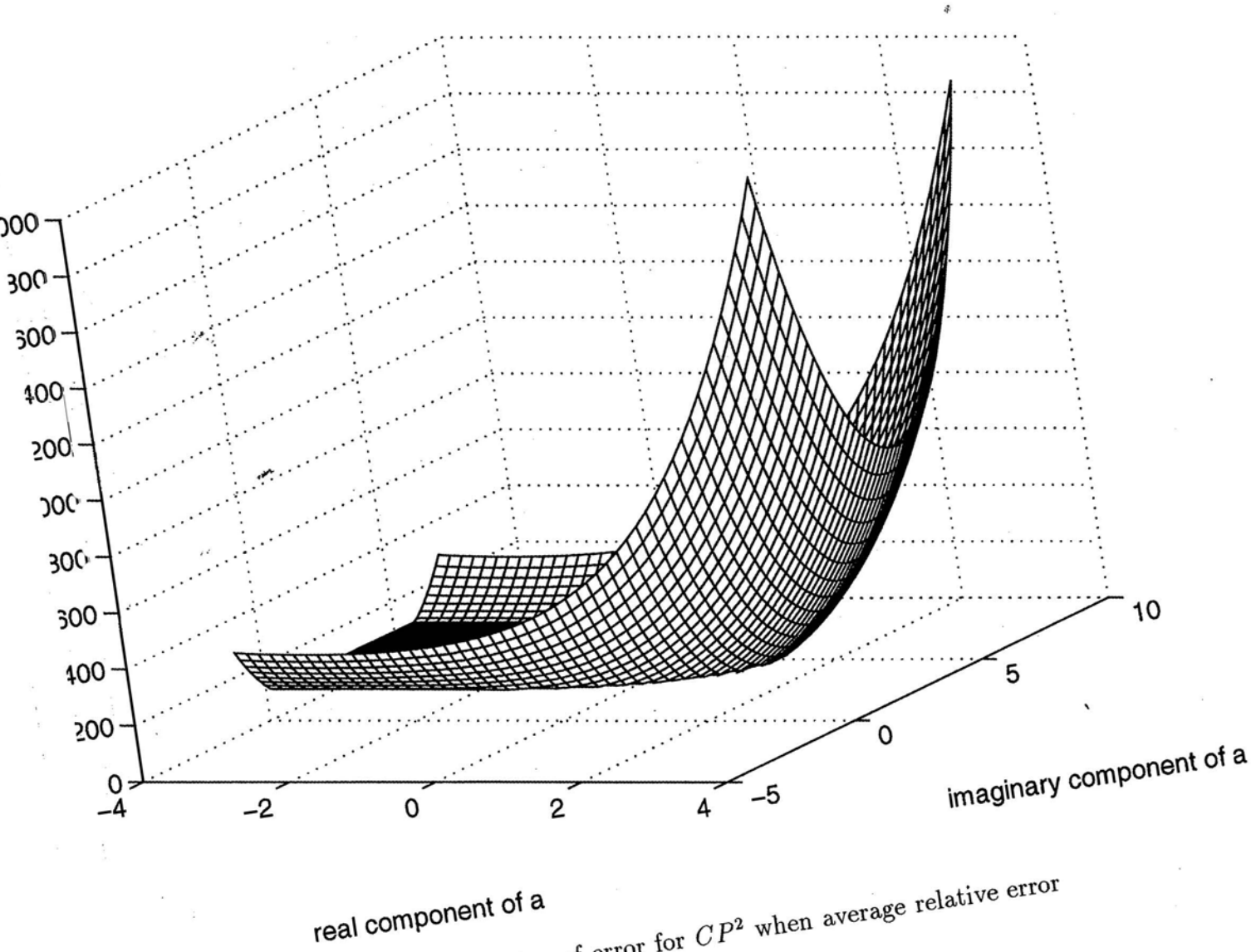

Figure V.8: Distribution of error for CP^2 when average relative error in $|f|^2$ is minimised

The distribution of the errors for λ was also considered. Due to the conclusions drawn from the previous chapter, it was believed that this should be constant throughout the evolution. All the tests agreed that it would remain real, and hence it is not necessary to consider three dimensional plots, only the real component of λ will be considered.

The results for the maximum and average error being minimised are shown in figures V.9 and V.10 respectively. They are both well defined and predict λ to be approximately 0.6, which was the initial value.

The relative average error (shown in figure V.12) is also well defined and agrees with the absolute error minimisation. However the relative maximum error (see figure V.11) is not as refined and gives a different value.

This is the first indication that it is preferable to test the average rather than the maximum error distribution. It also shows that there is no advantage in taking the relative error and, in fact, it could well be more vague.

All the evidence therefore suggests that this first test is too crude. There exists a range of values of a which it predicts to give the best fit. The programme keeps the first value it comes across and ignores the others, thereby missing the closest approximation.

There is not an obvious way to surmount this problem. The test has thus been shown to be unsatisfactory.

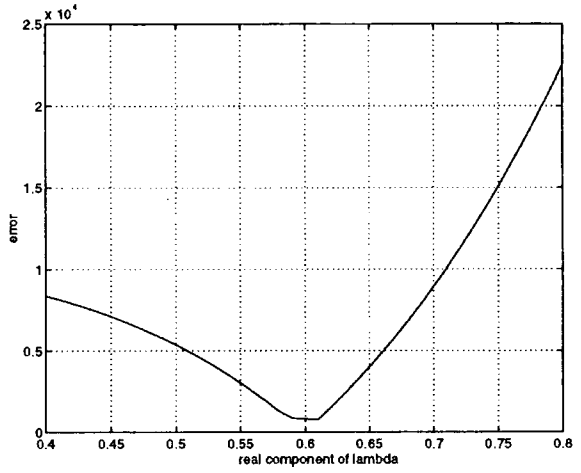

Figure V.9: Effect of the real component of λ on the maximum absolute error in $|f|^2$

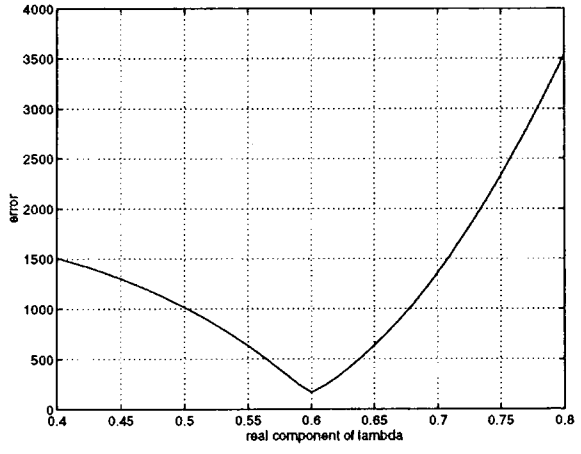

Figure V.10: Effect of the real component of λ on the average absolute error in $|f|^2$

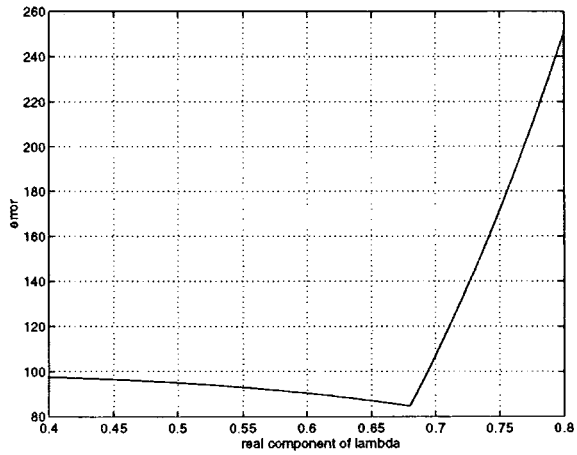

Figure V.11: Effect of the real component of λ on the maximum relative error in $|f|^2$

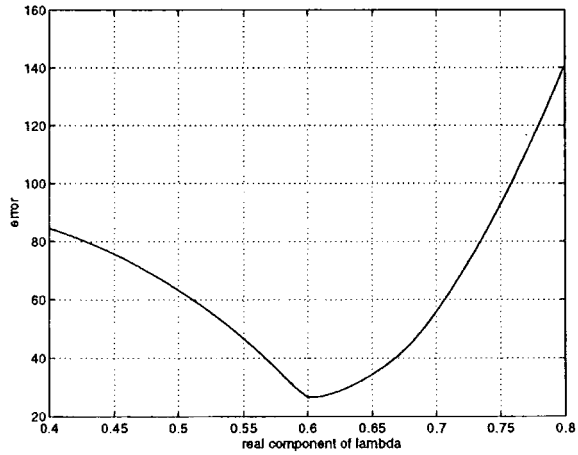

Figure V.12: Effect of the real component of λ on the average relative error in $|f|^2$

V.ii.c Minimising the difference in the fields

Now consider the second test. The distribution of the errors around the optimum value of a for fixed λ is shown in figure V.13 for the maximum error and figure V.14 for the average error. It can clearly be seen that these tests are more focused with the average being the better of the two.

The corresponding graphs for the real part of λ are shown in figures V.15 and V.16. Once again the average error minimisation gave the better focus. Therefore the average error in equation V.i.1 was minimised to find the nearest static solution for a range of time points.

V.ii. **Pure CP^2**

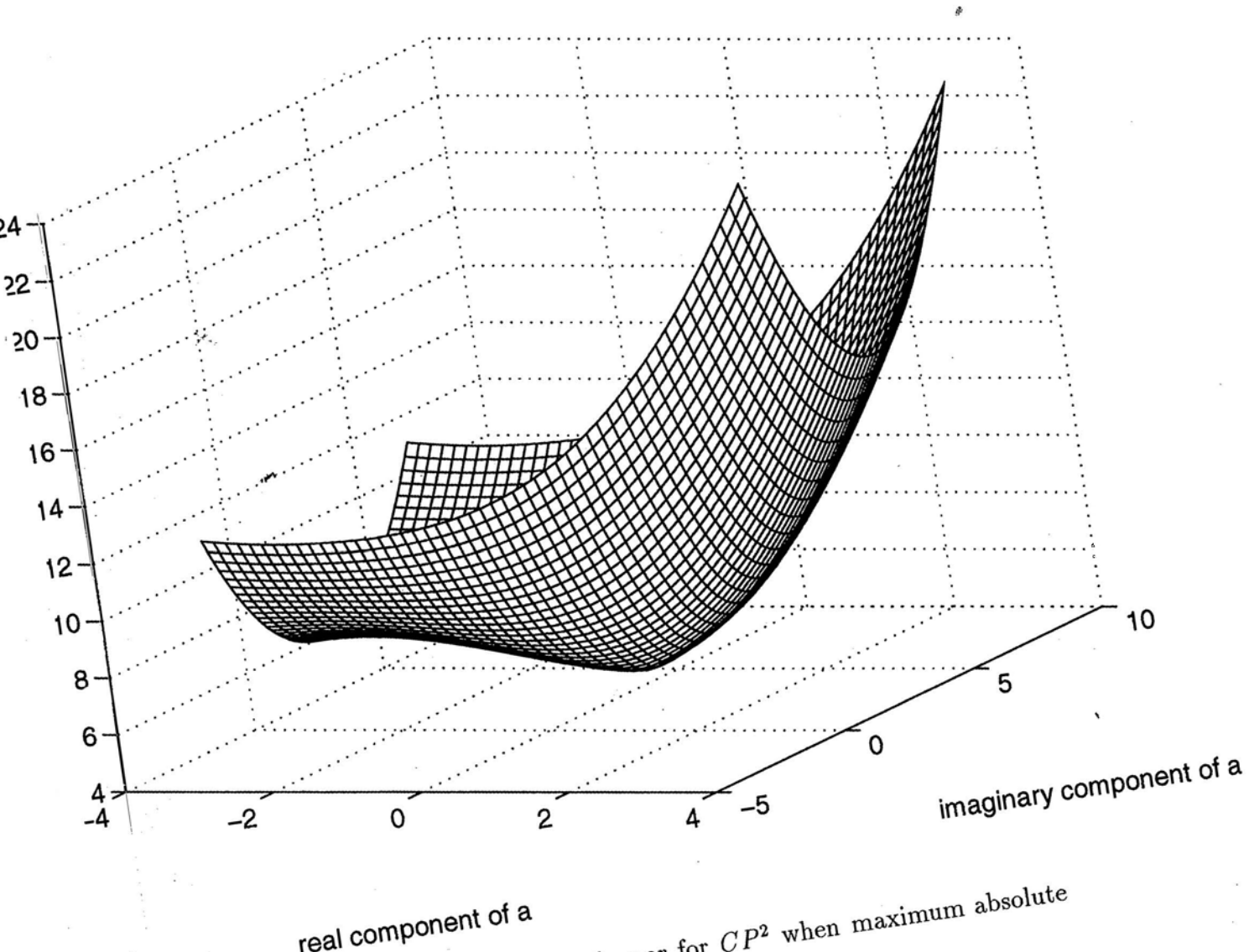

Figure V.13: Distribution of error for CP^2 when maximum absolute error for ntest V.i.1 is minimised

V.ii. **Pure CP^2**

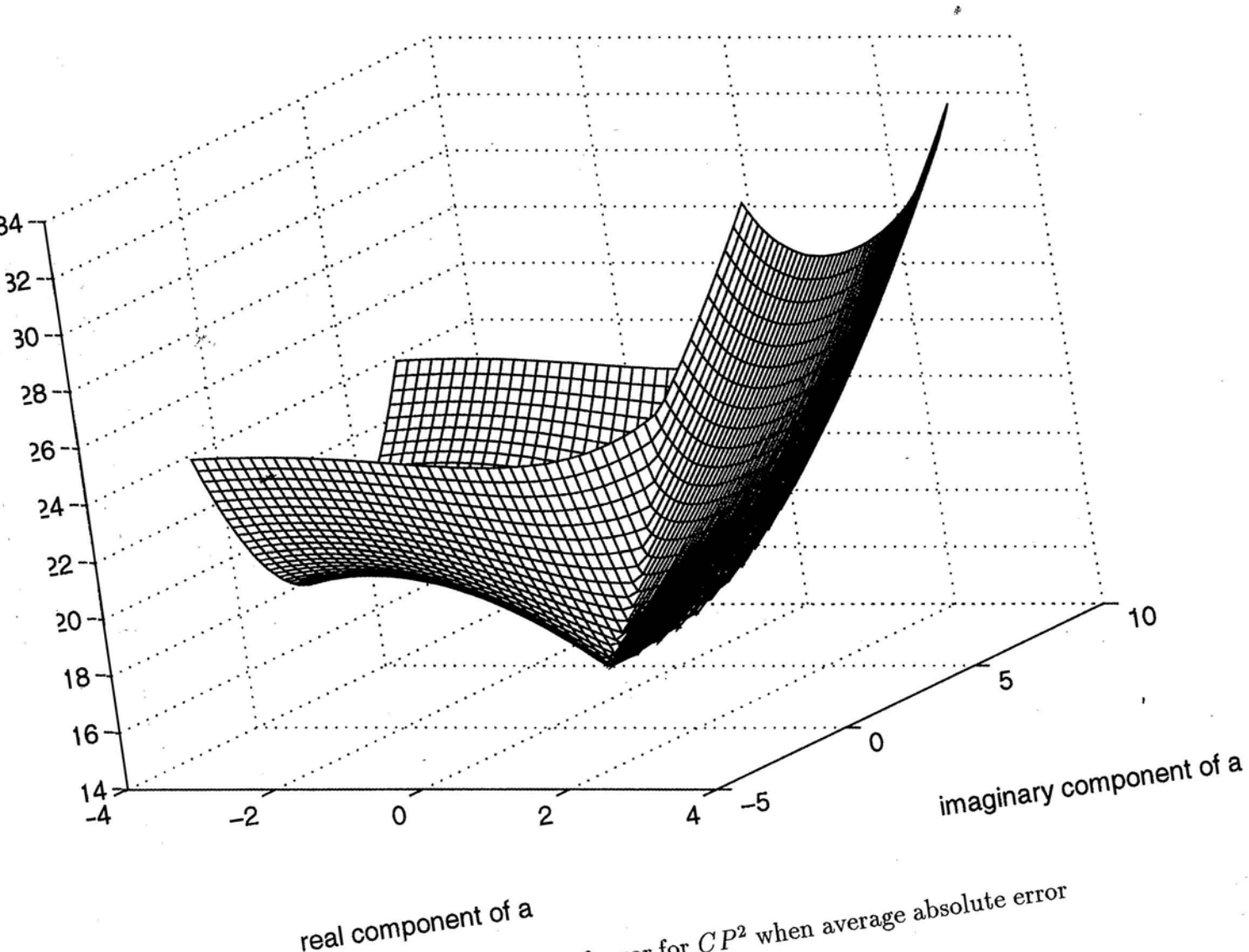

Figure V.14: Distribution of error for CP^2 when average absolute error for test V.i.1 is minimised

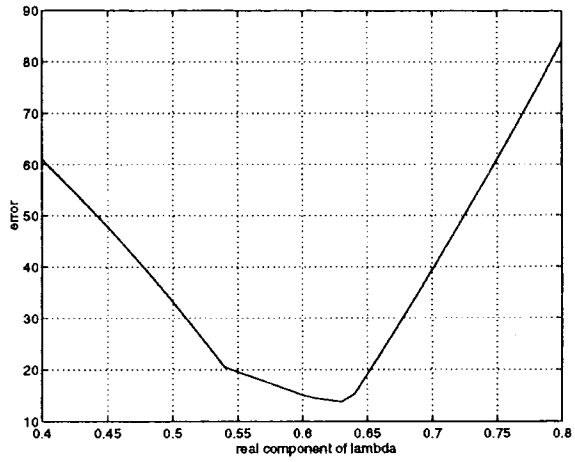

Figure V.15: Effect of the real component of λ on the maximum absolute error in the fields

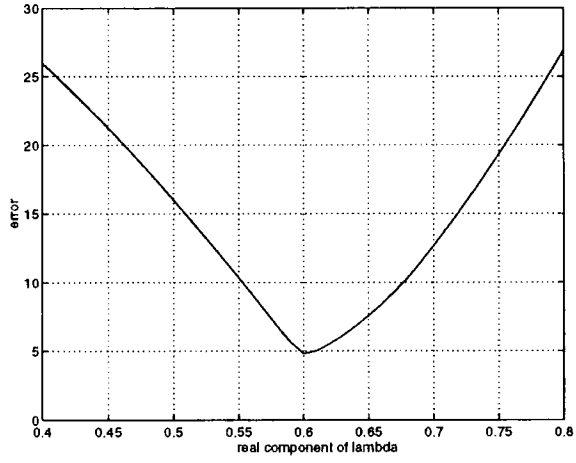

Figure V.16: Effect of the real component of λ on the average absolute error in the fields

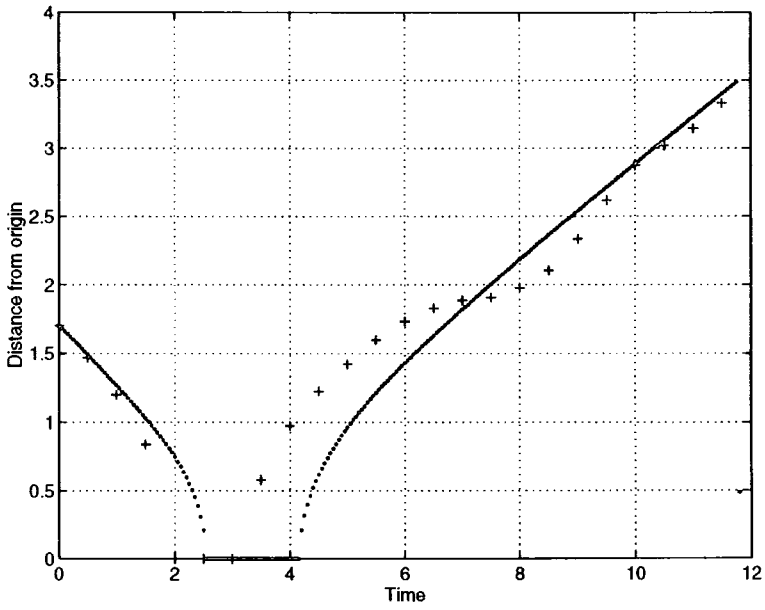

Figure V.17: Numerical prediction compared with closest static solutions

.... Numerical prediction
+++ Closest static solitons

Consider first the distance of the solitons from the origin. The programme calculates this from the maximum of the energy distribution and in figure V.17 this is compared with the results from the comparison procedure.

The positions are calculated from the optimal values for the parameters predicted by the comparison test, using the same method as for the evolution programme. There is still some discrepancy during the scattering, but by ten seconds it is converging on the known solution.

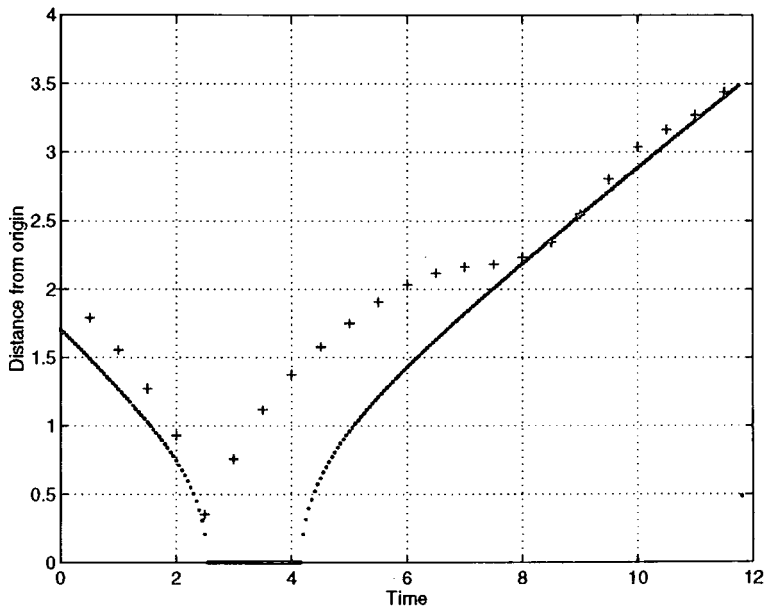

Figure V.18: Numerical prediction compared with predicted value of parameter a.

.... Numerical prediction
+++ a

In figure V.18 the distance predicted by the programme is compared with the parameter a associated with the closest static soliton solution. There is a discrepancy at the start because the solitons are initially placed close together. Therefore a is not expected to be equal to the position of the solitons.

Also, as expected the difference widens during the scattering itself. However, when the soliton are sufficiently far apart there is close agreement. This confirms the interpretation of a as being approximately the position of two well separated solitons.

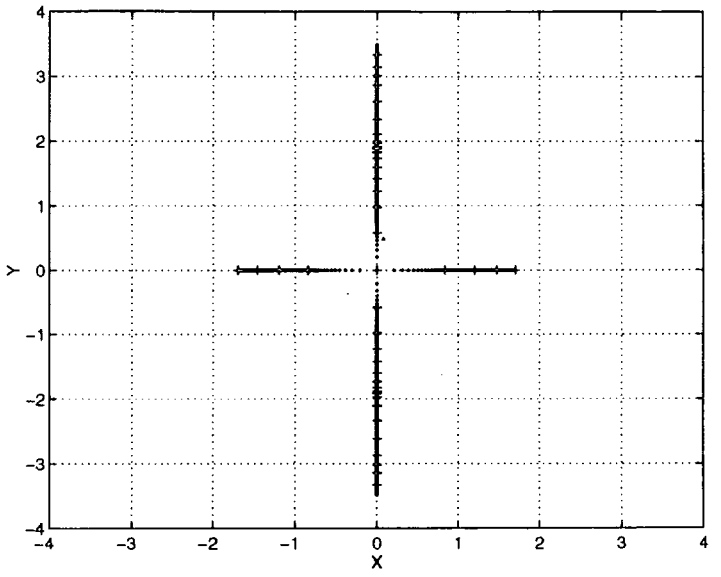

Figure V.19: Numerical prediction compared with closest static solutions

.... Numerical prediction
+++ Closest static solitons

Now consider the actual positions of the solitons in two space. These are compared in figure V.19. It can be seen that they are not inconsistent, they both predict orthogonal scattering.

In figures V.20 and V.21 the x and y co-ordinates respectively are plotted against time. It can be seen that the x co-ordinate is predicted well. The y coordinate disagrees during the scattering, but soon settles down to a good agreement after a finite time.

The last remaining concern is whether λ varies. Recall from chapter III that if this parameter varied, it caused the differential equations to diverge. As can be seen from figure V.22, the variation is insignificant until eight seconds.

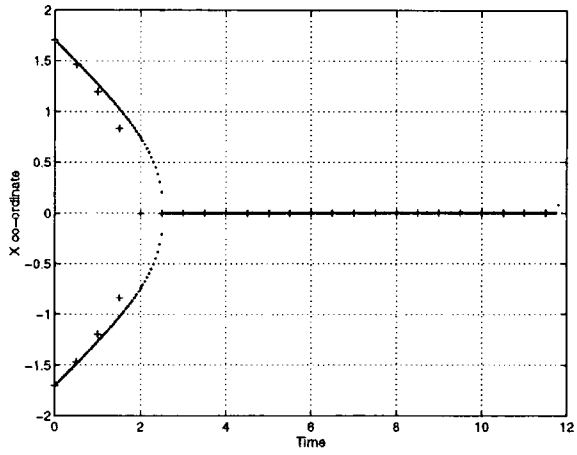

Figure V.20: Numerical prediction compared with predicted static solutions

.... Numerical prediction
+++ Closest static solitons

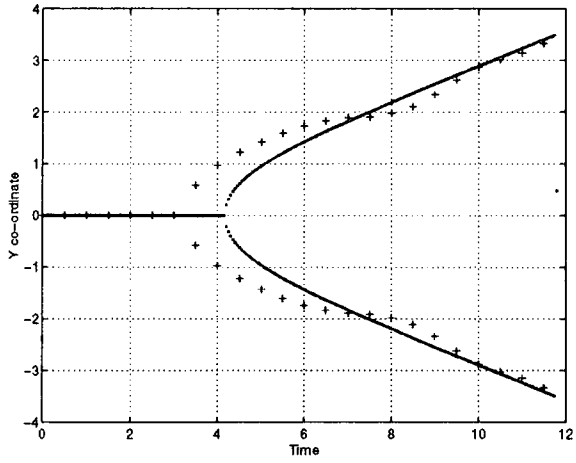

Figure V.21: Numerical prediction compared with predicted static solutions

.... Numerical prediction
+++ Closest static solitons

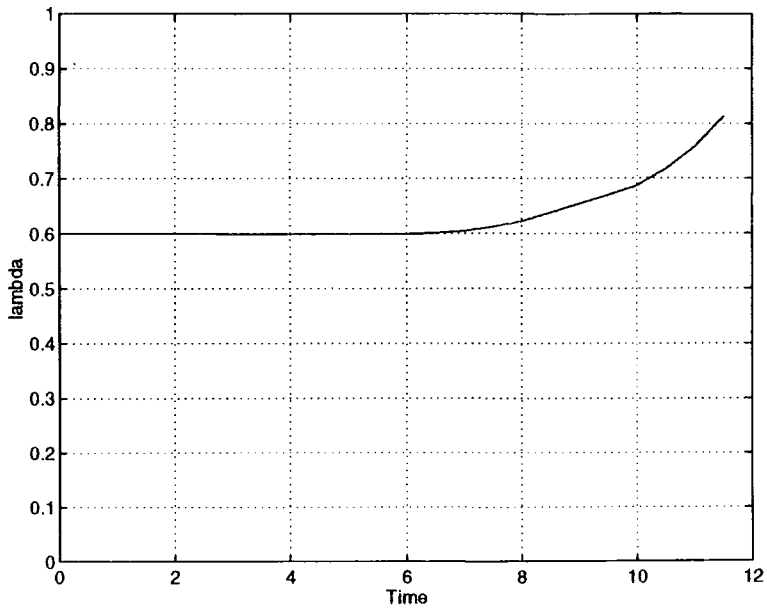

Figure V.22: Variation of λ during scattering process for pure CP^2

Examination of the three dimensionals plots suggest that the solitons are elongated during scattering. This could provide a reason for the variation in λ.

Alternatively, the discrepancy could simply be due to calculational errors. Note that computational problems caused the programme to crash just after eleven seconds.

Hence a relatively reliable test has been found for pure CP^2 and the simplified ansatz holds during the scattering process. The next section shall consider the effect of the Hopf term on this hypothesis.

V.iii Full Lagrangian

V.iii.a Minimising the difference in the fields

The results for the model with $K = 1$ is shown in figure V.23. The numerical results agree with the ansatz until just before scattering. It also agrees with the quantitative picture seen from a sequence of contour plots taken at half second intervals.

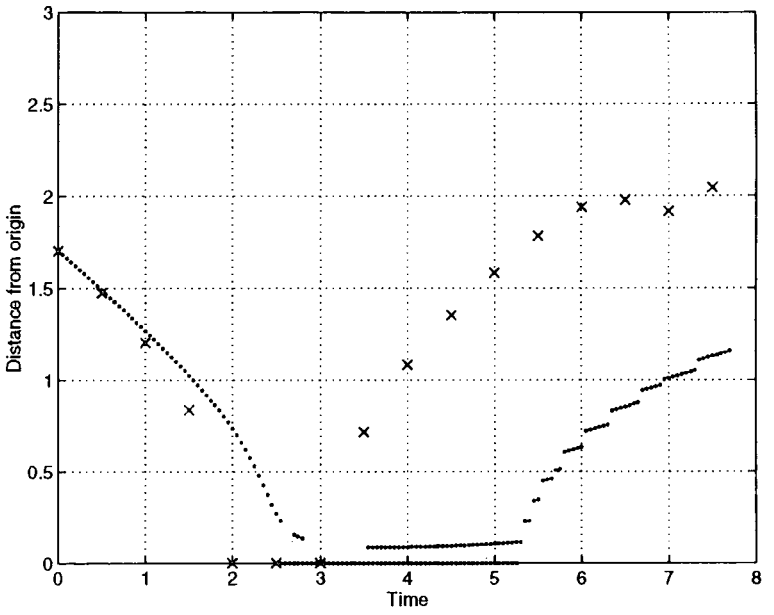

Figure V.23: Comparison of numerical prediction (dotted) with predicted static solutions (crossed)

However, there is severe disagreement after scattering. The predictions for the actual position of the solitons is even worse, see figure V.24. The reason for this had to be established.

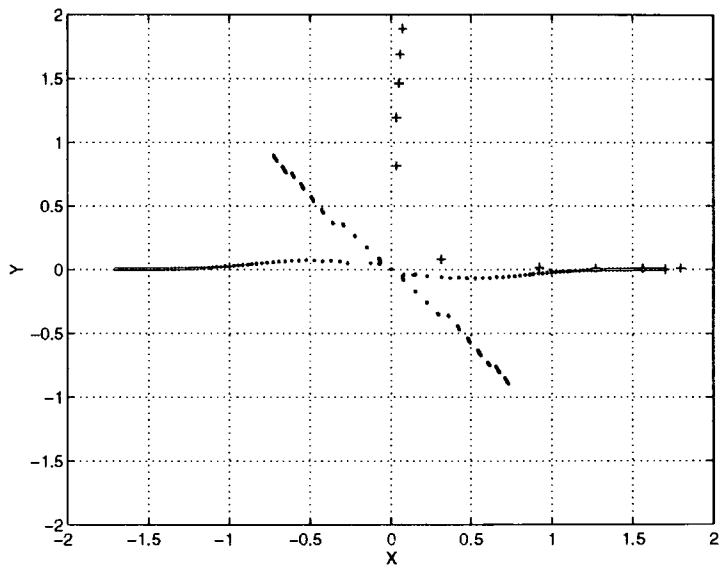

Figure V.24: Comparison of numerical prediction (dotted) with predicted static solutions (crossed)

The co-ordinates of the position were plotted against time, the results being shown in figures V.25 and V.26. Once again the x co-ordinate has been predicted fairly well but the comparison programme has a tendency to over estimate the y co-ordinate.

Therefore the validity of the comparison programme was once again under suspicion. The energy distributions were well behaved and hence did not suggest a fundamental problem.

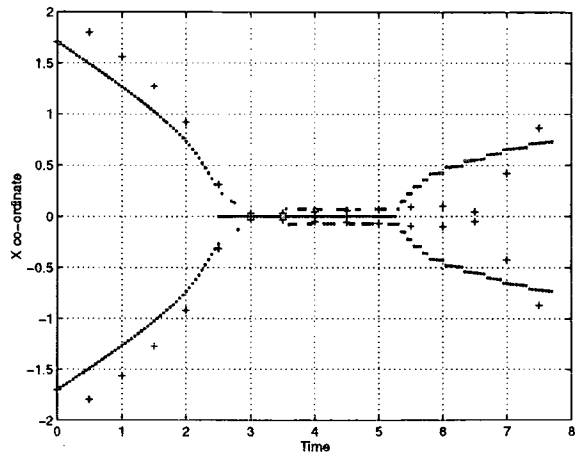

Figure V.25: Comparison of numerical prediction (dotted) with predicted static solutions (crossed)

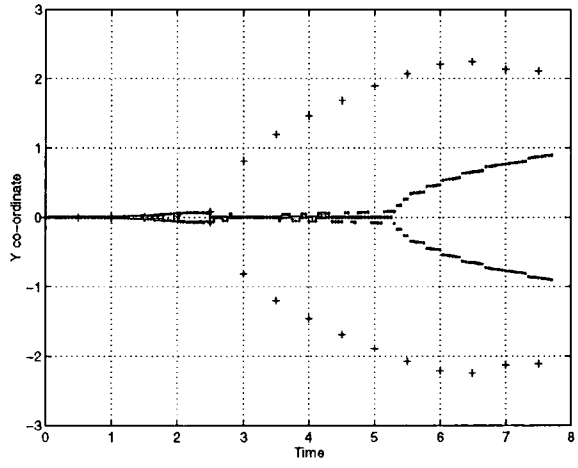

Figure V.26: Comparison of numerical prediction (dotted) with predicted static solutions (crossed)

It can be seen from figure V.27 that the modulus of λ is predicted to be approximately conserved. However it does pick up a small imaginary component. This is probably because the Hopf term affects the phase of the position.

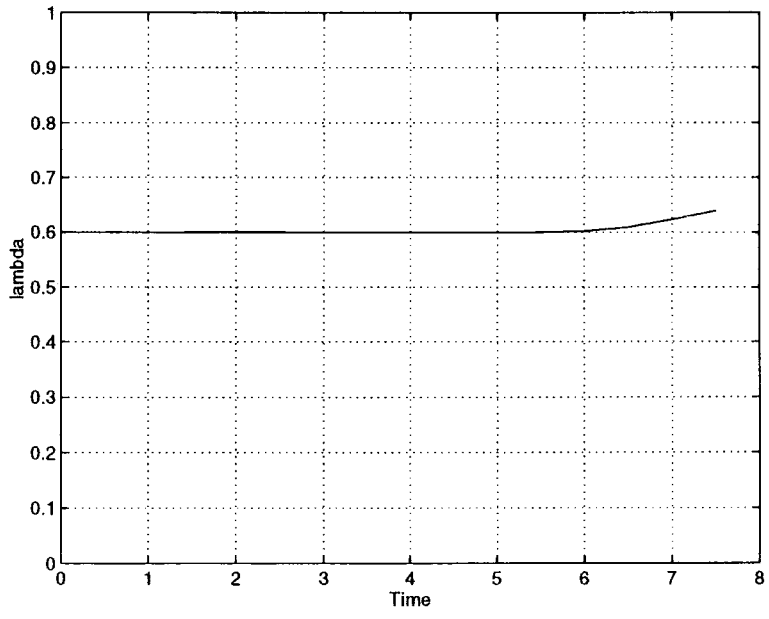

Figure V.27: Optimal values of μ for each static solution closest to the numerical results

However, a clue to the problem may have been given in figure V.25. There is an indication that the results may be starting to converge at seven seconds. It is possible that the programme crashed before agreement was reached.

The numerical evolution programme was more liable to crash for small velocities. Therefore, the comparison procedure was repeated for a faster velocity (v being set to 0.5 as opposed to 0.2).

The results for the distance from the origin is shown in figure V.28. There is good agreement before the solitons collide, but not during the collision itself. It can be seen that the results start to oscillate violently around the numerical solution after approximately six seconds.

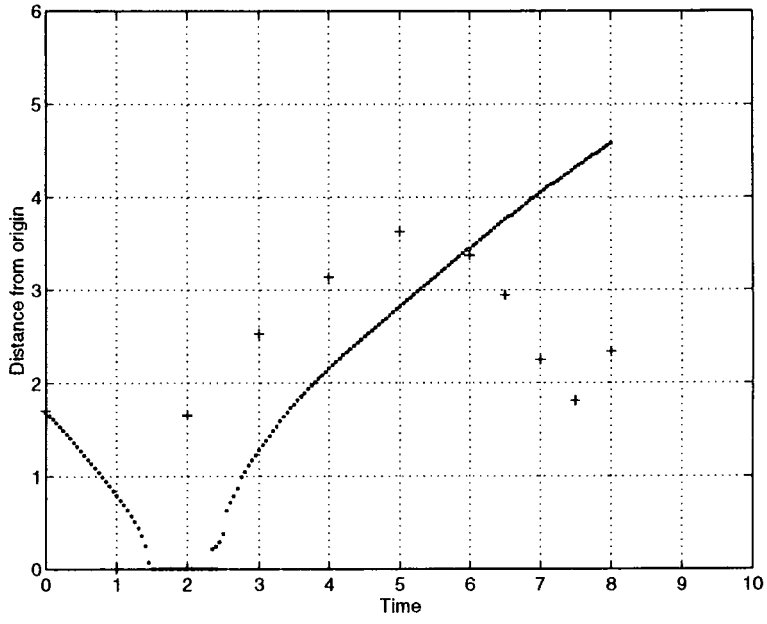

Figure V.28: Comparison of numerical prediction (dotted) with predicted static solutions (crossed)

The positions of the solitons are shown in figure V.29. These results are even worse. It shows that the procedure is clearly breaking down. When the coordinates are plotted against time (see figures V.30 and V.31), it can be seen that the major problem is with the imaginary component. The "closest fit" is not even close to the predicted solution.

For completeness, the variation in λ for each predicted solution is shown in figure V.32.

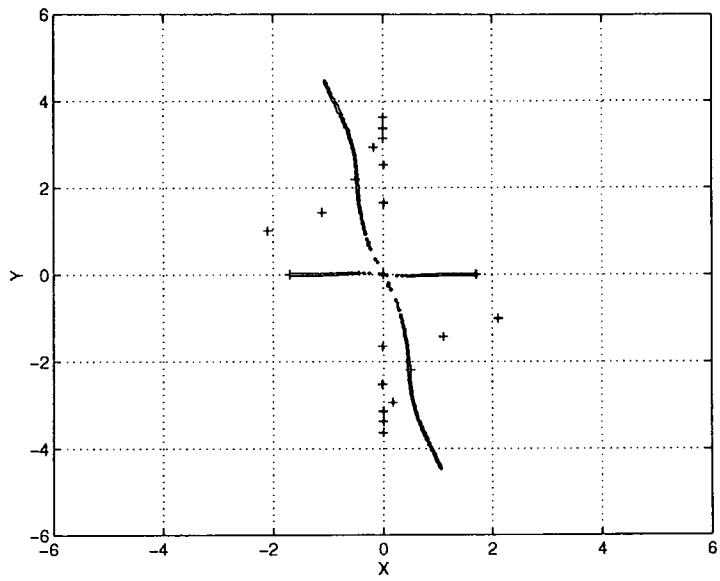

Figure V.29: Comparison of numerical prediction (dotted) with predicted static solutions (crossed)

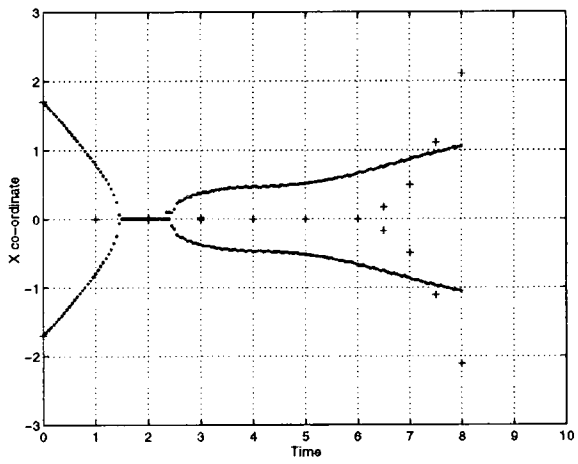

Figure V.30: Comparison of numerical prediction (dotted) with predicted static solutions (crossed)

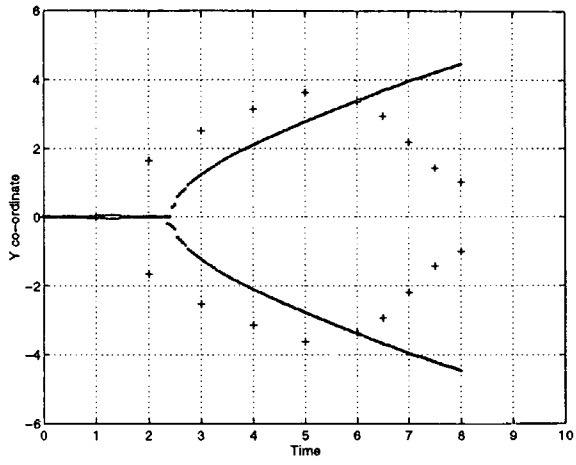

Figure V.31: Comparison of numerical prediction (dotted) with predicted static solutions (crossed)

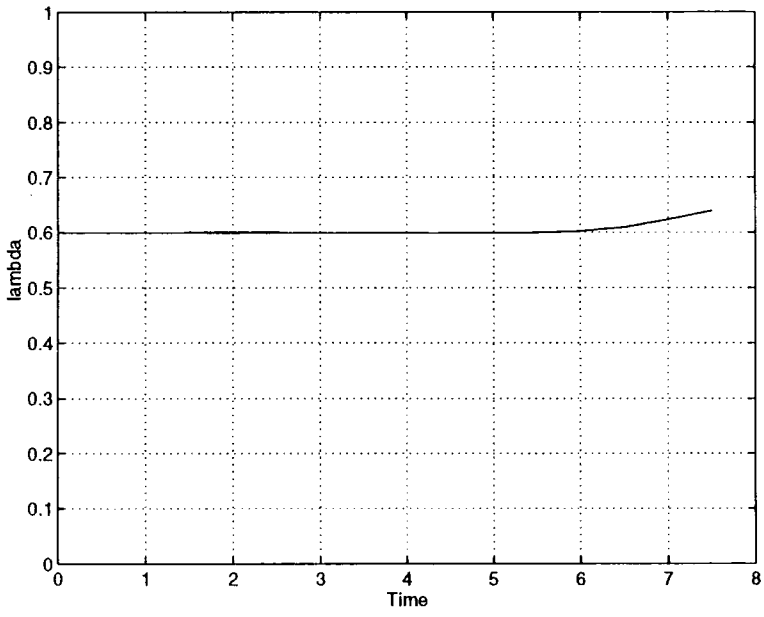

Figure V.32: Optimal values of λ for each static solution closest to the numerical results

The error distribution around the "optimal" value of a is shown on the next page. It can be seen that this is not well defined and hence the minimum value is blurred. Therefore, the comparison procedure is unsatisfactory for the full Lagrangian. It does not provide a useful means of testing for the closest solution.

A modified version of this test was also considered. It involved dividing the fields by $|\mathbf{f}|^2$ raised to some integral power. However, this did not affect the shape of the error distributions and hence will not be considered in detail.

V.iii. **Full Lagrangian**

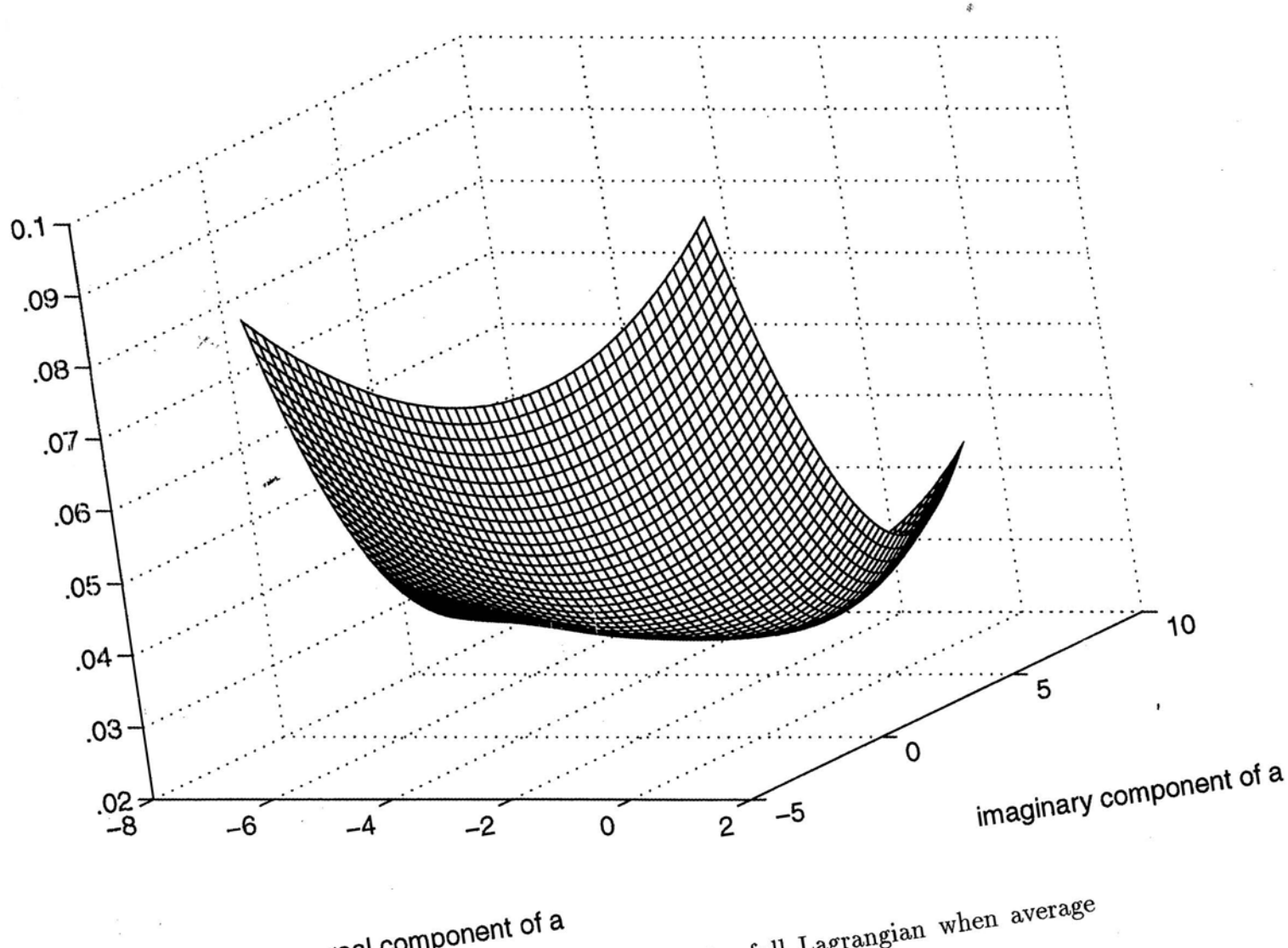

Figure V.33: Distribution of error for full Lagrangian when average absolute error for test V.i.1 is minimised

V.iii.b Crude Test

The crude test mentioned in the introduction was considered. As only five points wee considered, the fit was was not independent of the choice of points. However, it was hoped that some useful results would come from it.

The following expression,

$$w(z) = \lambda \frac{(z-a)(z-b)}{(z-c)(z-d)}, \qquad \text{(V.iii.1)}$$

was to be fitted to the data. The fields distributions are symmetrical and it was therefore decided to reflect this in the points chosen.

Therefore, because an odd number of points were needed, one of the points was taken to be the origin. The next two points were taken to be close to the location of the maximum of the field densities. This reflected the importance of fitting these points.

The final two points were taken to be near the boundary in the opposing quadrants. It was hoped that choosing data values in all the quarters of two space would minimise the errors.

The symmetry in the data was reflected in the fit given to the parameters. It indicated that a equalled $-b$ and c equalled $-d$, as was to be expected.

The three parameters c, d and λ were noticably affected by the position of the two data values located nearer the boundary. The closer they were to the boundary, the larger these parameters became.

This is compatible with the notion that they tend to infinity whilst their ratio remains finite. It does not confirm the result, but it gives an measure of plausibility to the simplified ansatz used in the simulations.

The procedure was used at various time points during an evolution for which the initial velocity was $v = 0.5$. The results are compared with the numerical predictions below

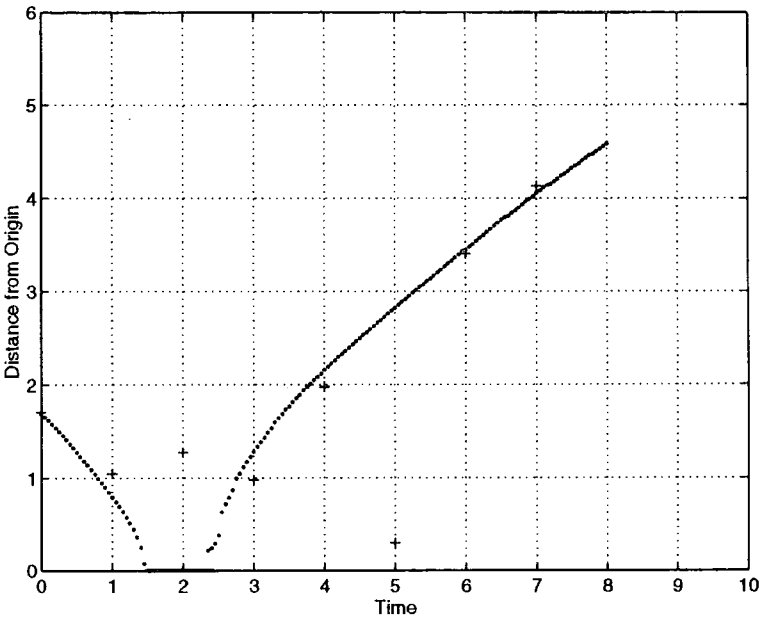

Figure V.34: Comparison of trajectory with points fitted by the crude test

There is good agreement except for during the scattering and at $t = 5$ seconds. The former was as expected. The latter is more of a concern. However, it should be remembered that this is a crude test. It is trying to match three dimensional structures with only five points.

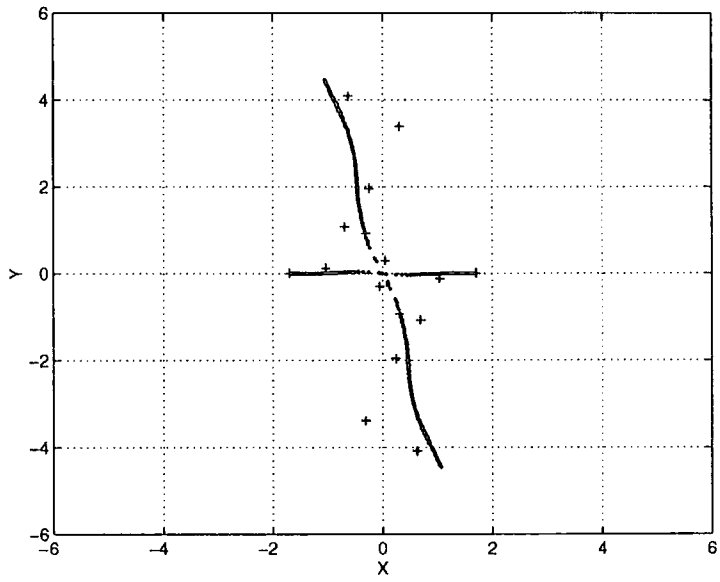

Figure V.35: Comparison of soliton positions with points fitted by the crude test

The value of a is highly sensitive to the points chosen to be close to the maximum of the energy distribution. This is reflected in the poor result for the point when t is five seconds. It is encouraging, however, that this method is able the otheer points so well.

The trajectory of the solitons are compared in figure V.35. The individual coordinates are shown in figures V.36 and V.36. There is reasonable agreement, except for the points referred to above.

Therefore, neither of the rigourous tests proposed at the start of this chapter were able to predict the trajectory of the full Lagrangian. However, some useful information was obtained which confirmed the validity of the simplified ansatz used in the programme.

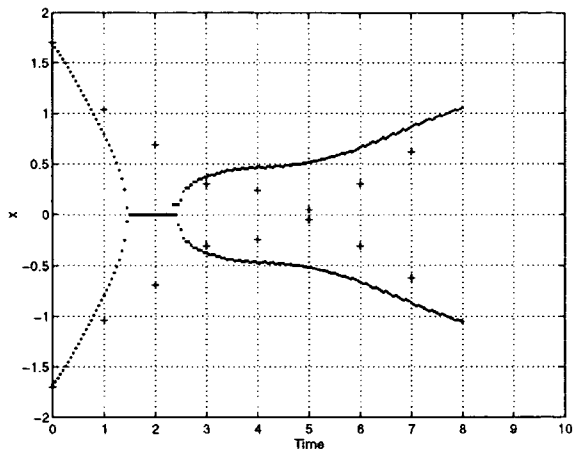

Figure V.36: Comparison of x coordinate with points fitted by the crude test

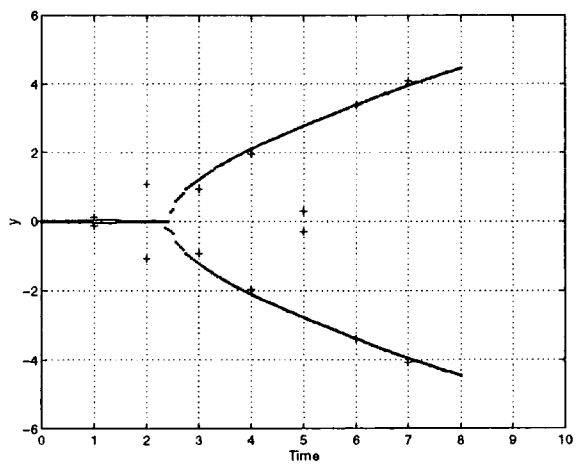

Figure V.37: Comparison of y coordinate with points fitted by the crude test

VI

Conclusion

Regrets? I've had a few,
but then again, too few to mention.
But more, much more than this,
I did it my way [1]

[1] Frank Sinatra, My Way

The work in this thesis was concerned with the CP^n nonlinear sigma model. This has two spatial and one time dimension. The nonlinearity arises from the compactification of two spatial dimensions into a sphere. Most of the work was concerned with the scattering of two solitons in CP^2.

In the simpler CP^1 model, it is possible to introduce a total divergent term which satisfies the numerical criteria of a Hopf term. The effect of this expression in the higher dimensional model was investigated.

After a review of earlier work in this area, a discussion on Noether's theorem was given. This associates a conserved charge with each symmetry of the Lagrangian which is used to define the model.

The charges associated with the internal symmetry in the model and the energy momentum tensor were calculated. They were used to explain the results obtained from numerical simulations of CP^1 and CP^2.

In CP^1 there are three charges arising from the internal $SU(2)$ symmetry. One of these was shown to be trivially zero. The remaining two are proportional to the real and imaginary components of the velocity of the solitons.

Moving on to pure CP^2, there will now be eight conserved charges. Two of them will also be proportional to the velocity of the solitons. This pair corresponds to the two non trivial charges in CP^1. The remaining charges were found to be trivially zero.

When the Hopflike term is added to the Lagrangian, the charges referred to above received a contribution which is independent of velocity. There are an additional two nontrivial charges which are related to the topological charge.

The project then diversified into two strands. The first used the charges which had been calculated to find expressions for the rate of change in the position of the solitons.

The ansatz used in the numerical simulations was

$$\begin{aligned} W &= \rho(x_+^n - a), \\ W^1 &= \mu(x_+^m - b) \end{aligned}$$

Initially it was assumed that only a was dependent on time.

It was able to provide a qualitative explanation for the behaviour of the solitons during the evolution. It explained why in pure CP^2 the phase of the solitons' position is constant before and after impact. It also predicted that when the Hopf term is added there will be a small phase change as the solitons move towards each other.

Hence they will no longer collide with a zero impact parameter. Thus the results could be compared with earlier work into the scattering of solitons which were forced to rotate away from the axis. This showed that a non zero impact parameter would lead to non orthogonal scattering in pure CP^2.

Also successfully predicted, was the fact that the absolute distance from the origin of the solitons would be approximately independent of the coefficient term associated with the Hopf term. It also showed that during and after scattering this was no longer expected to be the case.

However, the original ansatz used was only an approximation. Hence it led to inconsistencies in the equations and thus quantitative predictions could not be made.

The possibility of introducing additional time dependent parameters was investigated. However, due to the problems associated with trying to integrate numerically the expressions concerned, this did not provide any useful information.

The single soliton ansatz was then considered. It was able to confirm that, in this scenario, it is necessary for more than one parameter to be time dependent for the conserved charges to be finite.

An alternative method of investigation was then followed. It involved shadowing the trajectory of the solitons with the closest static approximation. A method was derived which was able to predict the trajectory for pure CP^2.

However, in the full Lagrangian, it was found that these methods were not able to predict the evolution after scattering. The explanation of this was found by plotting the error distributions around the optimal value of the parameters.

The minimum was not clearly defined. Hence the comparison test was unable to pick out the best fit. There is not an easy way to overcome this problem.

It was possible to provide some validation of the simple ansatz approximation. This involved crudely fitting the following ansatz to the data

$$w(z) = \lambda \frac{(z-a)(z-b)}{(z-c)(z-d)}.$$

This was able to confirm that it is possible to assume the denominator is constant. It also gave reasonable predictions for the soliton trajectory in the full Lagrangian.

Further work could concentrate on the time dependency of other parameters in the ansatz. This would fully test the veracity of the assumption that evolution could be predicted by only varying one. Is it sufficient to use only a Galilean boost?

It would also be of interest to consider the effect of the Hopflike term on the SU(3) conserved charges in the geodesic approximation. This involves the assumption that if the lumps are given a small amount of kinetic energy, then they will stay in a configuration close to a static approximation [32].

Therefore the parameters of the static ansatz are assumed to be time dependent. They are then substituted into the Lagrangian which is integrated over the spatial dimensions. The resulting ordinary differential equation can be integrated numerically. For the pure model, this gives results in close agreement to integrating the full model.

It would be useful to test further the validity of the initial ansatz used. For example, it would be interesting to perform the simulations with the initial lumps being exponentially localised (see [1]). This may provide more insight into the behaviour of the extended structures during the scattering.

Also, other methods for the shadowing procedure could be found and tested on the full Lagrangian. If a new procedure were able to predict the trajectory for the full Lagrangian, it would also need to be tested on pure CP^2.

More work could be performed on relating the effects of the Hopflike term with the effect of scattering rotating solitons. In particular, would it be possible for the two effects to cancel? This would provide confirmation that the additional term provides an internal rotation.

VII

References

Bibliography

[1] Ablowitz, M. Clarkson, P. *Solitons, Nonlinear Evolutution Equations and Inverse Scattering* LMS Lecture Note Series 149 Cambridge University Press (1991)

[2] Armstrong, M.A. *Basic Topology* McGraw-Hill (1979)

[3] Bailin, B. Love, A. *Introduction to Gauge Field Theory* Adam Hilger (1986)

[4] Boas, M.L. *Mathematical Methods in the Physical Sciences* John Wiley & Sons (1985)

[5] Bowick, M.J. Karabali,D Wijewardhana, L.C.R. *Nucl.Phys* **B271** *(1986) 417*

[6] Bronstein, I.N. Semendjajew, K.A. *Handbook of Mathematics* Verlag Harri Deutsch (1985)

[7] Char, B.W. et al *Maple V* Springer-Verlag (1991)

[8] Coleman,S. *Aspects of Symmetry* Cambridge University Press (1988)

[9] Din,A.M. Zakrzewski, W.J. *Phys.Lett.* **146B** *(1984) 341*

[10] Feynam R.P. *Phys.Rev.Lett* **23** *(1969) 1415*

[11] Gell-Mann, M. Levy, M. *Il Nuovo Cimento* XVI *(1960) 705*

[12] Goddard, P. Mansfield, P. *Rep.Prog.Phys* **49** *(1986) 725*

[13] Goldstein, H. *Classical Mechanics* Addison-Wesley (1980)

[14] Halzon, F. Martin,A.D. *Quarks and Leptons* John Wiley & Sons (1984)

[15] 't Hooft, G. *Nucl.Phys. B* **75** *(1974) 461*

[16] Hopf, H. *Fundamenta Mathematicae* **25** *(1935) 427*

[17] 't Hooft, G. NPB **75** (1974) 461

[18] Hu,S. *Homotopy Theory* Academic Press (1959)

[19] Itzyskin,C. Zuber, J.B. *Quantum Field Theory* McGraw-Hill (1980)

[20] Jackiw,R
Quantum Meaning of Classical Field Theory Rev.Mod.Phys. **49** (1977) 681

[21] Lamport, L. LaTeX Addison-Wesley (1985)

[22] Leese, R.A. Peyard M. Zakrzewski, W.J. *Nonlinearity* 1990 **3** 773

[23] Mandl, F. Shaw, G. *Quantum Field Theory* John Wiley & Sons (1993)

[24] MathWorks *Matlab Reference Guide* MathWorks, Inc.

[25] Merzbacher,E *Quantum Mechanics* John Wiley & Sons (1970)

[26] Ne'eman, Y. Kirsh,Y. *The Particle Hunters* Cambridge University Press (1987)

[27] NAG *Numerical Algorithms Group* Oxford

[28] Page, C.G. *Fortran 77 for Professional Programmers* Pitman (1988)

[29] Pennington, M.R. *Cornerstones of QCD* Rep.Prog.Phys **46** (1983) 393

[30] Piette, B. Zakrzewski, W.J. *Durham preprint DTP-91-298*

[31] Piette, B. Rashid, M.S.S. Zakrzewski, W.J. *Nonlinearity* **6** *(1993) 1077*

[32] Piette, P. Zakrzewski, W.J. *Durham preprint DTP-93-97*

[33] Rajaman, R. *Instantons and Solitons* North Holland (1987)

[34] Ryder, L.H. *Quantum Field Theory* Cambridge University Press (1985)

[35] Schoers, B.J. *Private Communication*

[36] Stokoe, I. Zakrzewski, W.J. *Z.Phys C* **34** *(1987) 491*

[37] Sutcliffe, P.M. *PhD Thesis, University of Durham*

[38] Wilczek F. Zee, A. *Phys.Rev.Lett.* **51** *(1983) 2250*

[39] Wu, Y. Zee, A. *Phys.Lett.* **147B** *(1984) 325*

[40] Zakrzewski, W.J. *Lecture Notes* XVII *Winter School of Theorectical Physics, Karpacz Poland (1980)*

[41] Zakrzewski, W.J. *Low Dimensional Sigma Models* Adam Hilger (1989)

[42] Zakrzewski, W.J. *Nonlinearity* **4** *(1991) 429*